ADAPTIVE POWER NETWORK PROTECTION USING SYNCHRONIZED DATA

Saumendra Sarangi

ADAPTIVE POWER NETWORK PROTECTION USING SYNCHRONIZED DATA

Thesis Submitted to the

Indian Institute of Technology, Kharagpur

For award of the degree

of

Doctor of Philosophy

by

Saumendra Sarangi

Under the guidance of

Prof. Ashok Kumar Pradhan

DEPARTMENT OF ELECTRICAL ENGINEERING

INDIAN INSTITUTE OF TECHNOLOGY KHARAGPUR

APRIL 2017

Dedicated

to

Lord Shiva

APPROVAL OF THE VIVA-VOCE BOARD

----/----/-------

Certified that, the thesis entitled **ADAPTIVE POWER NETWORK PROTECTION USING SYNCHRONIZED DATA** submitted SAUMENDRA SARANGI to Indian Institute of Technology, Kharagpur, for the award of the degree of Doctor of Philosophy has been accepted by the external examiners and that the student has successfully defended the thesis in the viva-voce examination held today.

(Member of the DSC) (Member of the DSC) (Member of the DSC)

(Supervisor)

(External Examiner) (Chairman)

CERTIFICATE

This is to certify that the thesis entitled **"Adaptive Power Network Protection using Synchronized Data "** submitted by Saumendra Sarangi, to Indian Institute of Technology, Kharagpur, is a record of bona fide research work under our supervision and we consider it worthy of consideration for the award of Doctor of Philosophy of the Institute.

(Supervisor)

Prof. Ashok Kumar Pradhan

Department of Electrical Engineering

Indian Institute of Technology Kharagpur

Kharagpur, 721302, India.

Date:

DECLARATION

I certify that

a. The work contained in the thesis is original and has been done by myself under the general supervision of my supervisors.
b. The work has not been submitted to any other Institute for any degree or diploma.
c. I have followed the guidelines provided by the Institute in writing the thesis.
d. I have conformed to the norms and guidelines given in the Ethical Code of Conduct of the Institute.
e. Whenever I have used materials (data, theoretical analysis and text) from other sources, I have given due credit to them by citing them in the text of the thesis and giving their details in the references.
f. Whenever I have quoted written materials from other sources, I have put them under quotation marks and given due credit to the sources by citing them and giving required details in the references.

Signature of the Student

Acknowledgements

It is great pleasure and proud privilege to express my sincere gratitude to my research supervisors Prof. Ashok Kumar Pradhan. I am grateful to Prof. Ashok Kumar him whose encouragement, supervision, guidance and personal support from the preliminary to the concluding level enabled me to develop an understanding of the subject. It is an honor for me to have been working under his supervision and being part of his working group. I express my indebtedness.

I acknowledge my deep sense of gratitude to the members of doctoral scrutiny committee Prof. Prabodh Bajpai, Prof. Sudipta Mohapatra and Prof. Debapriya Das for their valuable suggestions and scrutiny of this work.

I am immensely grateful for the co-operation and affection I received from past to present Heads of the Department Prof. Jayanta Pal and Prof. Siddhartha Sen. I express my sincere gratitude to all the faculty members of the department who enriched my research and learning.

I am indebted to my friends especially Premalata Jena, Paresh kumar Nayak, Pratim, Ganesh, Rabindra, Sirisha, Parul and Swaroop for providing a warm research atmosphere, sharing knowledge and encouragement. I am also thankful to the technical and laboratory staff of the department, Mr. Amitav Nandy for his support and constant encouragement.

I acknowledge Ministry of Human Resource and Development, India for the grant of scholarship for the last four years for the research program.

I owe my deepest gratitude to my parents and family members for their love, affection, care and constant encouragement throughout the research work.

Finally, I would like to thank my wife Rajalaxmi for her understanding, co-operation and sacrifice throughout the study period and encouraged me in completion of this work.

Dated: Saumendra Sarangi

Abstract

Power system, being dynamic, its states change continuously and also its parameters vary with time. Fixed setting approach in conventional relays causes protection malfunction at times. In order to meet the power demand and to exploit economic benefits series-compensation and multiterminal lines are being introduced. Available line protection schemes have limited performance for series compensated lines as compensation level varies with time and the metal oxide varistor (MOV) protecting it functions nonlinearly. Synchronized data from both ends of the series compensated line are applied to compute the compensation level and to identify the operation of MOV during fault. This is used to adapt the zone-2 and zone-3 characteristic which improves the protection performance. To overcome the limitations of conventional distance relays for the protection of three terminal lines, direct under reaching transfer trip (DUTT) scheme is being applied. Such scheme has problems with the increase in infeed current when portions of the lines may remain unprotected by the scheme. Prefault synchronized data of the three terminals are applied to estimate the infeed current during fault and used to adapt the relay settings to ensure more reliable operation of DUTT scheme.

Alpha plane method using ratio of both end currents is better scheme than differential relays. Such a scheme has limited performance during outfeed condition. An adaptive alpha plane relaying is proposed using phase angle between the voltage and current and magnitude of change in current at both ends of a line to confirm an internal fault which provides improved performance.

Zone 3 in distance relaying scheme uses local data and is unable to distinguish three phase fault and heavy loading condition. Whenever apparent impedance enters zone 3 the ratio of change in voltage magnitude to change in phase angle collected from nearby busses are applied to derive an index which discriminates load encroachment from three phase fault. This helps in avoiding relay malfunction during load encroachment.

All the proposed methods are tested for different systems and conditions and are compared with available methods. It is found that with the synchronized data available in a power system, there is great scope to improve protection scheme performance.

Key words: Phasor Measurement Unit, Synchronized data, Wide area measurements, Transmission line protection, Series-compensated line, Three-terminal line, Load encroachment, Direct under reaching transfer trip

List of Abbreviations and Symbols

CCVT	Capacitor Coupling Voltage Transformer
CT	Current Transformer
PT	Potential Transformer
DCB	Directional Comparison Blocking
DFT	Discrete Fourier Transform
DUTT	Direct Underreaching Transfer Trip
EMTDC/PSCAD	Electromagnetic Transients Including DC/Power Systems Computer Aided Design
FBI	Faulted Bus Identification
FFT	Fast Fourier Transform
FLI	Faulted Line Identification
GPS	Global Positioning System
MOV	Metal Oxide Varistor
NERC	North American Electric Reliability Council
PDC	Phasor Data Concentrator
PMU	Phasor Measurement Unit
POTT	Permissive Overreaching Transfer Trip
SPT	Single-pole Tripping
SVMs	Support Vector Machines
TCSC	Thyristor Controlled Series Capacitor
WAMS	Wide-Area Measurement Systems
WABP	Wide-Area Backup Protection
WSCC	Western Electricity Coordinating Council
WT	Wavelet Transform
CR	Current Ratio
SVM	Support Vector Machines
TTC	Total Transfer Capacity
TVE	Total Vector Error

ΔI_{diff}	Difference of both end change in current magnitude
$\Delta \dot{I}_R^a$	a-phase change in current magnitude at R-bus
$\Delta \dot{I}_L^a$	a-phase change in current magnitude at L-bus
δ	Angle between the voltages at buses M and N
$\emptyset_{th}$	Threshold for change phase angle during fault
ζ	Threshold change in current
ε	Constant
h	Magnitude ratio of both source volatge
$\emptyset_{min}$	Thresohold
Z_{err}	Error in apparent impedance
K_S	Percentage overlapping for S-bus relay
K_P	Percentage overlapping for P-bus relay
K_0	Zero compensating factor
C_S	Co-efficient for S-bus relay
C_P	Co-efficient for P-bus relay
Z_c	The characteristic impedance of the line
Z_{app}	Apparent Impedance
n	Time index
Z_{1RS}	Positive sequence impedance of line RS
$\overline{V}_{Spre}$	Prefault positive-sequence voltage at bus-S
$\overline{V}_{SF}$	Positive-sequence voltage at bus-S during fault
ΔV	Change in positive sequence voltage
ΔV_{nt}	Change positive-sequence voltage measured at n^{th} bus
$\Delta\theta_{nt}$	Change in positive-sequence voltage phase at n^{th} bus
ξ	Threshold for $\frac{\Delta V}{\Delta \theta}$
$\Delta\theta$	Change in positive sequence voltage phase
X_C	Capacitive Reactance
K_Z	Proportional coefficient of zero-sequence component
K_P	Positive-sequence proportional coefficient
ϕ_{1F}	Angle between positive-sequence current and voltage

Contents

Title Page i

Certificate of Approval v

Certificate vii

Declaration ix

Acknowledgements xi

Abstract xiii

List of Abbreviations and Symbols xv

Contents xix

List of Tables xxv

List of Figures xxvii

Chapter 1. Introduction 1

1.1 General……. 1

1.2 State-of-the-Art……. 4

1.2.1 Alpha Plane Based Line Protection……... 5

1.2.2 Communication Assisted Distance Protection for three terminal . . Line……. 6

1.2.3 Distance Relay for Series compensated Line……... 7

1.2.4 Load Encroachment Function in Distance Relay…….. 9

1.2.4 Synchrophasor and its applications to protection……. 10

1.3 Motivation……... 12

1.4 Thesis Objective……... 13

1.5 Brief Overview on Work Done……... 14

1.5.1 Adaptive Alpha Plane Transmission Line Protection …..... 14

1.5.2 Adaptive DUTT Scheme for Three Terminal Line Protection…….…….…….....…… 14
1.5.3 Adaptive Backup Protection for Series Compensated Line ……..… 15
1.5.4 Secured zone 3 Protection during Load Encroachment using Synchronized Data……..... 16
1.5.5 Overall Contribution in Adaptive relaying…… 17
1.6 Major Contributions from the Thesis Work……...…….…… 18
1.7 Thesis Organization……. 19

Chapter 2. Adaptive Alpha Plane Transmission Line Protection

2.1 Introduction ……..... 21
2.2 Alpha Plane Characteristic for Line Protection…….... 22
2.3 Characteristic of High Resistance fault……... 24
2.4 Phase Change During Fault…… 26
2.5 Proposed Adaptive Technique……..... 27
2.5.1 Threshold selection for $\Delta \boldsymbol{I}_{\boldsymbol{diff}}$……..... 29
2.5.2 Threshold selection $\emptyset_{\boldsymbol{th}}$……... 29
2.5.3 Steps for Computation of Proposed Method……. 30
2.6 Results…….…. 31
2.6.1 Test for Internal High Resistance Fault....……...……..... 33
2.6.2 Test for External High Line-to-ground Fault……..……..... 34
2.6.3 Test for CT Saturation with External Fault……...……...…….…… 34
2.6.4 Test for Series compensated Line…….……... 35
2.6.5 Test for Error due to Channel Equalization and Synchronization…..…..…… 37
2.6.6 Performance of the Proposed Method during Single Pole Operation……. 38
2.6.7 Test for Different Operating condition…… 38
2.6.8 Comparative Assesment……..……...……. 42
2.7 Conclusion……..……..... 42

Chapter 3. Adaptive DUTT Scheme for Three Terminal Line

3.1 Introduction……... 44

3.2 System Description and DUTT setting……..... 45
3.3 Estimated In-feed Current during fault …… 46
3.4 Limitations of communication Assisted Scheme…….. 48
3.4.1 Limitations of DCB and POTT Scheme…… 48
3.4.2 Limitations of DUTT Scheme……..... 49
3.5 Proposed Adaptive Method……..……. 52
3.6 Results……..……..... 57
3.6.1 Test for Variations in system condition……..……..…… 57
3.6.2 Test for variations in Source Impedance…….……..… 59
3.6.3 Simultaneous Adaptive Setting of all Three Relays……..... 60
3.6.4 Test for Unsymmetrical Fault…… 62
3.6.5 Sensitivity Analysis……...… 62
3.7 Comparative Assessment…….……. 63
3.7.1 Comparison with Current differential Scheme ….…….…... 63
3.7.2 Comparison with POTT and DCB Schemes…….…… 65
3.8 Conclusion……..……...… 65

Chapter 4. Adaptive Backup Protection for Series Compensated Line

4.1 Introduction ……...……... 67
4.2 Apparent Impedance Calculation for Series Compensated Line……..…….. 69
4.3 Problems with Distance Relay in the presence of Series compensation……. 75
4.4 Proposed Adaptive Backup scheme…….……. 76
4.5 Results ……...……... 78
4.5.1 Significance of MOV operation in Trip Boundary and corresponding Modelling……. 79
4.5.2 Inaccuracies in MOV Modelling…….…….. 79
4.5.3 Boundary Setting for Line-to-ground Fault with 60% Compensation Level……..…….……..... 80
4.5.4 Trip Boundary with series Compensation Bypassed at Middle of the Line for a Different system condition…… 81

4.5.5 Boundary Setting for line-to-ground fault with Compensation bypassed during fault…… 83
4.5.6 Zone 3 Boundary Setting for line-to-ground fault with series compensation at the end of the line……. 84
4.5.7 Zone 3 Boundary setting for Line-to-ground Fault with Series Compensation Bypassed during fault at End of the Line……. 85
4.5.8 Adaptive zone-2 setting for 60% series compensated line in modified 9-bus system…… 87
4.6 Conclusion…….……..……..... 88

Chapter 5. Secured Zone 3 Protection during Load Encroachment

5.1 Introduction……...…. 90
5.2 Impedance Trajectory during Load Encroachment…… 91
5.3 Proposed Supervised Scheme…….…… 92
5.3.1 Variation in Voltage Magnitude and Phase angle during Disturbance…….. 92
5.3.2 Selection of PMU Buses……. 94
5.3.3 PMU Group Selection for a Relay……. 95
5.3.4 The Discrimination Function……. 96
5.3.5 Threshold Selection……. 96
5.3.6 Steps for Supervised Scheme……..…… 97
5.3.7 Communication Requirement and Latency Issues……. 98
5.4 Results ……. 98
5.4.1 Test for Load Encroachment with High Reactive Loading……..…….. 99
5.4.1.1 Sudden Reactive Load Change…… 99
5.4.1.2 Slow Reactive Load Change…… 100
5.4.2 Test for Three Phase Fault during high Reactive Loading Condition…..... 101
5.4.3 Test with IEEE 118 bus with Series Compensation…… 102
5.4.3.1 Test for load encroachment……...…...…….……... 103
5.4.3.2 Test for Three Phase fault……...…….....…. 104
5.4.4 Comparative Assessment……. 105
5.5 Conclusion…….……..... 106

Chapter 6. Conclusions

6.1 Summary of the Work……..…..….. 107

6.2 Scope of Future Work……..……..... 109

References 111

Appendix A System Data for WSCC 3-Machine 9-Bus Power System (Chapter- 2).. 123

Appendix B System Data for 400-kV Thee-Terminal Line (Chapter -3)……. 124

Appendix C System Data for 400 kV Series Compensated Line (Chapter 4)…….. 125

Appendix D System Data for New England 10-Machine, 39-Bus Power System (Chapter 5)…… 126

Appendix E Single Line Diagram IEEE 118-Bus Power System (Chapter 5)…….. 130

Appendix F System Data for IEEE 118-Bus Power System (Chapter 5)…… 131

Publications from the Thesis……. 137

Author's Biography……... 139

List of Tables

Table 2.1.	Fault current for different surfaces	25
Table 2.2.	Performance of proposed method for different compensation levels at end of the line …….……..	36
Table 2.3.	Comparative assessment of proposed method for different types fault, fault location and fault resistances……..……..……...….....	40
Table 2.4.	Performance of proposed method for variations in δ and source impedance……..	41
Table 2.5.	Performance of Proposed method with different fault inception angle……	41
Table 2.6.	Comparison of Performance of Proposed method with method [26]……	42
Table 3.1.	Synchronized data and different indices *(*h_1=0.98, δ_1=-15˚, h_2=1.0 andδ_2=-5˚)…….	58
Table 3.2.	Synchronized data and different indices (h_1=1.01, δ_1=-10˚, h_2=1.06 and δ_2=-20˚)…….	59
Table 3.3.	Synchronized data and different indices (h_1=1.01, δ_1=-5˚, h_2=0.96 and δ_2=-10˚)……..	61
Table 3.4.	Adaptive setting with *h* and δ variation ……	63
Table 3.5.	Adaptive setting with source impedance variation……	63
Table 3.6.	Effect of line length variation……	63
Table 3.7.	Variation of overlapping with Line Length……..	64
Table 4.1.	Comparison of Calculated Impedance with and Without MOV Operation…….....	79
Table 4.2.	Variation in resistance and reactance due to inaccuracies in MOV Modeling……	80
Table 4.3.	Synchronized data with 60 % Compensation at middle with h = 1, δ = 10˚…….	81
Table 4.4.	Synchronized data for capacitor bypassed with h = 0.99, δ = -5˚…….....	82
Table 4.5.	Synchronized data for Capacitor Bypassed with h = 1, δ = 10˚…….....	83
Table 4.6.	Synchronized data for Capacitor at end of line with h = 0.95, δ = 20˚……	85
Table 4.7.	Synchronized data for capacitor bypassed with h = 0.99, δ = -5˚…….....	86
Table 4.8.	Synchronized data for 60% Compensation in 9-Bus System……	88
Table 5.1	PMU groups for 39 bus System…….....	95
Table 5.2	Data for three phase fault in the line 69-75…….	104

List of Figures

Fig.1.1	Adaptive protection scheme using synchronized data……	17
Fig. 2.1.	Two source equivalent system ..……..…..…….….....	23
Fig. 2.2.	Alpha plane characteristic showing operating and restraining regions ..……...……...……..	24
Fig. 2.3.	Phase angle between voltage and current during fault and normal operating condition……	27
Fig. 2.4.	Change in phase angle for line-to-ground fault with R_F= 0 Ω with (a) source impedance variation. (b) δ variation (c) voltage magnitude variation ..……..…..….....	31
Fig. 2.5.	Flow diagram of the Proposed Technique……..	32
Fig. 2.6.	WSCC 9-bus system for testing α-plane relay at bus 5 for line 5-4.....	32
Fig. 2.7.	Result for internal line-to-ground fault with R_F = 200 Ω. (a) Alpha plane characteristic (b) ΔI_{diff} (c) $\emptyset_1$ and $\emptyset_2$ in rad (d) $\emptyset_{min}$ in rad (e) index K_1	33
Fig. 2.8.	Result for external line-to- ground fault with R_F = 200 Ω (a) α-plane characteristic (b ΔI_{diff} in pu…….	34
Fig. 2.9.	Result for external fault three phase fault for CT saturation. (a) α-plane characteristic (b) ΔI_{diff} in pu. (c) $\emptyset_1$ and $\emptyset_2$ in rad (d) $\emptyset_{min}$ in rad (e) index K_1 ……..	35
Fig. 2.10.	Result for high resistance fault in series compensated line (a) Alpha plane characteristic (b) ΔI_{diff} (c) Phase angle deviation at both ends. (d) Φmin (e) Index K_1……	36
Fig. 2.11.	Result for channel equalization error(a) α-plane characteristic (b) ΔI_{diff} (c) Phase angle deviation at both ends. (d) Φmin .(e) Index K_1……..	37
Fig. 2.12.	Phase currents of line 4-5 during single pole tripping…….....	38
Fig. 2.13.	Result for single pole tripping (a) Alpha plane characteristic (b) ΔI_{diff} (c) Phase angle deviation at both ends. (d) Φmin .(e) Index K_1……..	39
Fig. 3.1.	The Three-terminal line……	46
Fig. 3.2.	The three-terminal line with fault in the TR section……..	49
Fig. 3.3.	Variation in percentage of Overlappings…….	51
Fig. 3.4.	Apparent impedance trajectory for 3-phase fault……	52
Fig. 3.5.	. Flow diagram for proposed adaptive technique…….	56

Fig. 3.6.	S and P relays zone 1 adaptive setting for DUTT scheme……..	58
Fig. 3.7.	S and P relays zone 1 adaptive setting for source impedance variation….	60
Fig. 3.8	S, R and P relays zone 1 adaptive setting for DUTT scheme……..	61
Fig. 3.9.	S Relay zone 1 adaptive setting for DUTT Scheme……..	62
Fig. 3.10.	Response of differential and DUTT schemes for CT saturation during three phase external fault ……	64
Fig. 3.11.	Apparent impedance at P and R relays during three phase internal fault	65
Fig. 4.1.	PMUs at the two buses in the series compensation system…….	69
Fig. 4.2.	Sequence diagram for ag -type fault after the series capacitor……...	71
Fig. 4.3.	Comparison of zone-2 trip boundaries with 60 % compensation at middle and capacitor……..	75
Fig. 4.4.	Flow diagram for the proposed adaptive technique…….	78
Fig. 4.5.	Trip boundary with 60% compensation at middle with h = 1, δ=10^0….	81
Fig. 4.6.	Trip boundary with capacitor bypassed at middle with h = 0.99, δ = -5^0..	82
Fig. 4.7.	Trip boundary with 60% series compensation bypassed during fault …..	83
Fig. 4.8.	Equivalent two-source system with series compensation at the end……..	84
Fig. 4.9.	Trip boundary with 60% series compensation at the end…….	85
Fig. 4.10.	Trip boundary with compensation bypassed during fault at the end with h = 0.95, δ =20^0……..	86
Fig. 4.11.	PMUs with the modified WSCC 9-bus system……	87
Fig. 4.12.	Trip boundary with 60% compensation at middle of bus-7 and 8 modified WSCC 9-bus system……	88
Fig. 5.1.	New England 39 bus System……	91
Fig. 5.2.	Impedance trajectory at bus-29 for different loading conditions…….	92
Fig. 5.3.	Single line diagram of two bus system……	92
Fig. 5.4	Phasor diagram for change in voltage at bus S during load increment at bus R.(b) Phasor diagram during three phase fault when voltage equal to 0.85 pu……	93
Fig. 5.5.	Phasor diagram for change in voltage at bus S for three phase fault…….	93
Fig. 5.6.	Ratio of change in voltage magnitude and voltage angle for three phase fault and load encroachment……	97
Fig. 5.7.	Flow diagram for proposed algorithm……	98

Fig. 5.8. (a) Change in voltage magnitude at PMU buses(pu.) (b) Change in Voltage angle (rad) (c) Impedance trajectory for the high reactive loading condition at bus 29. (d) Index D for zone 3 at bus 29 under high reactive loading in 39 bus system 99

Fig. 5.9. (a) Change in voltage magnitude at PMU buses (pu.) (b) Change in Voltage angle (rad) (c) Impedance trajectory for the relay at bus 29 during high reactive loading. (d) Index D under slow load increment during high reactive loading in New England 39 bus system…….. 100

Fig. 5.10. (a) Change in voltage magnitude at PMU busses(pu.) (b) Change in Voltage angle (rad) (c) Impedance trajectory for relay at bus 29. (d) Index D for three phase fault in New England 39 bus system during high reactive condition…… 101

Fig. 5.11. (a) Change in voltage magnitude at PMU buses(pu.) (b) Change in Voltage angle (rad) (c) Impedance trajectory for relay at bus 49 during load increment. (d) Index D during load increment in the presence series compensation in IEEE 118 bus system…….. 103

Fig. 5.12. (a) Impedance trajectory for relay at bus 49 during three phase fault. (b) Index D for three phase fault in the presence of series compensated in IEEE 118 bus system……. 104

Introduction

1.1 General

Deregulation, renewable sources and technological developments have made power system operation and control more challenging today. Relays protecting power system are designed to sense faults and isolate the faulted section as soon as possible. The relay settings, obtained through off-line calculation around an operating point, are fixed type in general. As the parameters and states of a power system vary continuously, it is not possible to incorporate all variations that may appear, in the calculation of relay settings. Analysis of several blackouts reveals relay maloperation as one of the important reasons [1]-[12]. The fixed setting approach therefore is a concern in relay performance during stressed operating conditions of power system [13]-[20]. With the invention of phasor measurement unit (PMU) and development in communication system, wide area measurement system (WAMS) is able to provide synchronized phasor data for monitoring power system dynamic states. Using WAMS data on current system status, it is possible to change the setting in a numerical relay to most appropriate one at that time. Such an adaptive setting approach ensures reliable operation of a protection scheme.

Available protection schemes for transmission lines use either local data or both end data. In the former approach, distance and overcurrent relays perform correctly most of the time, but they have limited discrimination capability for faults towards the remote end of the line and for high resistance faults. Using communication system transmission line protection scheme using data from both ends like current differential, phase comparison, directional comparison and carrier aided protection schemes [21] are possible. Such

techniques have advantage in speed and accuracy in protection decision. Uncertainties like failure of circuit breaker or communication or sensor failure ask for backup protection schemes.

Current differential protection while protecting long transmission line has problems because of high charging current, current transformer saturation and unequal line impedances [21]. Analysis on alpha plane based relay, which uses the ratio of currents of both ends of a line, reveals advantages over current differential protection particularly on CT saturation issue. It is found that such an approach has limitation during outfeed condition caused by high resistance fault and weak source conditions.

To exploit economic, technical and environmental benefits multiterminal lines are being used in power systems with three-terminal being the common configuration. Such a configuration imposes protection challenges for both local data based protection approach and methods using both end data [22]. Distance relay protecting a three-terminal line experiences underreach problem for a fault beyond the T-point. Communication assisted schemes like permissive overreaching transfer trip (POTT), direct underreacting transfer trip (DUTT) and directional comparison blocking (DCB) are preferred for protection of three terminal lines [23]. The DUTT scheme responds to fault when any of the three zone 1 elements detects an internal fault and the dependability of the protection scheme is ensured by maintaining overlappings among the three zone 1 elements. However zone 1 reach decreases with increase in infeed and at times the overlappings may vanish for certain infeed conditions.

Limited right-of-way and increased power demand have forced to include series capacitor in long transmission line and has advantages of high transfer capability, improved stability etc. However, a series capacitor in a line introduces challenge to distance relaying scheme [24]. Nonlinear nature of overvoltage protection devices of series capacitor, metal oxide varistor (MOV) and spark gap further complicates the protection. At times, the series capacitor may be bypassed during maintenance or by the overvoltage protection devices and during such period impedance seen by distance relay is similar to a normal transmission line. When the fault loop includes series capacitor the

seen impedance is modulated significantly and the distance relay requires information on compensation level present in the line for correct protection decision.

Zone 3 of a distance relay provides backup protection to the adjacent line and covers a large area in R-X plane. Zone 3 maloperates during heavy loading condition as the apparent impedance may enter inside the trip characteristic. Zone 3 maloperation may trigger cascaded tripping. Load encroachment functions are applied to prevent such maloperation [25]. They are set considering the maximum power factor angle and basically fixed in nature. During heavy reactive loading such fixed characteristic loses its ability to prevent maloperation. Investigations on large disturbances reveal that protection scheme maloperation is one of the major contributing reasons for cascaded tripping in power systems [5]. For example, the Northeast blackout in 2003 [5] and the recent 2012 blackouts in India [9] were initiated as a result of zone 3 maloperation due to load encroachment.

To improve the immunity of relays to the changes in system condition, adaptive protection is proposed [13]. Such a strategy permits a function within the protective relay that automatically adjusts the operating characteristic of the relay in response to changing power system conditions. The adaptive protection of a transmission line can be accomplished by changing the setting or by mapping the complex function of the relay on-line. It requires information on present system operating condition for setting calculation.

With the advent of global positioning system (GPS) based technology time stamped phasors are available from PMUs at different buses with an accuracy of 1 μs [26]. WAMS which integrates PMU data, can provide snapshot of whole power system in real time [27]. This has improved the monitoring and control of the power system. With synchronized data, WAMS has provided new opportunities for network protection to develop new algorithms. The adaptive protection for a transmission line can be accomplished using WAMS data.

This thesis proposes adaptive setting of relays using synchronised data which improves reliability of power network protection schemes. This is achieved by changing the relay setting in accordance with the system condition and deriving better protection

logic using additional features. An adaptive alpha plane transmission line protection scheme is proposed to improve the performance further for high resistance fault, CT saturation and single pole tripping. To nullify the effect of infeed, an adaptive DUTT scheme is proposed for three terminal lines. An adaptive zone 2 and zone 3 settings for series compensated line are achieved by computing the compensation level present in the line using synchrophasor data from both ends of the line. A secured zone 3 algorithm is developed using WAMS data to overcome the problem associated with load encroachment. These proposed algorithms are tested for different systems and fault conditions and found to be accurate. Available transmission line protection schemes supplemented by these algorithms using synchronized data will provide enhanced network protection for reliable power system operation.

1.2 Review of Existing State-of-the-Art Solutions

Transmission lines are protected by differential, POTT, DUTT and DCB schemes. In association with a differential scheme, distance relay may act as a backup protection. It is revealed that relay maloperation is a major cause of large scale disturbances in power system. With digital technology, adaptive protection scheme can improve the performance of relay. Synchronized phasor obtained from wide-area measurement system, has potential to provide accurate information on network condition. Numerous techniques are available to prevent relay maloperation during disturbances. A survey on these issues in relevance to the transmission line protection is carried out.

1.2.1 Alpha Plane based Line Protection

Local data based conventional relays protecting long transmission lines have limited performance in discriminating faults toward the ends of the lines. At times during stressed condition, such relays maloperate and is an important factor of recent blackouts [9]. Reliable line protection scheme can be achieved by utilizing information from both ends of a line. With fiber-optic communication [28], data availability from other end is feasible even for long transmission lines. Schemes which use both end data have inherent immunity to power swing, mutual coupling, series compensation if any and series impedance unbalances.

The widely applied scheme for line protection using both end information is directional comparison [29]-[32]. Such a protection scheme has limited performance as a result of distorted voltage signals during close-in fault or blown fuses or ferro-resonance problem associated with capacitor coupled voltage transformer (CCVT) [27]. A protection scheme which utilizes both end currents only can overcome these disadvantages. Phase comparison, charge comparison and current differential schemes require line currents to detect internal faults [33]. Current based techniques are sensitive to cross country fault. Conventional current differential protection has setting challenges because of current transformer (CT) saturation [34]. Both ends synchronized data also applied for differential protection to nullify the effect of charging current[35]-[38]

With the inputs to relay in complex form, it is convenient to represent the relay characteristic in a complex plane. In [39]-[40], alpha plane (α-plane) is introduced that uses ratio of both ends current phasors. The ratio during external fault and healthy condition remains within a restraining region of the complex plane. The phase current based alpha-plane relaying with large restraining region has advantages such as: tolerance to CT saturation and synchronization errors. The protection decision is compromised during high resistance fault and weak source condition. Though the sequence current based scheme has improved performance during high resistance fault, misoperates during single pole condition and operation of metal oxide varistor (MOV) in a series compensated line [41]. In [42], both sequence and phase currents are used to improve the sensitivity of alpha-plane principle. A modified alpha-plane characteristic is proposed which uses sequence components and phase currents along with an additional faulted phase detection logic to improve the reliability and sensitivity of the relay [43]. In these methods communication channel and computation requirements are high. During single pole tripping new sequence element logic is adopted to improve the sensitivity of the relay which depends on system parameters [44].

1.2.2 Communication Assisted Distance Protection for Three-Terminal Lines

Transmission lines are tapped in between two terminals to extract economical and technical benefits. The infeed or outfeed phenomenon during a fault in a three-terminal line creates challenge to distance relaying. Data from remote end provides better

performance to protect these lines. Current differential, directional comparison and communication assisted distance protection or unit protection scheme are available which has immunity to infeed [46]-[47].

Current differential principle adopted for three terminal line protection uses all three end currents to take the decision [48]-[49]. This scheme is faster in response and is free from problems associated with power swing and but may fail during outfeed condition. For detecting high resistance fault in a heavily loaded line such a scheme has limited performance [50]. In [49], current differential scheme is proposed using the sampled values of currents at all the terminals. This becomes more prominent when such faults occur during power swing [51]. The noise and spurious signals present during fault make it difficult to compare the currents. The differential scheme has limited performance in the presence of charging current, current transformer saturation issue and outfeed condition for internal faults [52].

Accurate fault detection is achieved for three-terminal line using derived signals from fault voltage and current [53]. Directional comparison technique based three-terminal line protection is proposed in [54]-[57] where polarity of fault generated transient current signals are compared. In [54], wavelet transform is applied to high frequency noise signals to detect internal fault of a three-terminal line.

The communication assisted distance protection schemes for such lines are DUTT, POTT, and DCB [23]. Out of these, POTT and DCB schemes are set with zone 2 coverage for protecting the line completely which needs to be extended to counter the infeed effect. Such schemes are vulnerable to load encroachment and power swing and also maloperate for outfeed condition [46]. Though zone 1 based protection DUTT scheme is more promising than schemes using zone 2, it has reach limitation problem [47].

DUTT scheme for protection of three-terminal line uses zone 1 distance element at each end which finds underreach problem due to the infeed from T-point [22]. The protection issue of three-terminal line with unequal branch lengths is more critical as they have limited overlapping regions between the zone 1 elements. These overlappings of zone 1 elements decrease with increase in infeed current from T-point. For high infeed

currents, the overlappings for distance relay settings may vanish which will lead to an unprotected line segment with DUTT scheme.

Adaptive setting for distance protection is addressed in [58]-[59]. It is shown that the trip boundary is significantly affected by the system conditions in particular for a transmission system with infeed. Influencing factors, e.g. load angle, voltage ratio, source impedance ratio and fault resistance. Finally an on-line method is proposed for tripping the available resistance and reactance components of apparent impedance. In [59], an adaptive zone 1 setting scheme for three-terminal line is proposed which considers voltage and line flow of all parts of system available through SCADA. Agent based technique is employed for adaptive relay setting of transmission line using power network information [60]. The latency of data will affect the performance of such adaptive scheme.

1.2.3 Distance Relay for Series Compensated Line

Series compensation has been utilized to improve the power transfer capability, power system stability, load division on parallel paths, reduced system losses, voltage regulation and flexible power flow control [61]–[62]. With the inclusion of series compensation in a line, the protection challenges are addressed in [63]–[66]. Problems in relaying of series compensated line include phenomena such as voltage and current inversions, subharmonic oscillations and additional transients caused by the air-gaps triggered for thermal protection of the MOV [66]. MOV protecting series capacitor imposes challenges to line protection because of subsynchronous resonance, and its non-linear operation [67]-[73]. Voltage inversion may cause maloperation of communication assisted and directional comparison protection schemes [24]. Differential relays also has problem for current inversion [64] and CT saturation. These limitations of available unit protection schemes ask for a backup protection which is achieved through distance relay.

Overreaching may cause maloperation of distance protection scheme of a series compensated line for a fault beyond zone-1 of the succeeding line. This can be avoided with a reduced setting in accordance with the compensation level [65]. At times, the series capacitor may be bypassed for maintenance or any other reason and apparent impedance is also modulated in case of MOV operation. At these conditions backup protection will

maloperate if accurate compensation level and MOV operation are not considered in online relay settings[66].

The MOV operation in a series compensated line complicates the protection problem further for a line-to-ground fault when MOV operates only in faulty phase. This introduces unbalance in the network and leads to non-zero values in the off-diagonal elements of line-impedance matrix. Therefore, sequence component analysis cannot be applied as usual for such a system. In such a case, MOV is preferred to be modeled in phase domain [67]. In [68], a quasilinear model is proposed to provide the inter-sequence mutual coupling during unbalanced fault with MOV operation. A superposition principle is applied with iterative approach to obtain accurate impedance offered by the MOV-protected series capacitor [69].

For line protection, different methods proposed to counter the effect of MOV while estimating fault distance, use local information [70]-[73]. Using relay current, the voltage across the series compensation is estimated for faults beyond the compensation [72]. Methods using wavelet transform [74] and high frequency noise signals [75] are also available for protection of series compensated lines.

Adaptive protection is applied to series compensated line to accommodate the variation in series compensation [76]-[78]. Using local data, methods are available for relay decision addressing MOV operation [77]-[78]. Adaptive protection using a hybrid parallel algorithm with distance relay function is proposed in [76]. In [77], adaptive Kalman filtering technique is employed to detect the fault position with respect to the series compensation. Neural network, to handle the complexity of varying system condition, is also applied for series compensated line [78]. In [79]-[81], adaptive setting of distance relay is proposed for FACTS devices.

1.2.4 Load Encroachment function in Distance Relay

Zone 3 of a distance relay provides remote backup protection for adjacent lines and covers a large area in R-X plane. During heavy system loading condition the load impedance may enter into zone 3 and the relay may confuse with three phase fault resulting undesirable tripping. Such maloperation has contributed cascade tripping of lines causing wide area disturbances [1]-[9].

Load encroachment function in distance relay, applied to prevent zone 3 maloperation is set with a fixed power factor angle [82]. Under extreme contingency and severe reactive loading condition, distance relay finds load impedance inside zone 3 but beyond the load encroachment function [83]. During such situations, for secured zone 3 decision additional information on system condition is necessary. Several methods are available to avoid zone 3 maloperation under heavy loading conditions [84]-[86]. Modified zone 3 characteristics like forward offset mho, lenticular and increased maximum torque angle are applied compromising the dependability of the relay [81]. Numerous techniques to obtain increased loadability are available in [84]-[86]. Blinders applied to discriminate heavy loading condition from fault are difficult to set and it requires accurate system study [85]. In [86], a neural network based blinder scheme to discriminate load from fault is proposed. Such a technique requires large number of training patterns to be generated for a system. In [87], a scheme combining the steady-state and the transient components using state diagram is proposed to prevent zone 3 maloperation. Rate of change of voltage is utilized to prevent undesirable tripping of distance relay during voltage instability and has challenges in threshold setting [86]. Transients present in current signal during fault and power factor angle are applied to support the zone 3 decision [88]. However this method has limitation in discriminating line end fault and transient caused by severe contingency condition. During stressed condition, tripping of a transmission line increases loadings of other lines and may cause zone 3 maloperation. Security analysis based zone 3 blocking scheme is proposed in [89] which utilizes line outage distribution factor (LODF) to compute the increased loading on lines and it is difficult to compute the LODF during cascade tripping.

Available methods using local information have limited capability in discriminating load to three phase fault. The adaptive schemes discussed in this section are based on local and network data received from SCADA. The measurements received from various substations are used in control centers to provide an estimate for all bus quantities and network parameters of the power system and updated in every 4-5 sec. As variation in power system is dynamic, it does not capture all the dynamic changes of the systems. Data having latency also does not guaranty the actual system condition. As a

result adaptive setting may not be proper. These issues are solved in the advent of Synchrophasor.

1.2.4 Synchrophasor and its applications to protection

In recent years with rapid advancement in communication and information technology, Wide area Measurement System (WAMS) technology has evolved. Phasor measurement Unit is a basic component of WAMs, which provides phasors with a synchronisation accuracy of 1 μs. Phasors from PMUs are gathered at a central location using advanced communication system. This has improved the ability to capture any dynamic changes of power system and also helps in better monitoring, protection and control of power networks [93]-[103]. Communication latency associated with WAMs data, restricts its application to slower form of protection schemes, e.g. backup protection schemes in general [93].

Significant research has been carried out on application of WAMs data to prevent relay maloperation and improve the security of the system. Its application can be classified in two categories, improving backup protection [101]-[114] and obtaining adaptive relay characteristic [116]-[117]. The former approach basically called as wide area backup protection scheme uses faulted line identification (FLI) approach. The wide-area information is used to identify the faulted line and then isolation of faulty section is achieved with high accuracy [101]–[114]. Such scheme can overcome the limitation of conventional backup protection which uses local data.

In [102]-[104], agent-based backup relay protection schemes built on low latency communication network is proposed. A WAMS based backup (WABM) protection using fault steady state component of voltage distribution is proposed for FLI [105]. A WABP algorithm based on the fault component voltage distribution is proposed in [106]. In this scheme the fault component of voltage at one terminal of the line is estimated by utilizing the measured values of fault component voltage and current at other terminals and the faulted line is identified based on the ratio of measured values to estimated values. In [107], on the basis of network topology and PMU placement, subsets of buses called as protection correlation regions (PCRs) are formed. The component of differential current in each PCR is applied to identify the fault.

In [108], changes in voltage magnitude at different buses and changes in current angle are applied to locate faulted section in a network and there from proper zone 3 decision is derived. It requires both system voltages and line currents. In [109], a state estimation approach is used to locate the faulted section which supports zone 3 that requires system topology and line parameters. Wide area network information and response of relays are applied to support the backup protection [110]. Apparent impedance calculated using synchrophasor data is used to discriminate three phase fault from other stressed conditions [111] which enhances the protection decision. Performance of the method depends on system topology and data from strategic locations. Load encroachment function applied to prevent zone 3 maloperation needs to be adaptive with changes in power system condition. In [112], wide area measurement based backup protection for series compensated line is proposed and it requires sequence components of voltage and currents form both ends of the line.

With the knowledge of accurate system condition an adaptive scheme is also feasible [113]-[115]. In [113], synchronized data is applied to three terminal line to improve the security. Using synchronized data estimated line parameter is applied to detect internal fault [114]. Adaptive power differential scheme is proposed in [115]. In [116], an adaptive current differential scheme using synchronized phasors is proposed, where the restraining region is varied using both end currents.

1.3 Motivation

In a deregulated, decentralized market in order to meet the power demand with limited right-of-way, utilities are trying for the optimum utilization of existing power assets. Incorporation of series compensation provides better utilization of an existing transmission line. Multiterminal lines are often used both at transmission and sub-transmission levels. Distance relay has underreach problem due to infeed issue with three terminal lines and overreach problem due to the presence of series compensation in a line. This may cause relay maloperation and such action may lead to cascaded outage when the power system operates at a stressed condition. Communication assisted scheme like DUTT is applied for protection of three terminal line has better performance than conventional distance relay using local information only. With increased infeed current

when the overlapping between zone 1 distance elements vanishes, fault in a section of three terminal line remains undetected by DUTT scheme. Similarly in a series compensated line as the compensation level varies distance relay seeks information on compensation level present in the line for correct relay decision. To detect and clear fault with a high degree of selectivity and dependability the relay setting must be changed according to current operating condition of the power system. To improve the relay performance data from both ends of the line are applied. Alpha plane protection scheme which uses both end data for protection suffers with relay maloperation for a high resistance fault.

Zone 3 element of distance relay takes decision based on local measurements. It encounters the problem of unwanted tripping during overload and is the main contributing reason of cascade outage and subsequent blackout. In today's competitive environment, transmission lines are operated close to their limits and zone 3 maloperation is often found in recent years [6]-[10]. At the same time, the recent advances in communication, computer networks and significant developments in phasor measurement units have drawn attention for the use of WAMS based synchrophasor data for improved protection. Communication latency in such technology allows mainly for improving protection functions having slow responses.

From the above discussion and as per the limitation of the existing methods following observations are made for the research work.

(i) Existing methods using both end phase current can detect an internal fault efficiently. But it has limited performance for high resistance fault. However sequence component based methods provides a solution to such an issue. Method using both sequence component and phase current form both ends is secured but requires more communication channel and has limitation during single pole operation, line impedance unbalances for MOV operation for series compensated line. Thus phase current based technique which has limitation during high resistance fault seeks an improved protection algorithm which can solve such issue.

(ii) Available protection technique for three terminal line has limited performance for changes in system conditions. Infeed form the tap point varies corresponding to the fault current and operating condition. DUTT scheme applied to protect unsymmetrical three terminal line maloperates for certain infeed conditions when overlapping between relay setting vanishes. This demands an adaptive setting in accordance with the infeed current.

(iii) Inclusion of series compensation which raises several protection challenges can be solved using both end data. However a reliable protection scheme requires a backup protection which is provided by distance relay. Performance of distance relay protecting series compensated line seeks information on compensation level present in the line for correct operation. Available adaptive protection scheme which uses single end data cannot compute the compensation level accurate which may leads to maloperation of backup protection. Synchronized data from both ends of the line can compute the accurate line compensation which can be utilized for appropriate decision.

(iv) Zone 3 protection of distance relay using local information is not sufficient enough to maintain the security of power system during stressed condition. In literature several methods available to prevent zone 3 maloperation which requires both end current information and system topology information. However such scheme suffers when system topology is not available. Therefore for effective protection, there is a need for improvement in existing backup protection schemes.

1.4 Thesis Objective

Employing numerical relay based protection scheme in power system has resulted significant performance improvement in the decision making process. The rapid advancement in communication and information technology has drawn attention for the use of wide-area synchronized measurements for protection. There is a scope to adapt the relay setting by using system condition information. The primary objective of this work is to obtain adaptive protection schemes for power networks with present day technology.

The following objectives are set for the research.

a) To enhance the alpha plane relaying using phase current from both ends.

b) To access the performance of the DUTT scheme for different operating condition using synchronized data and change the settings in accordance with the infeed condition.

c) To estimate the compensation level present in the line using both ends synchronized data to improve the coordination of the relay and prevent maloperation of the zone 2 and zone 3 relay.

d) To develop an algorithm using wide area measurement data which can prevent maloperation of zone 3 during load encroachment.

1.5 Brief Overview on Work Done

The work carried out in this research focuses on distance relaying issues for different networks (series-compensated or three-terminal line) and system conditions. Various techniques are developed and are tested on different systems for different situations to overcome the limitations of conventional settings. Simulations are carried out for different 400 kV systems with EMTDC/PSCAD. Discrete Fourier transform (DFT) estimation technique is used for extracting fundamental component of each input signal. The novelty of each technique developed in this work is highlighted below.

1.5.1 Adaptive Alpha Plane Transmission Line Protection

Alpha plane based protection schemes protecting transmission lines has immunity to channel delay, asymmetry has improved performance over differential relay. The scheme uses ratio of phase or sequence current from both ends of the line in the decision process. Phase based alpha plane relaying such scheme has limited performance during outdfeed. Sequence based scheme has better performance for out feed condition provides incorrect result during single pole condition and MOV operation in series compensated line.

In this work, an adaptive alpha-plane differential relaying using phase current is proposed which improves the performance for high resistance fault, unbalance caused by MOV operation in series compensated line and single pole operation. The phase angle between the voltage and current and magnitude of change in current from both ends are utilized for protection decision in the scheme when the trajectory in the alpha-plane lies in an overlapping region accommodating both internal faults with high resistance and external fault with CT saturation. The proposed method is tested for WSCC 9 bus system with and without series compensation. Simulation results show excellent performance of the proposed method.

1.5.2 Adaptive DUTT Scheme for Three Terminal Line Protection

Multiterminal lines are often used both at transmission and sub-transmission levels to exploit economic, technical and environmental benefits over two-terminal lines. Among the different multiterminal configurations, the simplest and the most used one is the three-terminal line. The use of three-terminal line imposes severe protection challenges to different protection schemes including distance relay. The presence of a third source-terminal causes distance relay to underreach for a fault beyond the tap point. The underreach problem can be overcome by extending the relay reach which limits the load carrying capability.

In this work, adaptive setting for DUTT scheme protecting three-terminal line using prefault synchronized data is proposed. The system operating condition is calculated from synchronized data and is used to check the overlappings between the zone 1 elements of DUTT scheme. For the loss of any overlapping, zone 1 setting of the lines are updated for improved protection decision. The method is tested for a three-terminal line simulated in EMTDC/PSCAD and the results show its high accuracy. The adaptive method is compared with other available methods; current differential, DCB and POTT.

1.5.3 Adaptive Backup protection for Series compensated Line

Series capacitors are installed in high voltage transmission systems for numerous technical benefits. Series compensation imposes challenges to different protection schemes including distance relay. Series capacitor may be bypassed at times for

maintenance purpose or by its overvoltage protecting devices MOV and spark-gap. Information on compensation level is required for accurate operation of the relay when fault loop includes the series compensation.

In this work voltage and current phasors obtained from both ends of the line are utilised to compute the compensation level present in the line. System condition is also estimated using the prefault data. Impedance offered by the MOV is computed using an iterative process to generate the boundary for any system condition. The performance of the method is tested for various compensation level, system operating condition and compensation at different location of the line. Two source equivalent 400 kV system is considered to test the proposed method and results show the proposed method works properly for all system condition.

1.5.4 Secured Zone 3 Protection During Load Encroachment using Synchrophasor Data

Conventional backup protection, in particular, zone 3 of distance relay takes decision based on local measurements and has limitation to distinguish a fault from heavy load. To prevent maloperation of zone 3 relay load encroachment functions are applied, which are based on fixed power factor. At times, during heavy reactive loading the power factor change is beyond the expected value and load encroachment function also maloperates. Such maloperation during heavy loading condition may lead blackout of the system.

The recent development in communication, information and computer network has drawn significant attention for the use of synchronised wide-area measurement for secure and reliable power system protection. Communication latency makes such technology viable mainly for improving the slower form protection functions. As zone 3 takes decision with a time delay WAMS based voltage data are applied during load encroachment. During a disturbance, the ratio of change in voltage magnitude and phase angle of selected buses is computed to discriminate load encroachment from three phase fault thus supplementing zone 3 protection. New England 39 bus and IEEE 118 bus systems are used to test the algorithm and results show high accuracy.

1.5.5 Overall Contribution in Adaptive Relay Setting

Adaptive protection can be applied to improve both the dependability and security of the relay. In the thesis data from both ends of the line and the system data are applied to improve both dependability and security. However relay decision can be enhanced according to the system operating condition using additional information or changing the setting of the relay. Relay decision may be instantaneous which provides primary protection or a delayed decision to provide backup as in case of Zone 2 and Zone 3 of distance relay as shown in Fig 1.1. However both end data based technique like alpha plane method and DUTT scheme provides decision without any time delay. Information with data synchronization gathered at central location called as Phasor data concentrator (PDC) or available to the relay, can fetch accurate system condition which can be applied for both instantaneous and delayed protection schemes as shown in the figure 1.1.

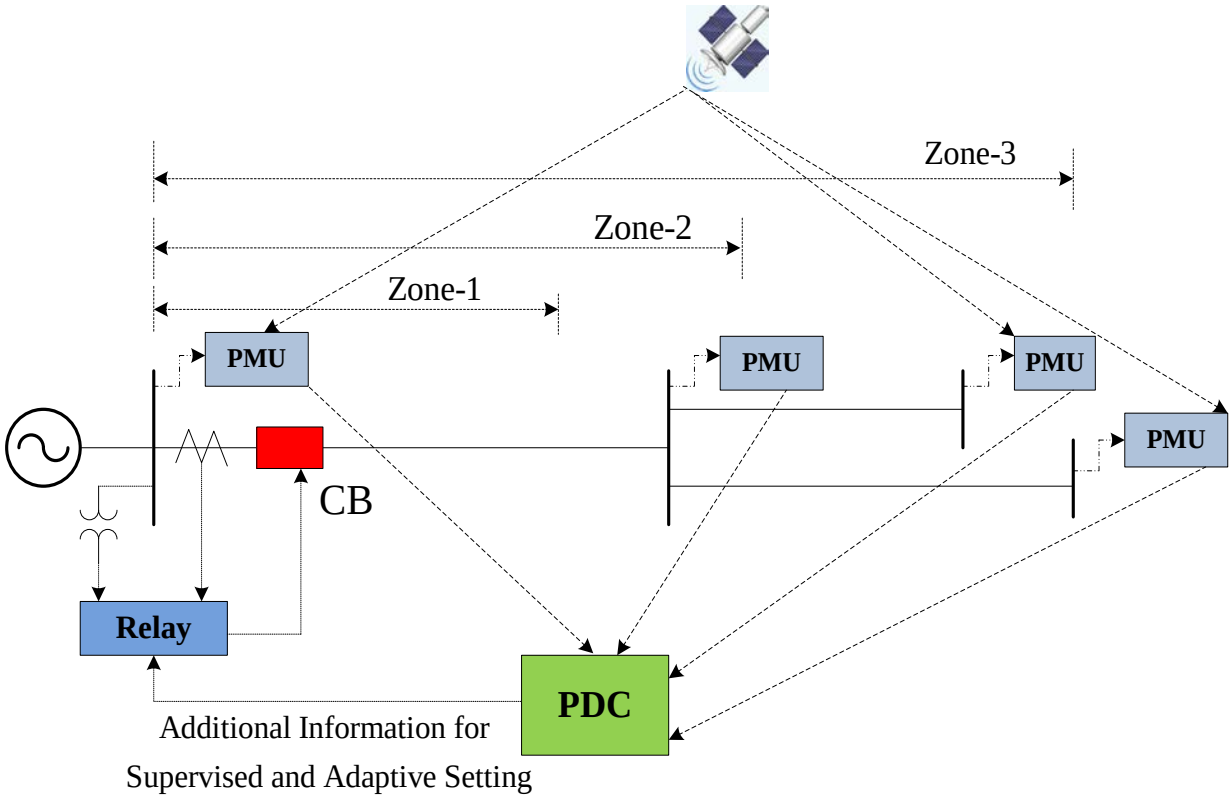

Fig. 1.1. Adaptive protection scheme using synchronized data .

In the first two chapters adaptive setting of faster protection scheme was sought. In alpha plane method an additional feature phase between voltage and current at both ends of the line is considered to support the relay decision. However the decision was taken based on the data during fault. In the second chapter adaptive DUTT scheme using synchronized data is proposed where infeed current for three phase fault is computed using prefault synchronized data. The settings were changed according to the data collected at the central location and information was send to the relay to change the setting. During fault only decision of the relays are shared as in the conventional scheme.

In the next two chapters, backup protection (zone 2and zone 3) is enhanced using synchronized data. Both ends synchronized voltage and current data are applied to compute the compensation level and adapt the relay setting. In the last chapter voltage form the synchophasors form selected busses are applied to discriminate three phase fault from load encroachment.

1.6 Major Contributions from the Thesis Work

The important contributions from the thesis are summarized below.

(i) Performance of phase current based alpha plane relaying is compromised during high resistance fault. An enhanced algorithm is proposed using the change in current magnitude at both ends of the line and angle deviation from the pre fault voltage to improve the performance of alpha plane relay using phase currents during high resistance fault.

(ii) The infeed current changes according to the system condition. The prefault system voltages obtained from the synchronised voltage and current measurements from all three terminal are considered to find out the overlappings between the zone 1 elements. If the any overlapping does not exist the adaptive setting is invoked at that condition.

(iii) The level of compensation of the series compensated line changes at times due its overvoltage protecting device and its maintenance purpose. When the compensation

level changes the setting of the zone 2 and zone 3 are adapted after calculating the compensation level using synchronised data from both ends of the line.

(iv) Conventional backup protection acts using local information. With only local measurements such scheme may maloperate during load encroachment. This may lead to cascade tripping and accelerate system collapse. Voltages collected from selected buses through a WAMS are applied to derive an index which discriminates fault from load encroachment and thereby better line protection is achieved.

1.7 Thesis Organization

The work carried out in this thesis has been presented in six chapters. The present chapter discusses few basic concepts and technical issues for power transmission protection. It presents state-of-the-art survey on the subject and sets the motivation behind the work related to distance relaying of different power networks under different system conditions.

Chapter-2 investigates the problem with the alpha plane protection schemes. A phase current based scheme is proposed using additional information on phase angle from both ends of the line, which improves the performance during high resistance fault.

Chapter-3 brings out the detail development of adaptive DUTT scheme for three terminal Line. Using the synchronized data from three ends of the line, the operating conditions at which DUTT scheme loses its dependability is found and latter the setting are changed to prevent such maloperation. This also provides how the proposed adaptive method is better than the conventional DUTT, POTT and differential protection schemes.

Chapter-4 provides adaptive backup protection of series compensated line is achieved using synchronized data from both ends of the line. The compensation level is computed using the prefault data and the system condition is computed with previously computed source impedances. Using the prefault system data the fault current through the MOV is computed and the equivalent impedance offered by MOV is computed and considered in the setting of the characteristic of the distance relay

In Chapter-5 a secured zone 3 method is presented using WAMS data. During load encroachment wide area measurement based voltage data are used. During a disturbance,

the ratio of change in voltage magnitude and phase angle of selected buses is computed to discriminate load encroachment from 3-phase fault thus supplementing zone 3 protection.

Chapter-6 concludes the important findings of the work presented in the thesis and suggests few areas for the future research.

Adaptive Alpha Plane Transmission Line Protection

Alpha plane based relay protecting a transmission line uses the ratio of the current phasors of both ends and has numerous advantages. Such an approach either uses phase or sequence components of currents. For a normal operating condition and external fault, the ratio remains within restraining region in the alpha plane. During high resistance internal fault, the computed ratio at times lies inside the restraining region resulting misoperation of the technique. The scheme which uses sequence components of the currents has limited performance for single pole tripping and line impedance unbalance conditions. In this work, two features; phase angle between voltage and current and magnitude of change in currents of both ends of the line supplement the relay in identifying an internal fault. This improves the performance of phase current based alpha plane relay. The proposed method is tested for WSCC-9 bus system and results for various cases show improved performance.

2.1 Introduction

Modern power system networks are not free from blackouts. Postmortem analysis of several blackouts reveals the main cause behind such events is failure of conventional relays, that use local data, in discriminating fault and heavy loading conditions [1]-[11]. With microwave and fiber-optic communications [21]-[28], protection schemes using both end data are sought to improve the security. Such schemes have inherent immunity

to power swing, mutual coupling and series impedance unbalance [29]. Both end current based schemes have advantage over voltage dependent directional comparison scheme due to the effect of CCVT transient on the latter. Convectional current differential schemes have limited performance during CT saturation for external fault.

In [39]-[40], alpha plane (α-plane) approach is introduced that uses ratio of both end current phasors and has advantages such as, tolerance to CT saturation and synchronization error. The scheme uses both sequence and phase currents in decision process. However phase current based scheme loses sensitivity due to outfeed during high resistance fault under heavy loading and weak source condition. Performance of relay has improved a lot for such conditions while sequence currents are considered as inputs [41]. However, its performance is compromised for single pole condition [42]-[43]. In [44], both sequence and phase currents are combined to improve the sensitivity of alpha plane principle, which demands increased communication channel.

In this work, an adaptive alpha plane relaying scheme using phase current is proposed which improves the performance for high resistance fault; unbalance caused by MOV operation in series compensated line and single pole operation. The phase angle between the voltage and current and magnitude of change in current of both ends are utilized for protection decision in the scheme when the trajectory in the alpha plane lies in an overlapping region accommodating both internal faults with high resistance and external fault with CT saturation. The proposed method is tested for several operating conditions for a two source equivalent system and WSCC 9 bus system with and without series compensation.

2.2 Alpha Plane Characteristic for Line Protection

A two bus power system as shown in Fig. 2.1 is considered to describe current based alpha plane scheme. For any operating condition, using both end current phasors ($\dot{I}_{\mathrm{L}}$and $\dot{I}_{\mathrm{R}}$) the current ratio (CR) is obtained as [39],

$$\mathrm{CR} = ke^{j\alpha} = \frac{\dot{I}_R}{\dot{I}_L} \tag{2.1}$$

Where k is the magnitude ratio and α is the phase angle difference between the currents. It is to be noted that the currents for the above relation can be either using individual phase current or any sequence currents. The generalized alpha plane characteristic is provided in Fig. 2.2.

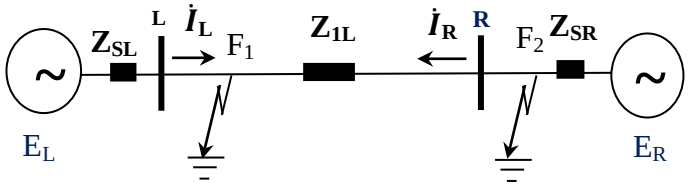

Fig. 2.1. Two source equivalent system.

During normal operating condition and for external fault the CR remains within the restraining region in the alpha plane. An internal fault is ensured when CR moves into the operating region. The boundary of the restraining region is defined as: the radius of arc k (typically between 5 and 10) and the angle α (typically between 160˚ to 210˚) [39]. Phase current based alpha plane relay with k=5 and α =210°, which bounds region 1 and 2 has inherent immunity to relay maloperation caused by communication delay, channel asymmetry and CT saturation.

Consider a line-to-ground fault with fault resistance of 0.1 Ω at 5 km from R bus on the 350 km line LR. For the case, the ratio CR is found in the operating region as shown in Fig. 2.2 (F_0). When the fault resistance is increased CR moves towards the restraining region and with R_F=130 Ω, CR is found at F_1 which is in the restraining region of the alpha plane and relay will interpret it as an external fault situation. If fault resistance is increased further, internal high resistance fault occurring close to R bus, the CR lies in the portions around the real axis as shown in the Fig. 2.2. To improve the sensitivity for high resistance fault, a smaller region (region 1) as shaded, is selected with $0.8 \leq k \leq 2.5$ and α =120° [44]. For external fault with CT saturation or channel asymmetry or communication delay, the CR remains in an extended portion; region 2 as marked in Fig. 2.2 and is outside region 1. However for high resistance internal fault, the CR lies in this region. To overcome this conflict more discriminating functions are required. It is to be noted that region 1 ensures no internal fault; a clear restraining region.

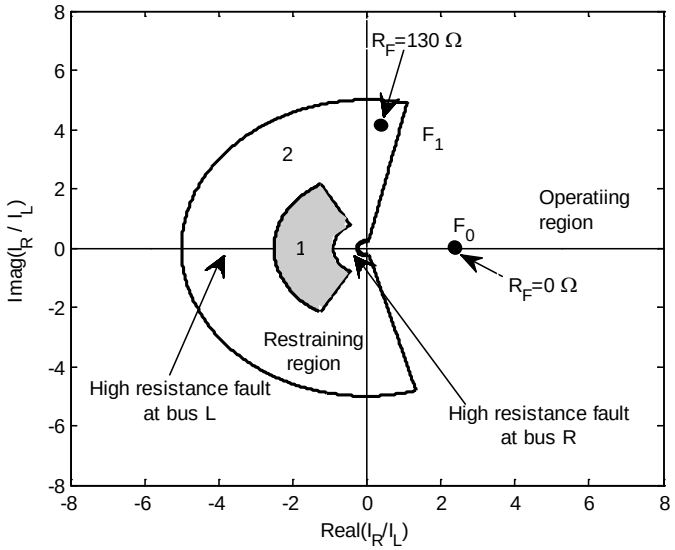

Fig. 2.2.Alpha plane characteristic showing operating and restraining regions.

2.3 Characteristic of high Resistance Fault

A high resistance fault results when an energized primary conductor comes in contact with a quasi-insulating object such as a tree, structure or equipment, or falls to the ground. Such undetectable high resistance fault poses a serious public safety hazard as well as a risk of arcing ignition of fires. A high resistance fault is characterized by having an resistance sufficiently high that it is not detected by conventional overcurrent protection, such as fuses and overcurrent relays. Unlike low impedance short circuits, which involve relatively large fault currents and are readily detectable by conventional overcurrent protection, these high resistance fault represent little threat of damage to power system equipment. High impedance faults produce current levels in the 0 to 50 ampere range. Typically, an high resistance fault exhibits arcing and flashing at the point of contact.

However the resistance of the fault is in the range of kilo Ohms. The maximum impedance can occur for tree touching the live wire is 100 kΩ.However for downed conductor it may increase up to 225 kΩ [133]. In addition to the low current magnitude and accompanied arc, the HIF results in several physical and electrical characteristics[134]-[135].

i) **Intermittence of the arc**: the arc does not generate current in a steady state pattern, instead it generates a few conduction cycles followed by several non-conduction cycles

ii) **Asymmetry in the current waveform**: due to difference in the break-down voltage against positive and negative voltage values, there is a difference between the peak value and shape of positive and negative half cycles of HIF current.

iii) **Current buildup and shoulder:** current magnitude gradually escalates (builds up) until it reaches and maintains a constant value for several cycles (shoulder).

iv) **Non-stationary Current:** the current frequency spectrum varies with time..

v) **Randomness:** Both the current magnitude and its conduction/non R conduction intervals are random values.

vi) **Non-linearity:** voltage–current characteristic of the HIF is non-linear due to the existence of the arc..

vii) **Low frequency components in current and voltage wave-forms:** due to non-linearity of HIF the waveforms contain harmonics up to 600 Hz for the current and up to 300 Hz for voltage..

viii) **High frequency components in current waveforms**: arc results in high frequency components in the current waveform.. including:

Typical results of staged faults at two different test sites for a typical 12.5 kV feeder are provided below in Table 2.1.

Table 2.1 Fault current for different surfaces

Surface	Current (A)
Dry asphalt	0
Concrete (non-reinforced)	0
Dry sand	0
Wet sand	15
Dry sod	20
Dry grass	25
Wet sod	40
Wet grass	50
Concrete (reinforced)	75

In this work both ends voltage current are applied to detect the internal high resistance fault.

2.4 Phase change during Fault

The source voltages at bus L and R as shown in Fig. 2.1, at any operating condition can be expressed as

$$he^{-j\delta} = \frac{\dot{\mathrm{E}}_{\mathrm{R}}}{\dot{\mathrm{E}}_{\mathrm{L}}} \tag{2.2}$$

where *h* is the magnitude ratio and δ is the angle difference. The prefault voltage of S bus can be expressed as,

$$\dot{V}_{\mathrm{pre}} = \dot{\mathrm{E}}_{\mathrm{L}} - \dot{\mathrm{I}}_{\mathrm{SL}}\mathrm{Z}_{\mathrm{SL}} - \dot{\mathrm{I}}_{\mathrm{pre}}\mathrm{Z}_{1\mathrm{L}} \tag{2.3}$$

where $\dot{\mathrm{I}}_{\mathrm{SL}}$ is the prefault current at bus. Using prefault voltage the fault current for a line-to-ground fault at F_2 in the Fig. 2.1 with a resistance R_F can be formulated as [126],

$$\dot{\mathrm{I}}_{\mathrm{F}} = \frac{\dot{V}_{\mathrm{pre}}}{Z_{\mathrm{SUM}} + 3\mathrm{R}_{\mathrm{F}}} \tag{2.4}$$

where,

$$\mathrm{Z}_{\mathrm{sum}} = 2\frac{\mathrm{Z}_{1\mathrm{L}}\mathrm{Z}_{1\mathrm{R}}}{\mathrm{Z}_{1\mathrm{L}}+\mathrm{Z}_{1\mathrm{R}}} + \frac{\mathrm{Z}_{0\mathrm{L}}\mathrm{Z}_{0\mathrm{R}}}{\mathrm{Z}_{0\mathrm{L}}+\mathrm{Z}_{0\mathrm{R}}}$$

$\mathrm{Z}_{1\mathrm{L}}, \mathrm{Z}_{1\mathrm{R}}, \mathrm{Z}_{0\mathrm{L}}$ and $\mathrm{Z}_{0\mathrm{R}}$are the Thevenin's impedances at fault point. The sequence currents through the line can be obtained as,

$$\dot{\mathrm{I}}_{1L} = \mathrm{w}_1\mathrm{w}_{11}\dot{\mathrm{I}}_{\mathrm{F}} \ , \dot{\mathrm{I}}_{0L} = \mathrm{w}_0\mathrm{w}_{10}\dot{\mathrm{I}}_{\mathrm{F}} \tag{2.5}$$

where,

$$\mathrm{w}_1 = \frac{\mathrm{Z}_{1\mathrm{L}}}{\mathrm{Z}_{1\mathrm{L}}+\mathrm{Z}_{1\mathrm{R}}}, \mathrm{w}_0 = \frac{\mathrm{Z}_{0\mathrm{L}}}{\mathrm{Z}_{0\mathrm{L}}+\mathrm{Z}_{10}}$$

and

$$\mathrm{w}_{11} = \frac{\mathrm{Z}_{\mathrm{C}}}{\mathrm{Z}_{\mathrm{C}}+\mathrm{Z}_{\mathrm{T}}}, \mathrm{w}_{01} = \frac{\mathrm{Z}_{0\mathrm{C}}}{\mathrm{Z}_{0\mathrm{C}}+\mathrm{Z}_{\mathrm{T0}}}$$

where Z_{T} and $\mathrm{Z}_{0\mathrm{T}}$ are the positive and zero sequence Thevenin's impedance looking towards the bus L.Z_{C} and $\mathrm{Z}_{0\mathrm{C}}$ are the positive and zero sequence impedances of the shunt capacitance.

The fault current at L and R bus can be computed as,

$$\dot{I}_L = \dot{I}_{1L} + \dot{I}_{2L} + \dot{I}_{0L} + \dot{I}_{pre} \tag{2.6}$$

$$\dot{I}_R = \dot{I}_{1L} + \dot{I}_{0L} + \dot{I}_{2L} - \dot{I}_{pre} \tag{2.7}$$

where nullifying the prefault shunt current the current can be represented as,

$$I_L = \left[2w_1 w_{11} + w_0 w_{10}\left[1 - \frac{Z_{1L} + Z_{SL}}{Z_{1L} + Z_{SL} + Z_{SR}}\left(1 - he^{-j\delta}\right)\right] + \frac{\left(1 - he^{-j\delta}\right)}{Z_{1L} + Z_{SL} + Z_{SR}}\right] E_L$$

Similarly, the voltage at the bus relay can be expressed as,

$$V_{aL} = 3R_F\dot{I}_F + \left(2\dot{I}_{1L} + \dot{I}_{pre}\right)Z_{1L} + \dot{I}_{0L}Z_{0L} \tag{2.8}$$

For the line-to-ground fault with a fault resistane of 0 Ω, the voltage can be respresented as,

$$V_{aL} = \left[2w_1 w_{11} Z_{1L} + w_0 w_{10} Z_{0L}\left[1 - \frac{Z_{1L} + Z_{SL}}{Z_{1L} + Z_{SL} + Z_{SR}}\left(1 - he^{-j\delta}\right)\right] + \frac{Z_{1L}\left(1 - he^{-j\delta}\right)}{Z_{1L} + Z_{SL} + Z_{SR}}\right] E_L$$

Expressing $I_L = a + jb$ and $V_{aL} = c + jd$, the phase angle between volatge and current can be represnted as

$$\emptyset = tan^{-1}\left(\frac{b}{a}\right) - tan^{-1}\left(\frac{d}{c}\right)$$

where $\emptyset$ can be expressed as a function $f(h, \delta, Z_{1L}, Z_{SL}, Z_{SR}, Z_C)$

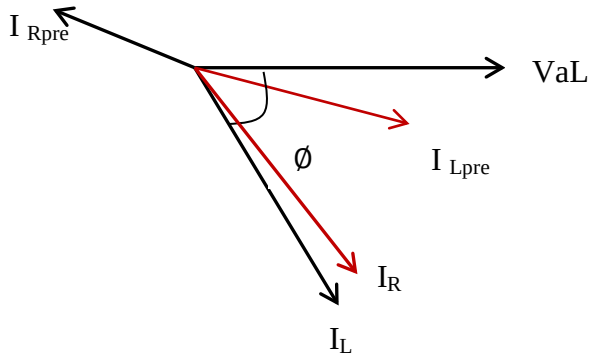

Fig. 2.3. Phase angle between voltage and current during fault and normal operating condition.

The phase angle between voltage and current can also be observed from the Fig. 2.3. Before the fault the prefault current lags with the power factor angle and during fault the angle increases to 70°-80° which is equal to line impedance angle. However as the fault resistance increases the angle decreases.

2.5 Proposed Adaptive Technique

For low resistance ground fault, the phase angle between the voltage and current is nearly to the transmission line impedance angle. As the fault resistance increases this angle decreases. To improve the performance of the alpha plane relay using phase currents, during high resistance internal fault (when CR lies in region 2) an additional feature, angle between voltage and current is first selected. During a fault, the angle deviation from transmission line impedance angle (θ) is obtained at both ends

$$\emptyset_1 = |\theta - \emptyset_{\mathrm{L}}|$$

$$\emptyset_2 = |\theta - \emptyset_{\mathrm{R}}| \tag{2.9}$$

where$\theta = \tan^{-1}\left(\frac{\mathrm{x}}{\mathrm{r}}\right)$ with x and r are transmission line reactance and resistance per kilometer respectively. $\emptyset_{\mathrm{L}}$and $\emptyset_{\mathrm{R}}$ are the angles between the voltage and current at L and R sides respectively. It is to be noted that $\emptyset_1$ and $\emptyset_2$are high for high fault resistance cases ($\emptyset_{\mathrm{L}}$ and $\emptyset_{\mathrm{R}}$ being small). This feature clearly identifies a high resistance fault when CR is in region-2 and thus useful in distinguishing the condition from CT saturation etc.

The angles $\emptyset_1$and $\emptyset_2$ for both internal and external high resistance faults is similar. For any external fault or load change, the magnitude of change in current at both ends of the line is equal. This feature is used to differentiate the internal and external high resistance faults. A feature for this is defined as,

$$\Delta \mathrm{i}^{\mathrm{a}}_{\mathrm{diff}} = \left|\Delta I^{\mathrm{a}}_{R}\right| - \left|\Delta I^{\mathrm{a}}_{L}\right| \tag{2.10}$$

where the change in currents

$$\Delta \mathrm{i}^{\mathrm{a}}_{\mathrm{R}} = \mathrm{i}^{\mathrm{a}}_{\mathrm{Rfault}} - \mathrm{i}^{\mathrm{a}}_{\mathrm{Rpre}}$$

$$\Delta \mathrm{i}^{\mathrm{a}}_{\mathrm{L}} = \mathrm{i}^{\mathrm{a}}_{\mathrm{Lfault}} - \mathrm{i}^{\mathrm{a}}_{\mathrm{Lpre}}$$

Similarly it can be computed for b and c phases. During external high resistance fault $\emptyset_1$ and $\emptyset_2$will be high but $\Delta \mathrm{I}_{\mathrm{diff}}$ will be small. On the other hand for internal high resistance

fault $\emptyset_1, \emptyset_2$ will be high and ΔI_{diff} will be also high. Both the features are combined to ensure detection of internal high resistance fault whenever the CR lies in restraining region 2. To identify internal fault when CR is in region-2 an index K_1 is defined as,

$$K_1 = \begin{cases} 1 & \text{if } \Delta I_{diff} > \zeta \text{and } \emptyset_{min} > \emptyset_{th} \\ 0 & \text{if } \Delta I_{diff} > \zeta \text{ and } \emptyset_{min} < \emptyset_{th} \end{cases} \quad (2.11)$$

Where $\emptyset_{min} = \min(\emptyset_1, \emptyset_2)$, $\emptyset_{th}$ and ζ are thresholds selected considering possible operating conditions. During a high resistance fault when the CR lies in restraining region-2, K_1=1 and the proposed method concludes an internal fault. Thus using the system condition information the decision is derived incase the trajectory in region-2.

2.4.1 Threshold selection for ΔI_{diff}

For internal fault ΔI_{diff} is very high and for an external fault it is negligible (without CT saturation). Shunt capacitance may cause difference in current magnitude at both ends but is be of negligible effect on change in current. There may be difference in current during normal loading condition due to CT error but this will be small. These are considered in threshold setting to discriminate high resistance internal fault to load change. Considering 2 % error for C class protection CT at both ends and to provide a secured operation, a threshold ζ is selected as 0.08 pu. Thus by this normal condition are filtered out except CT saturation during external fault.

2.4.2 Threshold selection $\emptyset_{th}$

Angle deviates for high resistance fault and for CT saturation [46]. The scheme finds problem during CT saturation. To differentiate CT saturation from internal high resistance fault minimum of $\emptyset_1, \emptyset_2$ is considered. Minimum change for line-to-ground fault is observed for R_F=0 and it also depends on system condition and parameters are derived in the previous section. To select the threshold for $\emptyset_{min}$, a line-to-ground fault with R_F=0 at one end of the line is considered (Fig. 2.1).

Considering an external line-to-ground fault with R_F=0 at F_2 for the two source equivalent system as in Fig. 2.1, the phase angle deviation is observed at bus L. The phase angle between a-phase voltage V_{aL} and line current I_L is computed for different prefault loading conditions. To observe the effect of source impedance variation on phase

angle between voltage and current, the source impedance at one end is varied for the maximum possible change in source impedance from 0.2 pu. to 2 pu [128]. The variation of $\emptyset_1$ is plotted in Fig.2.3 (a) and the maximum value is found to be 0.362 rad. Similarly the maximum deviation of angle is observed for h and δ (magnitude ratio and angle difference of source voltages at two busses) which is plotted in Fig. 2.4 (b) and (c). The h is varied from 0.9-1.1 pu. and δ is varied form 0-0.61 rad [128]. The maximum deviation of ∅ at L bus for h and δ variations is found to be 0.362 and 0.4178 rad respectively. It depicts that variation in $\emptyset_1$ is mostly for the changes in h and δ. With these values for heavy loading condition and from all above observations the threshold $\emptyset_{th}$ is selected as 0.436 rad.

2.4.3 Steps for computation of Proposed Method

In this method to obtain improved performance of current based alpha plane scheme two features are selected depending on system condition. The different steps of the proposed method are given in the following steps

Step 1 : Current ratio is calculated using (2.1).

Step 2 : If the ratio lies inside region-1, the relay is blocked.

Step 3 :(a) When the ratio lies inside the restraining region 2, $|\Delta \dot{I}_R|$ and $|\Delta \dot{I}_L|$ for all three phases are computed, followed by calculation of ΔI_{diff}.

(b) If $\Delta I_{diff} > \zeta$ then Φ_{min} is calculated using $\emptyset_1$ and $\emptyset_2$.

(c) Whenever $\Delta I_{diff} > \zeta$ and $\Phi_{min} > \Phi_{th}$, K_1 is set as 1 ensuring the internal fault case.

Step 4: When the ratio is beyond region-1 it is an internal fault and $K_1 = 1$.

The flow diagram of the proposed technique is provided in the Fig. 2.5. The inputs to the proposed technique are the voltage and current data form both ends of the line. Using both end current information the ratio as in (2.1) is computed and the phase angle between voltage and current at both ends of the line is computed as additional feature is selected. Region 1 is secured region where help of additional is not required. However, when the current ratio present in the region 2, additional features are checked and for $K_1=1$ according to (2.11) internal high resistance fault is detected. This also improves the maloperation during CT saturation.

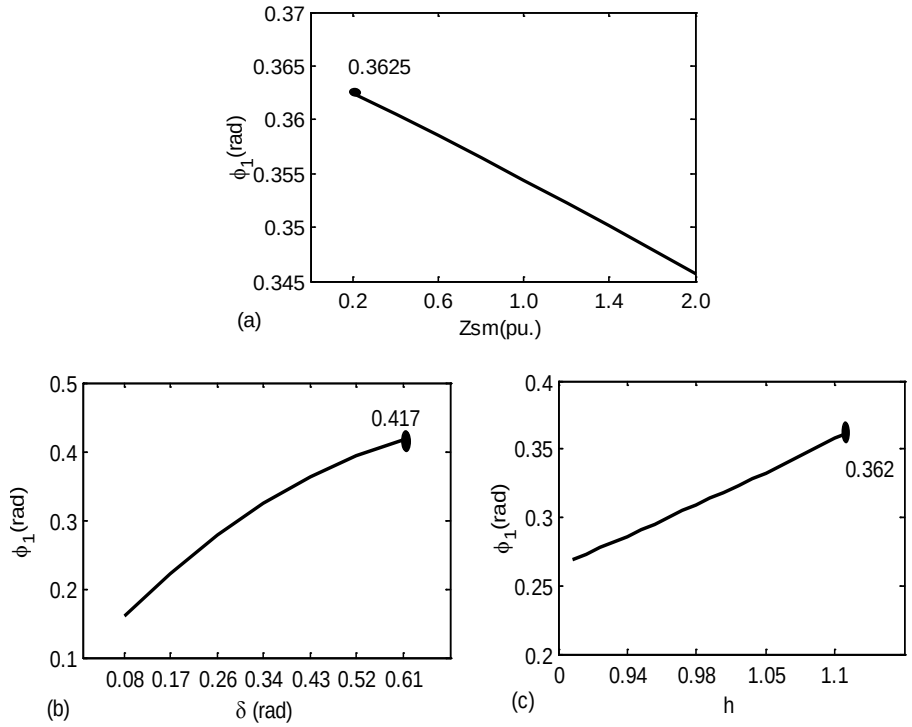

Fig. 2.4. Change in phase angle for line-to-ground fault with R_F= 0 Ω with (a) source impedance variation. (b) δ variation (c) voltage magnitude variation.

2.6 Results

230 kV, 50 Hz 9-bus WSCC system as shown in Fig. 2.6 is used to test the effectiveness of the proposed method. The line connected between bus 4 and bus 5 are selected. For testing the algorithm simulations are carried out using EMTDC/PSCAD for various system conditions such as internal and external high resistance line-to-ground faults, CT saturation and load increment. The method is also tested for series compensated line for different compensation level and compensation present at different position of the line. Fault resistance at both ends of the line is varied and performance of the checked. Few results are provided in this section. Comparison with previously existing method is also provided in this section. For all the cases the phase angle between the voltage and current at buses 5 and 4 are denoted as $\emptyset_1$ and $\emptyset_2$ respectively. Current phasors are obtained by using one cycle discrete Fourier transform (DFT). Data sampling rate is maintained at 1 kHz. Phasor data are collected at 50 frames per second from the other end for the 50 Hz system.

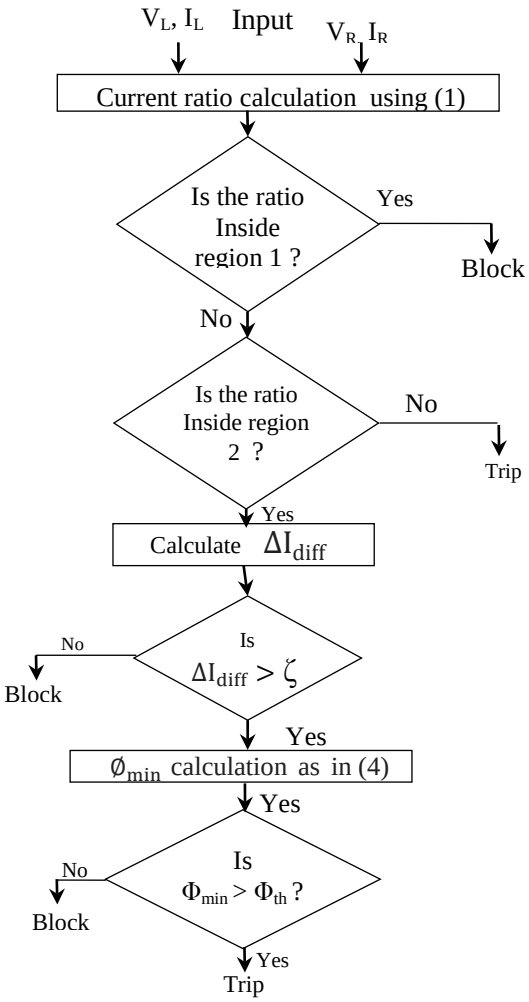

Fig. 2.5. Flow diagram for proposed Technique

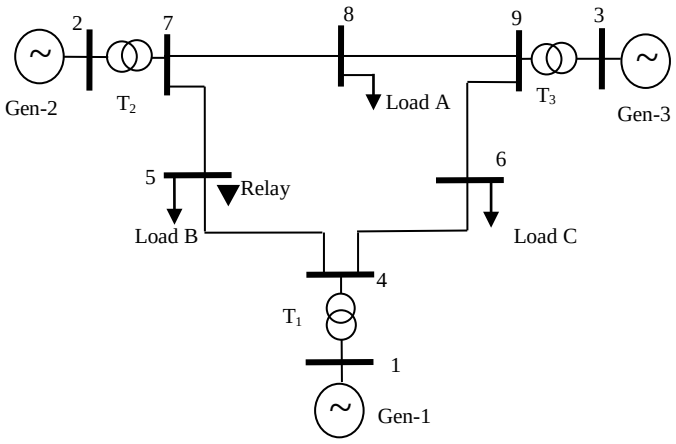

Fig. 2.6. WSCC 9-bus system for testing alpha plane relay at bus 5 for line 5-4.

2.6.1 Test for Internal High Resistance Line-to-ground fault

The performance of the proposed method is tested for an internal high resistance fault. In the prefault condition power flows from bus 5 to bus 4. A line-to-ground fault at 5 km from bus-4 with R_F =200Ω, in line 5-4, is created at 1.0 s. The current ratio (CR) is calculated using (2.1) and plotted in Fig. 2.7. From the figure, it is observed that before fault the current ratio was inside restraining region 1. outside the restraining region 1 but inside the region 2. The conventional alpha plane relay will send a block signal for this internal fault. During this period current phasors obtained from both ends are applied to compute ΔI_{diff} using (2.10) and plotted in Fig. 2.7 & (a).With $\Delta I_{diff} > \zeta$, angle deviations between voltage and current is calculated for each end and plotted in Fig. 2.6 (b). The minimum of both the angles is obtained and plotted in the Fig.2. 6 (c). The index K_1 is obtained using (4) and plotted in Fig. 2.7(d). With K_1=1 for the case, an internal fault is confirmed which is correct. The proposed scheme provides a correct decision where the conventional alpha plane fails during high resistance internal fault (Fig. 2. 7).

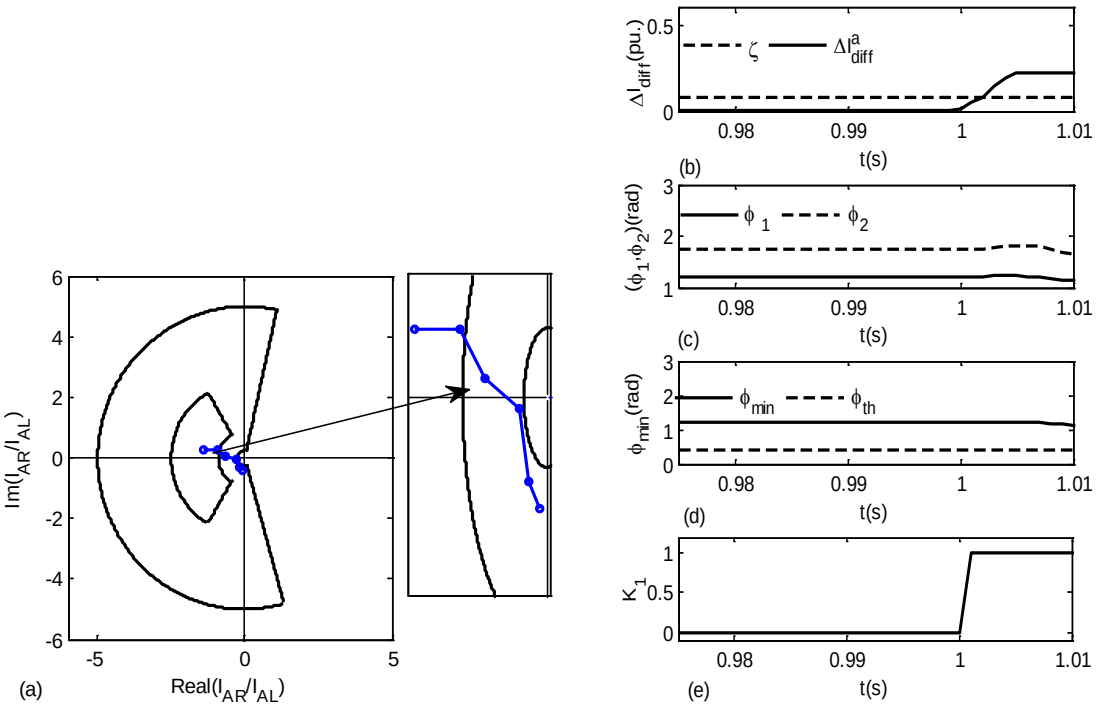

Fig. 2.7. Result for internal line-to-ground fault with R_F = 200 Ω. (a) alpha plane characteristic (b) ΔI_{diff} (c) $\emptyset_1$ and $\emptyset_2$ in rad (d) $\emptyset_{min}$ in rad (e) index K_1.

2.6.2 Test for external high resistance line-to-ground fault

The performance of the proposed method is tested for external high resistance fault. A line-to-ground fault with R_F =200 Ω is simulated at 5 km from the bus 5 on the line 5-7. Current ratio calculated for line 4-5 is plotted in Fig. 2.8 (a). The CR settles in region-2. ΔI_{diff} for this case is plotted in Fig. 2.8(b). From the figure it is noticed that $\Delta I_{diff} < \zeta$. The proposed method will remain silent to this situation which is correct. Both the conventional alpha plane and proposed schemes provide the correct decision for this case.

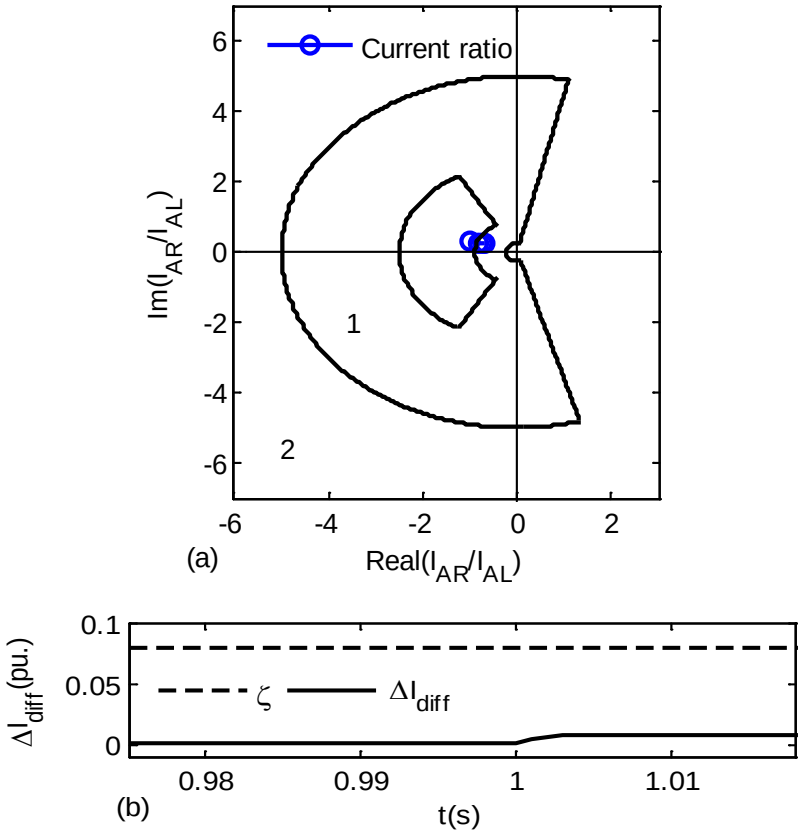

Fig. 2.8. Result for external line-to- ground fault with R_F = 200 Ω (a) alpha plane characteristic (b ΔI_{diff} in pu.

2.6.3 Test for CT Saturation with external fault

Differential relays protecting high voltage transmission line have limited performance for external fault with CT saturation. To test the performance of the proposed method for CT saturation, line 4-5 of the nine bus system in Fig. 2.5 is considered. With magnetization characteristic as in [117], the burden of CT at bus 4 is increased from 0.4 Ω

to 2.5 Ω. A three phase fault is created beyond bus 4(external fault). The CR is plotted in Fig. 2.8(a). It is observed that the CR moves out of region 1 and remains in region 2 as CT saturates. ΔI_{diff} is plotted in Fig. 2.7 (b) and Φ_{min} in Fig. 2.8 (d). From the figure it is observed that though $\Delta I_{diff} > \zeta$, $\Phi_{min} < \Phi_{th}$, and thus $K_1 = 0$.This concludes an external fault which is correct.

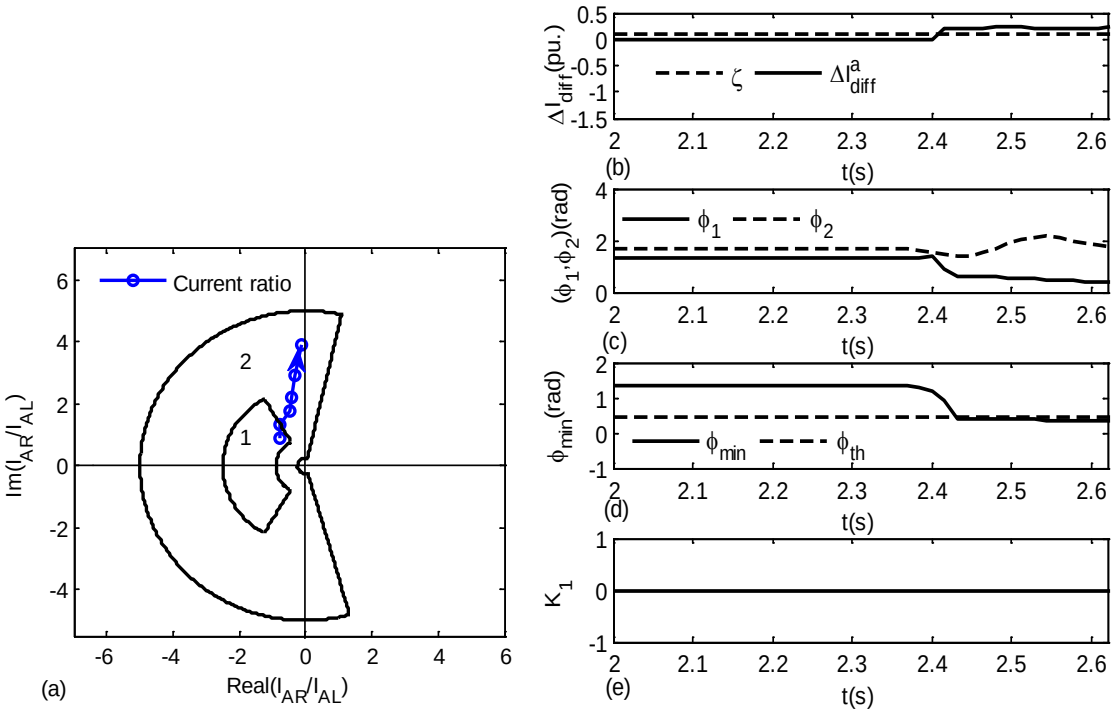

Fig. 2.9. Result for external fault three phase fault for CT saturation. (a) alphaplane characteristic (b) ΔI_{diff} in pu. (c) $\emptyset_1$ and $\emptyset_2$ in rad (d) $\emptyset_{min}$ in rad (e) index K_1 .

2.6.4 Test for Series Compensated Line.

Protection of series compensated line is challenging due to operation of its over-voltage protective devices (MOV and air-gap). The MOV operation depends on fault resistance, type of fault, prefault current and distance up to the fault point. MOV operation introduces asymmetry in the phase impedances [29] and computation of the sequence components becomes erroneous and therefore phase based approach as proposed in the method is advantageous. To test the accuracy of the proposed method a 40 % series compensation is considered in line 4-5, at bus 5 of Fig. 2.6. The rating of MOV is selected as in [117]. A line-to-ground fault with R_F =180 Ω, at 5 km from the bus 4 on the line 4-5 is created at

0.99s. As observed form Fig. 2.10 (a), CR remains inside region 2. ΔI_{diff} for a-phase is computed. From Fig. 2.10 (b), K_1=1 during the fault and the method identifies it as an internal fault which is correct.

The performance of the proposed method is tested for different compensation level at end and middle of the transmission line with line-to-ground fault of 200 Ω . Table. 2.2 depicts that the proposed method provides accurate decision for any compensation level at end of the line.

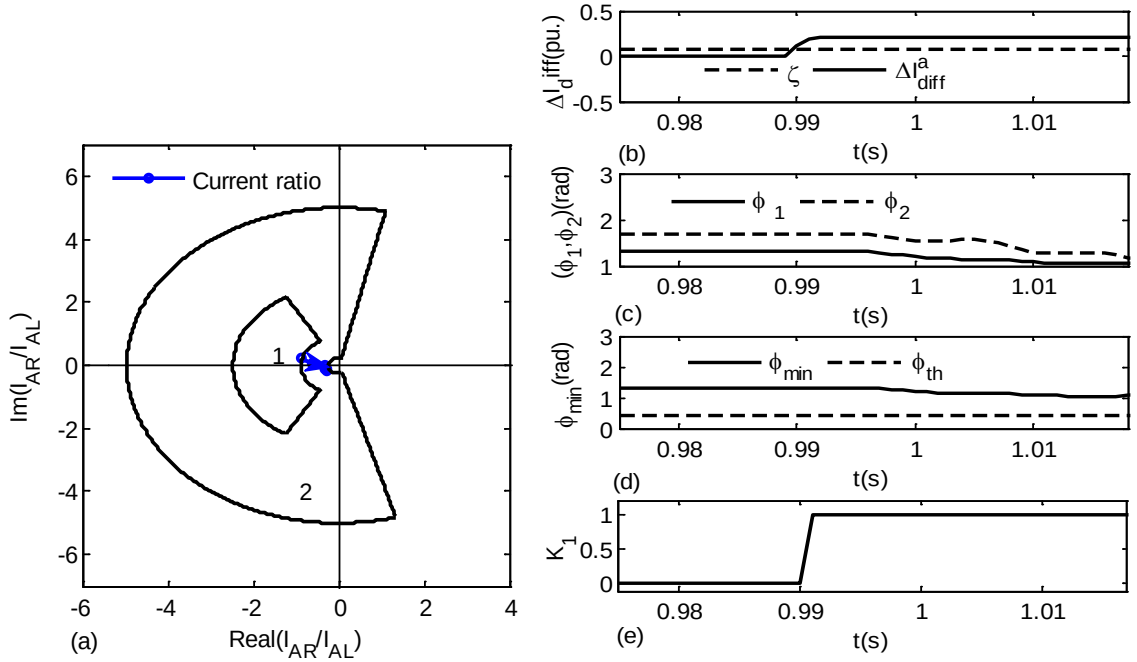

Fig. 2.10. Result for high resistance fault in series compensated line (a) alpha plane characteristic (b) ΔI_{diff} (c) Phase angle deviation at both ends. (d) Φmin (e) Index K_1.

Table 2.2
Performance of Proposed method for different Compensation levels at end of the line

Sl No	Position of the compensation	Percentage of the compensation	CR	Conventional method	Proposed Method		
					Indices		Decision
					ΔI_{diff} (pu)	Φ_{min} (rad)	
1	End of the Line	20%	3.58∠160°	Block	0.242	1.10	Trip
2		35%	3.25∠164°	Block	0.273	1.19	Trip
3		50%	2.48∠167°	Block	0.293	1.32	Trip
4	Mid of the line	20%	3.3∠160°	Block	0.23	1.34	Trip
5		35%	2.8∠165°	Block	0.237	1.23	Trip
6		50%	2.31∠167°	Block	0.239	1.03	Trip

2.6.5 Test for error due to Channel Equalization and Synchronization.

The communication channel delay produces an apparent phase shift between the data collected from both ends. The algorithm must compensate for the channel delay to prevent erroneous current ratio calculation. The level of asymmetry depends on the architecture of the communication system [123].

To test the performance of the proposed scheme for channel delay, a 4 ms channel delay is considered while receiving data (equivalent to 72° phase error). During normal operating condition the synchronized data are used for CR as plotted in Fig. 2.11 (a). It is observed that the ratio computed without any delay remains in the region 1, whereas with delayed data it is inside region 2. Presence of the CR in region 2 dose not confirm a healthy condition and requires additional information to check internal fault if any. This is achieved by calculating ΔI_{diff} and Φ_{min} which are provided in Fig. 2.11. (b) and (d) respectively. The index K_1=0 for this, which reveals no internal fault which is correct. The proposed method is correct for even for large synchronization error and is advantageous compared to the method in [117] with synchronized data.

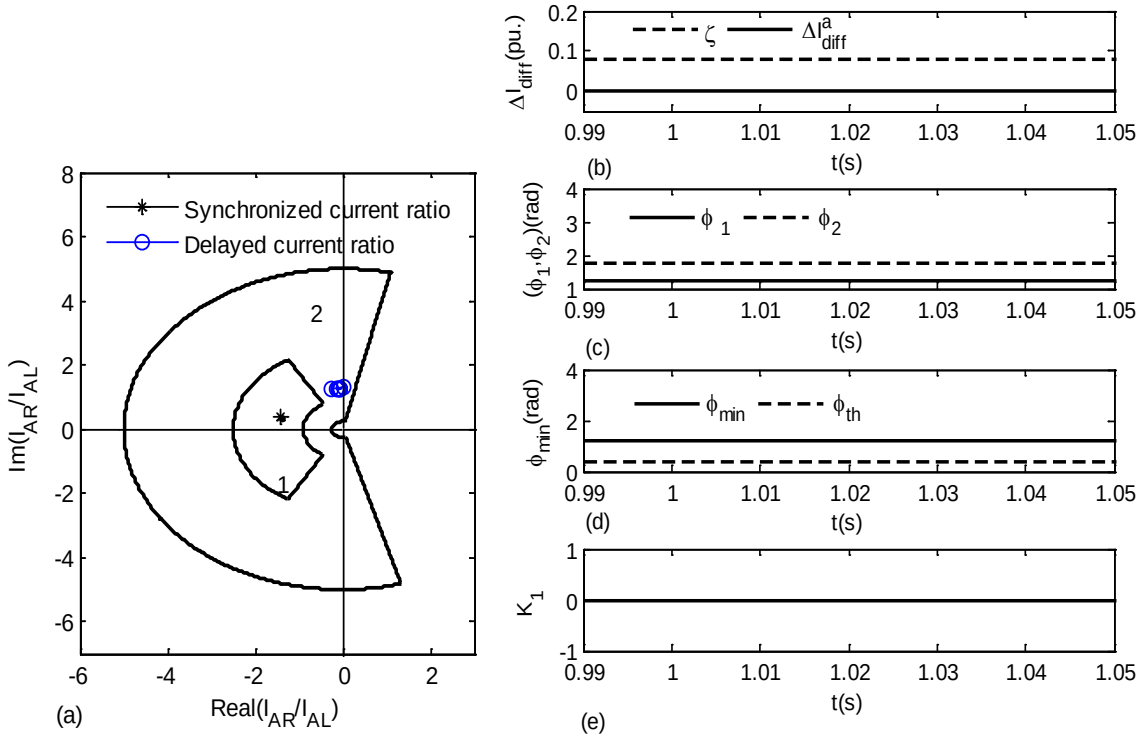

Fig. 2.11. Result for channel equalization error(a) alpha plane characteristic (b) ΔI_{diff} (c) Phase angle deviation at both ends. (d) Φmin .(e) Index K_1.

2.6.6 Performance of the proposed method during single pole operation

To test the performance of the proposed method during single pole operation phase-B of line 4-5 is tripped due to a fault at 1.0 s and the phase currents are shown in Fig. 2.12.The CRs for phase current, negative and zero sequence currents are plotted in alpha plane as shown in Fig. 2.12 (a). The CRs for negative and zero sequence currents settle outside the restraining region at t=1s with pole tripping in phase-B. This show alpha plane relay based on sequence currents will maloperate. The CR for phase-A current remains inside region-1.

During this period a line-to-ground fault with R_F=150 Ω at 1.05 s is created at 4 km from bus 4 and the locus of CR of phase currents are observed. The CR remains within the restraining region, which causes the maloperation of the conventional scheme. For this case, ΔI_{diff} andΦ_{min} are computed and K_1=1 consistently following fault as shown in Fig 2.12 (e). This confirms an internal fault which is correct. The proposed method performs correctly during single pole operation whereas method in [26] using negative sequence components may malfunction.

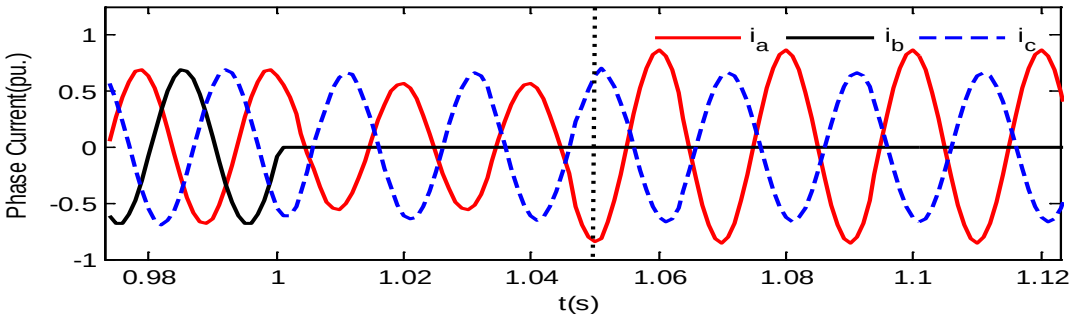

Fig. 2.12. Phase currents of line 4-5 during single pole tripping.

2.6.7 Test for different operating conditions

The performance of the proposed algorithm is verified for different operating conditions and different types of fault by using a two source equivalent system as shown in Fig.2.1 with the systems parameters as in Appendix C. All four types of fault is simulated at different location by varying the fault distance from relay end to end of the line with a system condition of h=1.1 and $\delta = 30°$. A few special cases such as line-to-line fault, three phase fault, high resistance line-to-ground and line-line-to-ground faults at end of the line and mid-point of the line are provided in the Table. 2.3. The current ratio (CR)

remains within the restraining region-2 of Fig. 2.1 for high resistance line-to-ground fault with fault resistance of 200 Ω and 450 Ω (refer Table 2.3), which causes maloperation of conventional method. However Table 2.3 depicts that indices proposed in this method, provide correct decision for all types of fault at different location of the line. For line-to-line and three phase fault the maximum fault resistance is considered as 10 Ω and for such cases the CR remains in the trip region, proposed indices are not computed as marked (NC) in the Table 2.3 and both methods operates correctly.

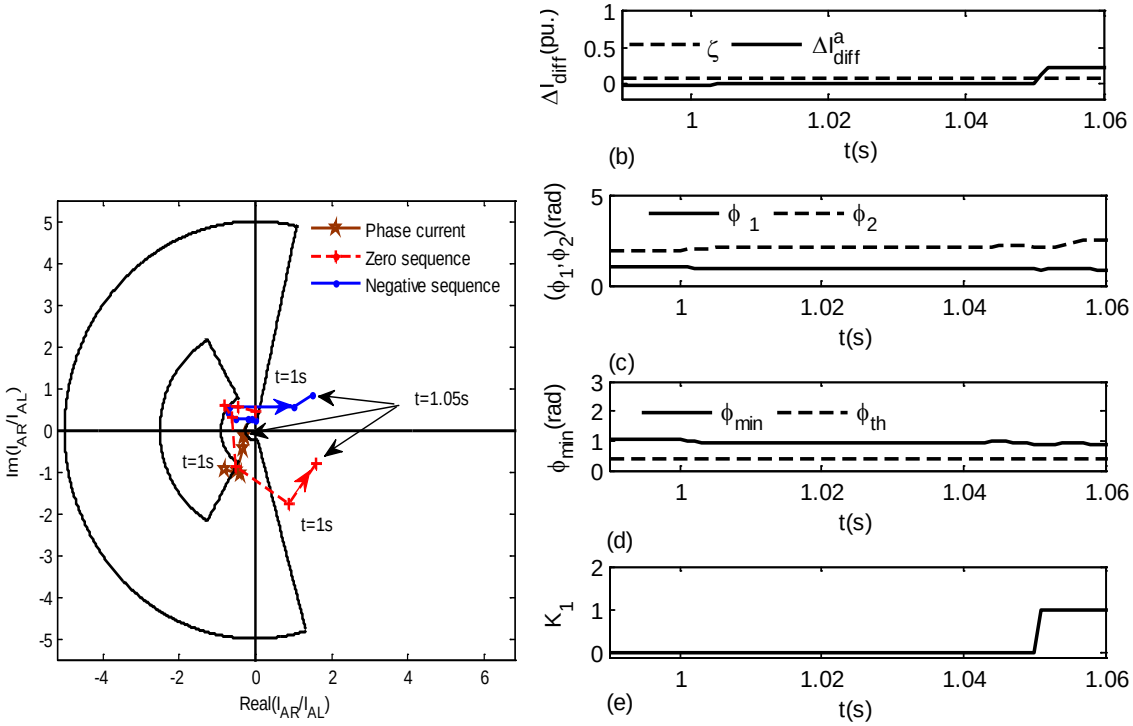

(a)

Fig. 2.13. Result for single pole tripping (a) alpha plane characteristic (b) ΔI_{diff} (c) Phase angle deviation at both ends. (d) Φmin .(e) Index K_1.

Another case is tested for different types of fault at the electrical center of the line. During normal loading conditions the current ratio for both low and high resistance fault at electrical center remains outside the restraining region and features are not required for the decision process. However for high resistance fault during heavy loading condition the current ratio remains inside the restraining region and features of the proposed schemes are helpful in providing correct decision.

Table 2.3
Comparative Assessment of proposed method for different types of internal fault, fault locations and fault resistances

Fault Distance	Fault Resistance (Ω)	Fault Type	CR	Conventional Method	Proposed Method		
					Indices		Decision
					ΔI_{diff}	Φ_{min}	
5km from L -bus	10	LL	$117\angle -81°$	Trip	NC	NC	Trip
		LLL	$69\angle 37°$	Trip	NC	NC	Trip
	40	LG	$8.19\angle -162°$	Trip	NC	NC	Trip
		LLG	$7.76\angle -162°$	Trip	NC	NC	Trip
	200	LG	$2.46\angle -162°$	Block	0.31	1.41	Trip
		LLG	$2.24\angle -161°$	Block	0.289	1.4	Trip
	450	LG	$1.95\angle -152°$	Block	0.13	1.38	Trip
		LLG	$1.82\angle -189°$	Block	0.129	1.34	Trip
	1000	LG	$1.88\angle -179°$	Block	0.128	1.31	Trip
		LLG	$1.79\angle -178°$	Block	0.127	1.30	Trip
	10 kΩ	LG	$1.88\angle -177°$	Block	0.126	1.29	Trip
		LLG	$1.79\angle -176°$	Block	0.126	1.28	Trip
Mid of the Line	10	LL	$1.07\angle -27.6°$	Trip	NC	NC	Trip
		LLL	$1.51\angle 27.6°$	Trip	NC	NC	Trip
	40	LG	$1.97\angle 62.7°$	Trip	NC	NC	Trip
		LLG	$3.04\angle 31.8°$	Trip	NC	NC	Trip
	200	LG	$3.27\angle 174°$	Block	0.25	1.174	Trip
		LLG	$3.09\angle -173°$	Block	0.241	1.14	Trip
	450	LG	$1.7\angle -168°$	Block	0.15	1.30	Trip
		LLG	$1.65\angle -166°$	Block	0.149	1.29	Trip
	1000	LG	$1.68\angle -171°$	Block	0.15	1.30	Trip
		LLG	$1.63\angle -163°$	Block	0.149	1.29	Trip
	10 kΩ	LG	$1.58\angle -177°$	Block	0.145	1.29	Trip
		LLG	$1.53\angle -173°$	Block	0.135	1.27	Trip
5km from R -bus	10	LL	$0.21\angle -24°$	Trip	NC	NC	Trip
		LLL	$0.04\angle -28°$	Trip	NC	NC	Trip
	40	LG	$0.24\angle 34°$	Trip	NC	NC	Trip
		LLG	$0.29\angle 30°$	Trip	NC	NC	Trip
	200	LG	$0.72\angle 144°$	Block	0.31	1.374	Trip
		LLG	$0.82\angle 145°$	Block	0.241	1.164	Trip
	450	LG	$0.63\angle -143°$	Block	0.118	1.31	Trip
		LLG	$0.58\angle -163°$	Block	0.117	1.15	Trip
	1000	LG	$0.65\angle 164°$	Block	0.116	1.32	Trip
		LLG	$0.62\angle 165°$	Block	0.113	1.114	Trip
	10 kΩ	LG	$0.55\angle -163°$	Block	0.112	1.21	Trip
		LLG	$0.53\angle -173°$	Block	0.111	1.109	Trip

The proposed method is also tested for variation in load angle δ and source impedance at both ends of the line. For all the cases a line-to-ground fault at 5 km from L-bus with a fault resistance of 250 Ω is considered. The current ratio CR for few cases is presented in Table 2.3. The impact of the source impedance variation on the decision process is minimal as observed from Table 2.3. At lower loading the conditions the

conventional and proposed scheme both provides satisfactory result. As the loading increases the decision of the conventional method is compromised for high resistance fault. During such condition the supplementing features of the proposed method prevent relay maloperations.

The fault inception angle is varied for a line-to-ground fault near to L-bus with fault resistance of 200 Ω from 0° to 300°. For each case the current ratio is obtained and current ratio (CR) for few cases is provided in the Table 2.4. It is validated that the CR is not dependent upon the fault impedance angle and the relay detects internal high resistance fault for any variations in source impedance.

Table 2.4
Performance of Proposed method for variations in δ and source Impedance

δ In (°)	Source Impedance		CR	Conventional Method	Proposed Method		
	Z_{1L}	Z_{1R}			Indices		Decision
					ΔI_{diff}	Φ_{min}	
10°	Z_{1L}	10* Z_{1L}	0.81∠13°	Trip	NC	NC	Trip
	Z_{1L}	Z_{1L}	0.66∠16°	Trip	NC	NC	Trip
	Z_{1L}	0.1* Z_{1L}	0.64∠17°	Trip	NC	NC	Trip
20°	10* Z_{1R}	Z_{1R}	2.43∠ − 158°	Block	0.31	1.174	Trip
	Z_{1R}	Z_{1R}	2.43∠ − 158°	Block	0.29	1.14	Trip
	0.1* Z_{1R}	Z_{1R}	3.67∠ − 143°	Block	0.31	1.18	Trip
30°	Z_{1L}	10* Z_{1L}	1.98∠-162°	Block	0.30	1.28	Trip
	Z_{1L}	Z_{1L}	2.26∠-160°	Block	0.38	1.165	Trip
	Z_{1L}	0.1* Z_{1L}	1.99∠-160°	Block	0.37	1.155	Trip

Table 2.5
Performance of Proposed method with different fault inception angle

Inception Angle	CR	Conventional Method	Proposed Method		
			Indices		Decision
			ΔI_{diff} (pu.)	Φ_{min} (rad)	
10°	2.07∠-162°	Block	0.32	1.346	Trip
100°	2.07∠-162°	Block	0.318	1.46	Trip
200°	2.07∠-162°	Block	0.317	1.346	Trip
300°	2.07∠-162°	Block	0.316	1.346	Trip

2.6.8 Comparative Assessment

The proposed method is compared with the phase co relation method in [45], which uses the cosine of phase angle between the both end currents to compute the operating quantity. It works for high resistance fault less than 400 Ω. However as the fault resistance cosine of the phase angle between current becomes negative. As it is observed form the Table. 2.6, CR for high resistance line-to-ground fault nearby L bus with h= 1.1 and delta= 30° remains in the region 2 of the Fig 2.1. For line-to-ground faults above 400 Ω, the operating quantity is less than zero, which depicts that the method in [45] provides a block signal which is incorrect. However, the proposed method indices show the decision is correct (refer Table 2.6). This reveals the proposed improves the sensitivity of the conventional method during high resistance fault. The proposed method can detect internal high resistance fault up to a resistance of 750 Ω.

In comparison with the sequence based method proposed in [45], during single pole tripping condition the proposed method provides better sensitivity for high resistance internal fault as shown in the section F. In [44], additional external fault detection logic improves the performance during CT saturation for external fault, but has limited performance for high resistance internal fault. However the proposed method provides accurate result during CT saturation and high resistance internal fault.

Table 2.6
Comparison of Performance of Proposed method with the method [45]

Fault Resistance In (Ω)	CR	Method [45]		Proposed Method		
				Indices		Decision
		I_{OP}	Decision	ΔI_{diff} (pu.)	Φ_{min} (rad)	
410	2.37∠-148°	-8.3	Block	0.119	1.145	Trip
450	2.31∠-151°	-10.2	Block	0.118	1.255	Trip
500	2.17∠-155°	-11.1	Block	0.13	1.251	Trip
520	2.14∠-165°	-13	Block	0.124	1.235	Trip

2.7 Conclusion

Alpha plane based relay using phase current has limitations for high resistance fault. In this chapter the phase angle between the voltage and current and magnitude of change in current at both ends of a line are used to confirm an internal fault when the ratio lies in the conflicting region. The adaptive scheme is advantageous over current differential schemes during CT saturation for external fault. The adaptive technique is tested for numerous situations including that for series compensated line, high resistance fault, single pole operation and channel delay and found to be accurate. If voltage data are not available during close in fault or so, the scheme uses the conventional alpha plane technique.

Adaptive Direct Underreaching Transfer Trip Protection Scheme for Three Terminal Line

Direct underreaching transfer trip scheme used for protection of three terminal transmission line operates when at least one of the three zone 1 elements detects an internal fault. This scheme uses dedicated communication system to transfer the decision from one end to other ends. DUTT scheme is reliable till the overlappings between zone 1 settings exist. The infeed through the tapped line reduces the overlapping between the zone 1 distance elements in the scheme. At times, the overlappings vanish resulting an unprotected region in the line. In this work, an adaptive DUTT scheme is proposed using prefault synchronized data where zone 1 relay settings are updated to ensure overlappings always resulting a more reliable protection scheme.

3.1 Introduction

Transmission lines are tapped in between two terminals to extract economical and technical benefits. It creates protection challenges for the line as the fault current flowing from the tapped point affects the voltage and current at the two terminals. DUTT scheme for protection of three-terminal line uses zone 1 distance element at each end which finds underreach problem due to the infeed from T-point [22]. The protection issue of three-terminal line with unequal branch lengths is more critical as they have limited overlapping regions between the zone 1 elements [22], [47]. These overlappings of zone 1 elements decrease with increase in infeed current from T-point. For high infeed currents, the

overlappings with distance relay settings may vanish which will lead to an unprotected line segment with DUTT scheme.

Communication assisted protection schemes like DUTT, permissive overreach transfer trip and directional comparison blocking, are used for three-terminal line protection. The DCB and POTT schemes based on zone 2 overreaching elements are vulnerable to load encroachment and power swing. These schemes also maloperate for outfeed condition. Zone 1 based protection scheme like DUTT is more promising than schemes using zone 2 for the purpose. However available DUTT scheme has reach limitation problem [47].

In this work an adaptive DUTT scheme for protection of three-terminal line is proposed where the relay settings are modified using prefault synchronized data. The system operating condition is obtained from synchronized data and is used to check the overlappings between the zone 1 elements of DUTT scheme. When any overlapping is lost, zone 1 settings of the lines are updated to overcome this problem, resulting improved protection decision. The method is tested for a three-terminal line simulated in EMTDC/PSCAD and the results show its high accuracy.

3.2 System Description and DUTT Settings

A three-terminal line with unequal branch lengths as shown in Fig. 3.1 is considered where the line lengths are in the increasing order of PT, ST and RT. The DUTT scheme protecting the lines uses zone 1 trip signals to be shared by the three distance relays at P, R and S buses. As an example demonstrated in this work, zone 1 of relay R is set with 80% of Z_{RP} which covers up to point F. P relay is set with 80% of Z_{SP}which covers up to M and H as shown in TR and TS sections of Fig. 3.1 respectively. In a similar way the setting of S relay is 80% of Z_{SP} which covers beyond Fand within M on TR section and up to G on TP section**.**

The system of Fig. 3.1 is considered where distance relays (GPS time synchronized) are available at the three buses and are linked with a communication system. The distances of the line segments from the three ends to the T-point are provided in Appendix B.

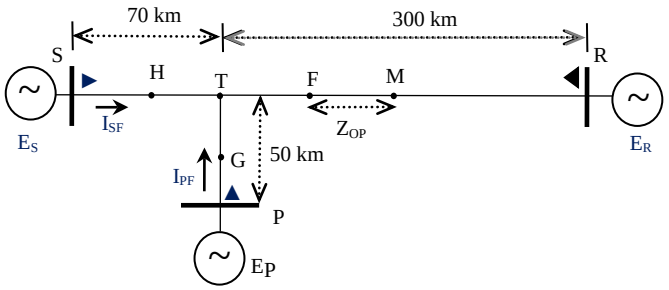

Fig. 3.1. The three-terminal line.

For each relay, zone 1 is set 80% of the shortest line section in the forward direction. For the 50 Hz system, the positive sequence phasor data available at a rate of 50 frames per second from the three buses are processed at each relay end to estimate the operating condition.

$$\bar{E}_S = \bar{V}_S + Z_{1sS}\bar{I}_S \tag{3.1}$$

$$\bar{E}_R = \bar{V}_R - Z_{1sR}\bar{I}_R \tag{3.2}$$

$$\bar{E}_P = \bar{V}_P + Z_{1sP}\bar{I}_P \tag{3.3}$$

whereZ_{1sS}, Z_{1sR} and Z_{1sP} are the source impedance at S, R and P buses. The relation between voltage sources are defined by,

$$h_1 e^{-j\delta_1} = \frac{\bar{E}_R}{\bar{E}_S}, h_2 e^{-j\delta_2} = \frac{\bar{E}_R}{\bar{E}_P} \tag{3.4}$$

where ($h_1$and h_2) are voltage magnitude ratios and and(δ_1 and δ_2) are phase angle differences of source voltages at R and S and P and S buses respectively.

3.3 Estimated infeed current during fault

The infeed current during fault During fault beyond T point in the system due to the infeed for the other terminals can be obtained from the system condition information. The prefault currents at bus S and P are obtained by applying superposition principle [92], [93].Prefault current at S-bus is obtained as,

$$I_{preS} = E_S\left(\frac{1}{Z_{Seq}} - K_1 - K_2\right) \tag{3.5}$$

where.

$$K_1 = \frac{Z_P h_1 e^{-j\delta_1}}{(Z_P + Z_S)Z_{Req}}, K_2 = \frac{(Z_{TF} + Z_R)h_2 e^{-j\delta_2}}{(Z_R + Z_S + Z_{TF})Z_{Peq}}$$

and $Z_P = Z_{1sP} + Z_{PT}, Z_S = Z_{1sS} + Z_{ST}$, $Z_R = Z_{1sR} + Z_{RF}$.

whereZ_{PT} and Z_{ST} are impedances from P and S buses to T point respectively.$Z_{\mathrm{RF}}$is the impedance between R and F.$\mathrm{Z_{TF}}$is the impedance between T and F. $Z_{1\mathrm{sS}}$,$Z_{1\mathrm{sP}}$ and $Z_{1\mathrm{sR}}$ are the positive sequence source impedance at S, P and R buses respectively. WhereZ_{Seq}, $Z_{\mathrm{Req}}$and Z_{Peq} are Thevenin's equivalent impedance seen from S, R and P sources respectively. Prefault current in TF is obtained as

$$I_{\mathrm{pre2}} = E_{\mathrm{S}}\left(\mathrm{K_3} + K_4 - \frac{h_1 e^{-j\delta_1}}{\mathrm{Z_{Req}}}\right) \tag{3.6}$$

where

$$\mathrm{K_3} = \frac{\mathrm{Z_P}}{(\mathrm{Z_P} + \mathrm{Z_R} + \mathrm{Z_{TF}})\mathrm{Z_{Seq}}}\ ,\ K_4 = \frac{\mathrm{Z_S} h_2 e^{-j\delta_2}}{(\mathrm{Z_R} + \mathrm{Z_S} + \mathrm{Z_{TF}})\mathrm{Z_{Peq}}}$$

Considering the prefault current voltage at F can be obtained as:

$$V_{pre} = E_{\mathrm{S}} - I_{\mathrm{preS}}\mathrm{Z_S} - I_{\mathrm{pre2}}\mathrm{Z_{TF}} \tag{3.7}$$

Using I_{preS} and I_{pre2} in (3.5) and (3.6)V_{pre} becomes,

$$V_{\mathrm{pre}} = E_S(1 - Z_S\left(\frac{1}{Z_{Seq}} - \mathrm{K_1} - \mathrm{K_2}\right) - (\mathrm{K_3} + \mathrm{K_4} - \frac{h_1 e^{-j\delta_1}}{\mathrm{Z_{Req}}})\ \mathrm{Z_{TF}})) \tag{3.8}$$

For a three phase fault with fault resistance $\mathrm{R_F}$at F, the fault current will be,$I_F = \frac{V_{\mathrm{pre}}}{Z_{\mathrm{SUM1}} + \mathrm{R_F}}$

where

$$Z_{\mathrm{SUM1}} = \frac{(\mathrm{Z_S Z_P}/(\mathrm{Z_S} + \mathrm{Z_P}))\mathrm{Z_{TF}}}{(\mathrm{Z_S Z_P}/(\mathrm{Z_S} + \mathrm{Z_P})) + \mathrm{Z_{TF}}} + \mathrm{Z_R}$$

The currents at bus S and P are obtained as,

$$I_{\mathrm{S}} = I_{\mathrm{F}}\mathrm{C_1 C_{11}}\ ,\ I_{\mathrm{P}} = I_{\mathrm{F}}\mathrm{C_1 C_{12}} \tag{3.9}$$

The distribution factors used in (3.9) are,

$$\mathrm{C_1} = \frac{\mathrm{Z_R}(\mathrm{Z_S}+\mathrm{Z_P})}{\mathrm{Z_S Z_P} + (\mathrm{Z_{TF}} + \mathrm{Z_R})(\mathrm{Z_S}+\mathrm{Z_P})}, \mathrm{C_{11}} = \frac{\mathrm{Z_P}}{(\mathrm{Z_S}+\mathrm{Z_P})}, \mathrm{C_{12}} = \frac{\mathrm{Z_S}}{(\mathrm{Z_S}+\mathrm{Z_P})}$$

Fault current at S and P buses are defined as,

$$\begin{aligned} I_{\mathrm{SF}} &= I_{\mathrm{S}} + I_{\mathrm{PRES}} \\ I_{\mathrm{PF}} &= I_{\mathrm{P}} + I_{\mathrm{PREP}} \end{aligned} \tag{3.10}$$

Substituting I_S and I_{PRES}, current during fault at S-bus becomes,

$$I_{SF} = E_S\,(\frac{1}{Z_{Seq}} - \mathrm{K_1} - \mathrm{K_2} + \,(\,(1 - \mathrm{Z_S}\left(\frac{1}{\mathrm{Z_{Seq}}} - \mathrm{K_1} - \mathrm{K_2}\right) - \left(\mathrm{K_3} + \mathrm{K_4} - \frac{1}{\mathrm{Z_{Req}}}\right)\mathrm{Z_{TF}})/(\mathrm{Z_{SUM1}} + \mathrm{R_F}))\mathrm{K_5}) \tag{3.11}$$

Similarly fault current at P-bus becomes,

$$I_{PF} = E_S\,(\mathrm{K_9} - \mathrm{K_7} - \mathrm{K_8} + \,(\,(1 - \mathrm{Z_S}\left(\frac{1}{\mathrm{Z_{Seq}}} - \mathrm{K_1} - \mathrm{K_2}\right) - \left(\mathrm{K_3} + \mathrm{K_4} - \frac{1}{\mathrm{Z_{Req}}}\right)\mathrm{Z_{TF}})/(\mathrm{Z_{SUM1}} + \mathrm{R_F}))\mathrm{K_5}) \tag{3.12}$$

Where the constants in (3.11) and (3.12) can be expressed in terms of system parameters as:

$$\mathrm{K_5} = \frac{\mathrm{Z_{TF}Z_P}}{\mathrm{Z_{TF}(Z_S{+}Z_P) + Z_SZ_P}}, \mathrm{K_6} = \frac{\mathrm{Z_{TF}Z_S}}{\mathrm{Z_{TF}(Z_S{+}Z_P) + Z_SZ_P}}, \mathrm{K_9} = \frac{h_2 e^{-j\delta_2}}{\mathrm{Z_{Peq}}}$$

$$\mathrm{K_7} = \frac{\mathrm{Z_S}h_1 e^{-j\delta_1}}{(\mathrm{Z_P} + \mathrm{Z_S})\mathrm{Z_{Req}}}, \mathrm{K_8} = \frac{\mathrm{Z_{TF}} + \mathrm{Z_R}}{(\mathrm{Z_{TF}} + \mathrm{Z_P} + \mathrm{Z_R})\mathrm{Z_{Seq}}}$$

3.4 Limitations of Communication Assisted Schemes

Three-terminal lines are protected by communication assisted distance protection schemes or phase-segregated current differential protection scheme due to the limited performance of the distance relays in protecting such lines.. Communication based distance protection scheme especially POTT or DCB scheme when used for protecting such lines may maloperate during stable power swing due to their operating principle [22]. On the other hand current differential protection scheme has immunity to power swing. However, such a scheme has limitation to detect high-resistance fault at higher value of prefault current during power swing. This scheme also finds difficulty to detect an internal fault that causes significant outfeed during power swing [26]. The performance of the communication assisted schemes are discussed in the preceding section.

3.4.1 Limitations of POTT and DCB Scheme

Communication assisted distance protection schemes such as POTT and DCB schemes are set with overreaching zone-2 element to overcome infeed effects in a three-terminal

line. Zone 2 element at ends of the line shared decision information to detect internal fault. The output of the POTT scheme is set '1' for internal fault and '0' otherwise. To compensate the infeed effect the setting of the zone2 element has increased which suffers from maloperation during overloading condition and power swing. As shown in the Fig. 3.2 for a fault in TR section the current direction at P-bus may be reverses and due to this relay at P bus dose not responds to this condition. This causes mloperation of the POTT scheme for outfeed.

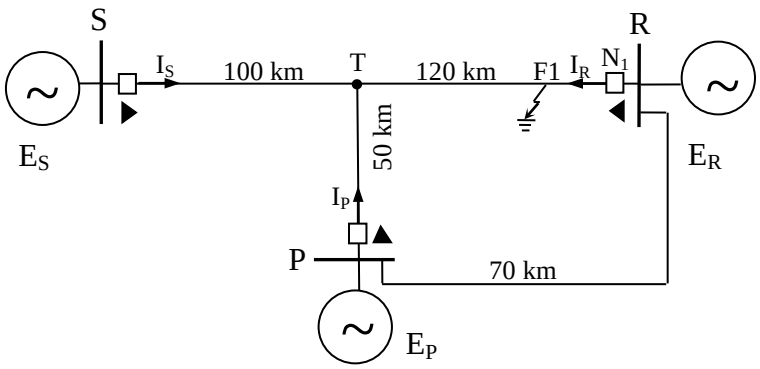

Fig. 3.2. The three-terminal line with fault in the TR section.

Similarly DCB scheme protected three-terminal line is more susceptible to power swing compared to POTT scheme. This is because during swing if the apparent impedance enters into one of the three relay characteristics and at the same time apparent impedances at the other two terminals are beyond their reverse zone setting then trip command would be initiated by such scheme [23]. It is observed that the DCB scheme also maloperates for the swing case demonstrated above.

3.4.2 Limitations of DUTT Scheme

Zone 1 relays at the three buses S, R and P as shown in Fig. 3.1 should have overlappings to ensure that at least one of the three relays will be able to detect any internal fault in the lines. The overlapping impedances between P and R relays (Z_{OP}) and between S and R relays (Z_{OS}) are defined as,

$$Z_{OP} = kZ_{SP} - (Z_{PT} + Z_{TF})$$
$$Z_{OS} = kZ_{SP} - (Z_{ST} + Z_{TF}) \quad (3.13)$$

where k = 0.8 for all the cases.The overlapping impedances between relays S and R and P and R depend on infeed from the tapped line. The apparent impedance seen by S relay for a three phase fault at F in Fig. 3.1 can be expressed as,

$$\mathrm{Z_{app}} = \mathrm{Z_{ST}} + \left(1 + \frac{\bar{I}_{\mathrm{PF}}}{\bar{I}_{\mathrm{SF}}}\right) Z_{\mathrm{TF}} \tag{3.14}$$

where$\bar{I}_{\mathrm{SF}}$and $\bar{I}_{\mathrm{PF}}$ are fault currents at S and P buses during a three phase fault at F respectively as derived in the previous section.

Thus the error to the apparent impedance caused by infeed current will be,

$$\mathrm{Z}_{err} = \frac{\bar{I}_{\mathrm{PF}}}{\bar{I}_{\mathrm{SF}}} \mathrm{Z_{TF}} \tag{3.15}$$

$\mathrm{Z_{err}}$relates to underreach amount of the relay and reflects the decrease in overlapping between S and R relays zone 1 elements. The underreach effect caused by the infeed current varies in accordance with system condition including source impedances. At certain infeed conditions, the overlapping vanishes which will result in DUTT maloperation.

For proper DUTT decision, the overlappings between the three relays have to be ensured. Three phase fault current is more compared to current during any other type of fault in a line. For a fault at one location, the error caused by the infeed current is maximum for three phase fault. Thus, if the overlapping is ensured for three phase fault, it would satisfy for all other faults. R relay zone 1 setting protects up to F and is not affected by infeed from P-bus. If a fault in the TF section is not detected by any of S or P relays (due to underreach), DUTT scheme will malfunction for this case. Therefore, decrease in overlapping is checked for three phase fault at F (reach of R relay) to ensure proper relay decision. With the infeed effect, the overlappings between relay settings of S and R($\mathrm{C_{OS}}$) and P and R($\mathrm{C_{OP}}$)at one instant can be formulated as,

$$\mathrm{C_{OS}} = |\mathrm{Z_{OS}}| - \left|\frac{|\bar{\mathrm{I}}_{\mathrm{PF}}|}{|\bar{\mathrm{I}}_{\mathrm{SF}}|} \mathrm{Z_{TF}}\right| \tag{3.16}$$

$$\mathrm{C_{OP}} = |\mathrm{Z_{OP}}| - \left|\frac{|\bar{\mathrm{I}}_{\mathrm{SF}}|}{|\bar{\mathrm{I}}_{\mathrm{PF}}|} \mathrm{Z_{TF}}\right| \tag{3.17}$$

whereZ_{OS} and Z_{OP} are as defined in (3.13). The percentage of overlappings between S and P relays with R relay are defined as,

$$K_{\mathrm{S}} = \frac{\mathrm{C_{OS}}}{|\mathrm{Z_{OS}}|} \times 100 \tag{3.18}$$

$$K_{\mathrm{P}} = \frac{\mathrm{C_{OP}}}{|\mathrm{Z_{OP}}|} \times 100 \tag{3.19}$$

As the infeed current increases the overlapping decreases and at some operating conditions, any overlapping(s) may vanish.

A 400-kV, 50 Hz three terminal transmission system as in Fig. 3.1 is simulated for different operating conditions to observe the variation in percentage of overlapping. The magnitude and angle of voltage at R-bus is maintained constant for all cases. The voltage magnitude, angle and source impedances at S and P buses are varied in each case. The variation in percentage overlapping between zone 1 of S and R and P and R relays with infeed current ratio is plotted in Fig. 3. 3.The dotted line in the plot separates overlapping and non-overlapping zones. The percentage of overlapping reduces with the increase in infeed current and for a range of infeed current ratio, portion of three-terminal line remains unprotected by DUTT scheme.

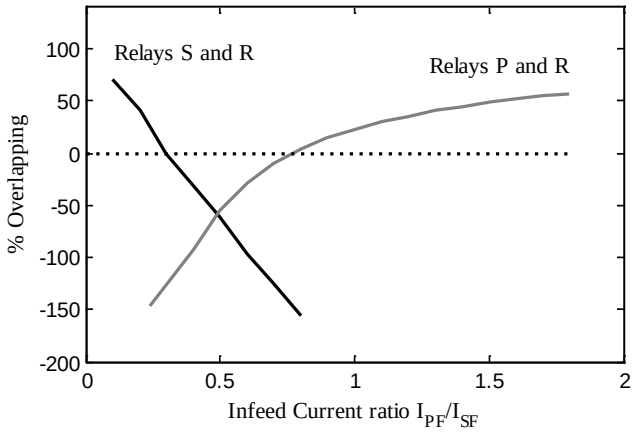

Fig. 3.3. Variation in percentage of overlappings.

The performance of DUTT scheme is tested for a 3-phase fault at 85% of the line RP section from R-bus (which is outside the zone 1 setting of R relay). The prefault loading condition of the three-terminal line is fixed ath_1=0.98, δ_1=-15˚,h_2=1.0andδ_2=-5˚ (refer (3.4)).The apparent impedances seen at S,P and R relays are plotted in Fig. 3.4 (a)

and (b). It is observed that the trajectory of apparent impedance settles outside the set zone 1 characteristics of these S, P and R relays. Thus the fault will not be detected by any of the zone 1 element of the DUTT protection scheme and it fails to identify the internal fault. This happens due to the infeed.

For proper operation of DUTT scheme the zone 1 setting of S and P relays should be monitored continuously. For this the overlappings are calculated and then relay settings are changed when required to ensure proper decision by DUTT scheme.

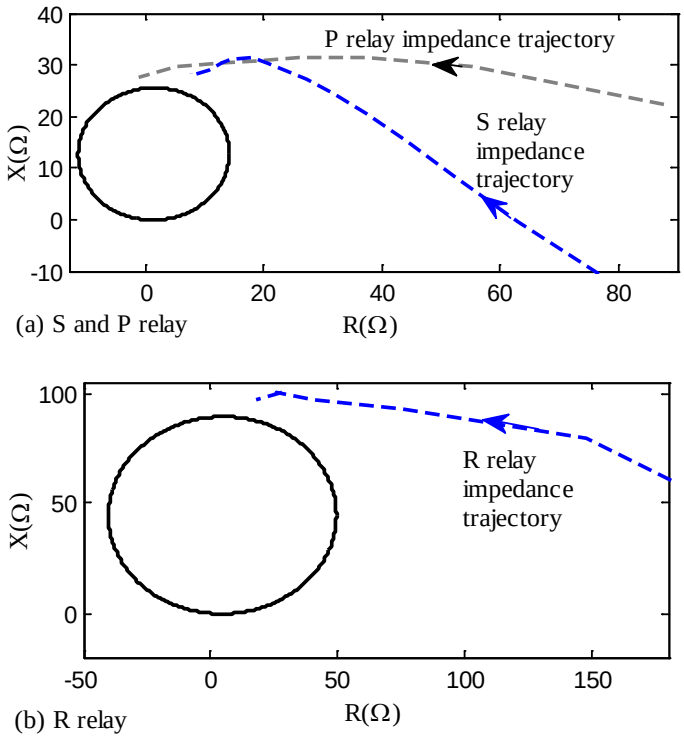

Fig. 3.4. Apparent impedance trajectory for 3-phase fault.

3.5 Proposed Adaptive Method

The system of Fig. 3.1 is considered to be protected by DUTT scheme where zone 1distance elements (GPS time synchronized) are available at the three buses and are linked with a communication system. Zone 1 of R-bus relay remains within the T-point and is not affected by the infeed current. The relays at buses S and P face underreach problem and need to be adapted in accordance with the infeed condition. For the 50 Hz system, the positive sequence phasor data available at a rate of 50 frames per second from

the three buses are processed at each relay end to estimate the operating condition. Using this information percentage of overlapping for S relay is calculated by (3.18). Zero or negative value of $K_S$implies that the overlapping is lost. In such a case the overlapping between S and R relays zone 1 characteristics can be retained by increasing the zone 1 setting of S relay by ΔZ_S as below,

$$\Delta Z_S = \frac{|\bar{I}_{PF}|}{|\bar{I}_{SF}|} Z_{TF} \tag{3.20}$$

80% setting of S relay protects up to G (say) in TP section as shown in Fig. 3.1. The increase in S relay setting may overreach TP section which is not desirable. To ensure that the setting of S relay does not go beyond P, the adaptive setting has to be modified. This requirement can be assured if the reach of adaptive setting at S relay is restricted up to G. This is only possible when the increased setting ΔZ_S is less than the error in apparent impedance of S relay caused by the fault current from R-bus for a three phase fault at G. The error in seen impedance can be expressed as,

$$Z_{Ser} = \frac{|\bar{I}_{RG}|}{|\bar{I}_{SG}|} Z_{TG} \tag{3.21}$$

where$\bar{I}_{RG}$ and $\bar{I}_{SG}$ are fault currents from R and S buses. While the settings are changed, S relay setting may overreach the TP section. To verify S relay zone 1 reach, a three phase fault at G is considered for same operating condition. The fault currents can be expressed as,

$$I_{SG} = E_S\left(\frac{1}{Z_{Seq}} - K_1 - K_2 + \frac{K_{p1}K_{p2}}{Z_{SUM2} + R_F}\left(h_2 e^{-j\delta_2} - (K_9 - K_7 - K_8)(Z_P - Z_G)\right)\right) \tag{3.22}$$

$$I_{RG} = E_S\left(K_3 + K_4 - \frac{h_1 e^{-j\delta_1}}{Z_{Req}} + \frac{K_{p1}K_{p3}}{Z_{SUM2} + R_F}\left(h_2 e^{-j\delta_2} - (K_9 - K_7 - K_8)(Z_P - Z_G)\right)\right) \tag{3.23}$$

whereZ_G is the impedance of the section T to G in Fig. 3.1. The constants used can be expressed in terms of system parameters as,

$K_{p1} = \frac{(Z_P - Z_G)}{((Z_R + Z_{TF})Z_S/(Z_R + Z_{TF} + Z_S)) + Z_P}$, $K_{p2} = \frac{Z_P}{(Z_S + Z_P)}$, $K_{p3} = \frac{Z_S}{(Z_S + Z_P)}$ and

$$Z_{SUM2} = \frac{((Z_S+Z_{TF}+Z_R)Z_G) + Z_S(Z_R+Z_{TF}))(Z_P - Z_G)}{(Z_S+Z_R+Z_{TF})(Z_P) + Z_S(Z_R+Z_{TF})}$$

Using I_{SG} and I_{RG} in (3.22) and (3.23) S relay overreach is checked. Positive C_S confirms overreaching and. for such a case both S and R relays settings are adapted using (3.16). When$|\Delta Z_S| > |Z_{Ser}|$, adaptive setting of S relay may reach beyond TP section. In order to maintain overlapping without overreach, setting of S relay is decreased and R relay setting is increased simultaneously by the same amount. The renewed S relay reach for TP section is checked by,

$$C_S = |\Delta Z_S| - |Z_{Ser}| \tag{3.24}$$

In case, C_S is positive, the setting for S relay should be updated with,

$$Z_{S_{New}} = Z_{S_{SET}} + Z_{Ser} \tag{3.25}$$

Simultaneously, R relay setting is changed to,

$$Z_{R_{New}} = Z_{R\_SET} + (\Delta Z_S - Z_{Ser}) \tag{3.26}$$

whereZ_{S_SET} and Z_{R_SET} corresponds to the fixed 80% setting for S and R relaysrespectively. If $|\Delta Z_S| \leq |Z_{Ser}|$, S relay setting is increased by ΔZ_S as in (3.20).

Similarly the percentage of overlapping between P and R relays zone 1 is calculated as in (3.19). Zero or Negative overlapping implies adaptive setting is required. In that case, the overlapping between P and R relays is maintained by increasing the setting by

$$\Delta Z_P = \frac{|\bar{I}_{SF}|}{|\bar{I}_{PF}|} Z_{TF} \tag{3.27}$$

P relay adaptive setting may overreach TS section (say beyond S). The 80% setting of P relay covers up to H on TS section (refer Fig 3.1). As mentioned earlier for S relay reach, P relay setting should be limited up to H. For this, the error in P relayapparent impedance caused by fault current from R-bus can be obtained for a three phase fault at H as,

$$Z_{Per} = \frac{|\bar{I}_{RH}|}{|\bar{I}_{PH}|} Z_{TH} \tag{3.28}$$

$\bar{I}_{RH}$and$\bar{I}_{PH}$ can be derived using the system condition and can be expressed as:

$$I_{PH} = E_S(K_9 - K_7 - K_8 + \frac{K_{t1}K_{t2}}{Z_{SUM3} + R_F}(1 - (\frac{1}{Z_{Seq}} + K_1 + K_2)(Z_S - Z_H))) \quad (3.29)$$

$$I_{RH} = E_S(K_3 + K_4 - \frac{h_1 e^{-j\delta_1}}{Z_{Req}} + \frac{K_{t1}K_{t3}}{Z_{SUM3} + R_F}(1 - (\frac{1}{Z_{Seq}} + K_1 + K_2)(Z_S Z_H))) \quad (3.30)$$

whereZ_H is the impedance between T and H in Fig. 3.1.The constants used in (3.29) and (3.30)can be represented as:

$$K_{t1} = \frac{(Z_S - Z_H)}{((Z_R + Z_{TF})Z_P/(Z_R + Z_{TF} + Z_P)) + Z_S}$$

$$K_{t2} = \frac{Z_R + Z_{TF}}{(Z_R + Z_P + Z_{TF})}, K_{t3} = \frac{Z_P}{(Z_R + Z_P + Z_{TF})} \text{ and}$$

$$Z_{SUM3} = \frac{((Z_P + Z_{TF} + Z_R)Z_H) + Z_P(Z_R + Z_{TF}))(Z_S - Z_H)}{(Z_P + Z_R + Z_{TF})(Z_S) + Z_P(Z_R + Z_{TF})}$$

Using I_{PH} and I_{RH} reach of P relay adaptive setting is verified. The reach of adaptive P relay setting, for TP section is checked by

$$C_P = |\Delta Z_P| - |Z_{Per}| \quad (3.31)$$

In case required to satisfy the reach requirement the settings of P and R relays are changed simultaneously. In case of, C_P is positive, the setting for P relay should be,

$$Z_{P_{New}} = Z_{P_{SET}} + Z_{Per} \quad (3.32)$$

Simultaneously, R relay setting is modified to

$$Z_{R\_New} = Z_{R\_SET} + (\Delta Z_P - Z_{Per}) \quad (3.33)$$

whereZ_{P_SET}corresponds to 80% setting for P relay. For $|\Delta Z_P| \leq |Z_{Per}|$, the P relay setting is increased by ΔZ_P. It is observed that both the renewed settings never overreach simultaneously.

The flow diagram for adaptive DUTT setting scheme is provided in Fig. 3.5. The different steps of the proposed adaptive technique is provided below

Step 1: The input for the proposed method is the voltage and current phasors.

Step 2 : Estimation of the system condition.

Step 3 : Computation of percentage of overlapping using (3.18) and (3.19).

Step 4 : For any negative or zero value of percentage overlapping, increments in impedance required for S and P relays are calculated.

Step 5 : The settings are updated for S and P bus relays .

Step 6: Adaptive setting is checked by (3.24) and (3.31) and the settings are modified in case of any violation in reach.

Proposed scheme uses three ends prefault data and the settings are updated in each cycle when required. During fault it needs only decision signal from the other end as used in conventional DUTT scheme. In case of communication failure it switches to the conventional fixed setting approach.

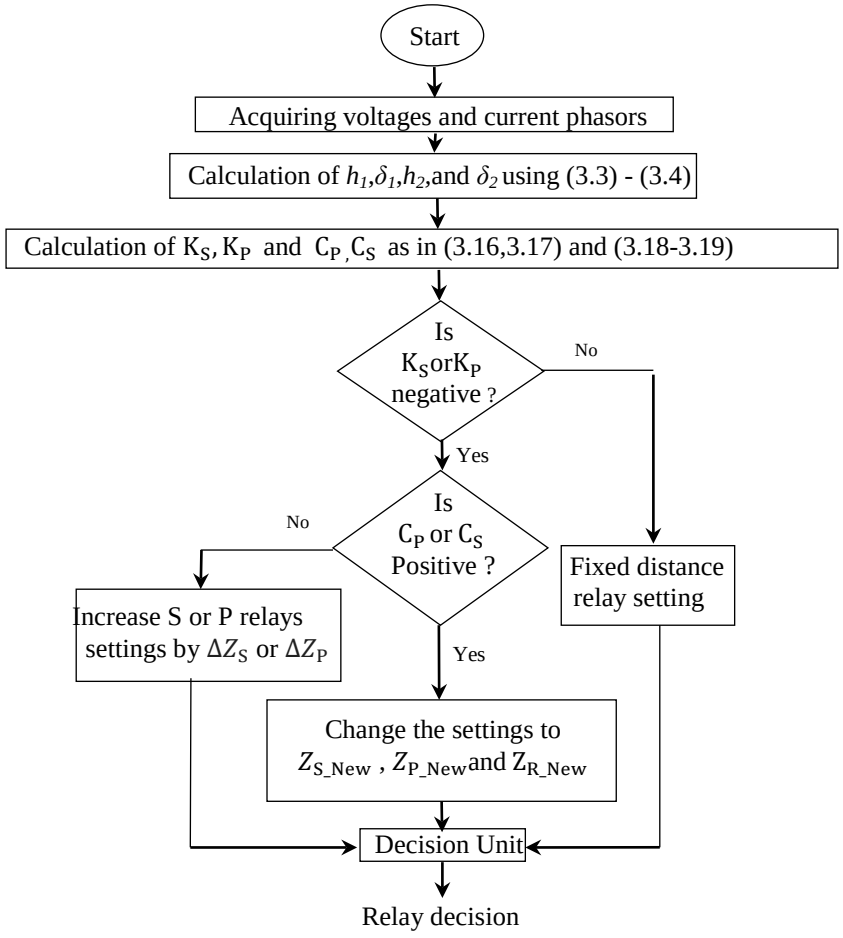

Fig. 3.5. Flow diagram for proposed adaptive technique.

The source impedance varies with time. It can be computed from a two port equivalent of any system which is obtained from a power flow solution of the network,

with protected component being removed [128]. In this work the source impedance is assumed to be available using WAMs data and network information. The changes in source impedance are updated with the arrival of a new set of data. Up to the next computation, the previous source impedance is considered for the proposed algorithm.

3.6 Results

The method proposed for adaptive setting of three-terminal line is tested for a 400 kV, 50 Hz three bus system as shown in Fig. 3.1. Few important results are demonstrated in this section. The system is simulated using EMTDC/PSCAD. One-cycle discrete Fourier transform is used to compute the phasors from data sampled at 1 kHz in MATLAB platform. The Synchronized prefault voltage and current data collected at central location are used to estimate the overlapping. In case required, adaptive trip boundary is generated and tested for the same system condition.

3.6.1 Test for variation in system condition

Power system is dynamic in nature and its operating condition changes with time. To test the adaptive DUTT scheme changes in system operating condition is considered. The system was initially operating at a condition with $h_1=1.01$, $\delta_1=0^\circ$, $h_2=1.01$ and $\delta_2=5^\circ$.The condition is changed to$h_1=0.98$, $\delta_1=-15^\circ$, $h_2=1.0$ and $\delta_2=-5^\circ$. The prefault synchronized data obtained from three buses are used to calculate the voltage magnitude ratio and phase angle differences (refer Table 3.1). The computed phasor are applied to compute the overlapping present between zone 1 elements of the DUTT scheme. Using (3.18) and (3.19) the percentage overlappings for S and P relays with R relay are calculated. Negative K_S and K_P infer overlappings of all the three settings are lost. For proper operation of DUTT scheme, S and P relays settings are obtained by increasing it as in (3.20) and (3.27) respectively. Both fixed and adaptive settings are plotted in Fig. 3.6 (a) and (b) for S and P relays respectively.

The accuracy of the adaptive setting is checked for a 3- phase fault created at 85% of line RP from the R-bus with negligible fault resistance during the latter operating condition. The fault impedances seen by S and P relays are plotted in Fig. 3.5 (a) and (b) respectively. It is observed from the figures that the fault impedances settle outside the

fixed zone 1 characteristic and inside the adaptive settings of the two relays. Thus fault is identified correctly it shows the accuracy of the proposed adaptive method. Increased setting of S and P relays may overreach for TP and TS sections. From Table 3.1 it is observed that C_S and C_P are negative which confirms the new S and P relays settings do not have overreach problem and therefore adaptive setting for R relay is not required

Table 3.1
Synchronized data and different indices (h_1=0.98, δ_1=-15˚, h_2=1.0 andδ_2=-5˚)

Bus	Voltage (kV)	Line Current (kA)	System Condition				Indices			
			h_1	h_2	δ_1 (˚)	δ_2 (˚)	K_S	K_P	C_S	C_P
S	236.87 ∠-1.66°	0.69∠-10.4°	0.98	1.0	-14.13	-4.7	-67.2	-54.7	-1.8	-1.3
P	238.81 ∠-2.89°	0.21 ∠166.1°								
R	232.69 ∠-15.3°	0.46 ∠-21.7°								

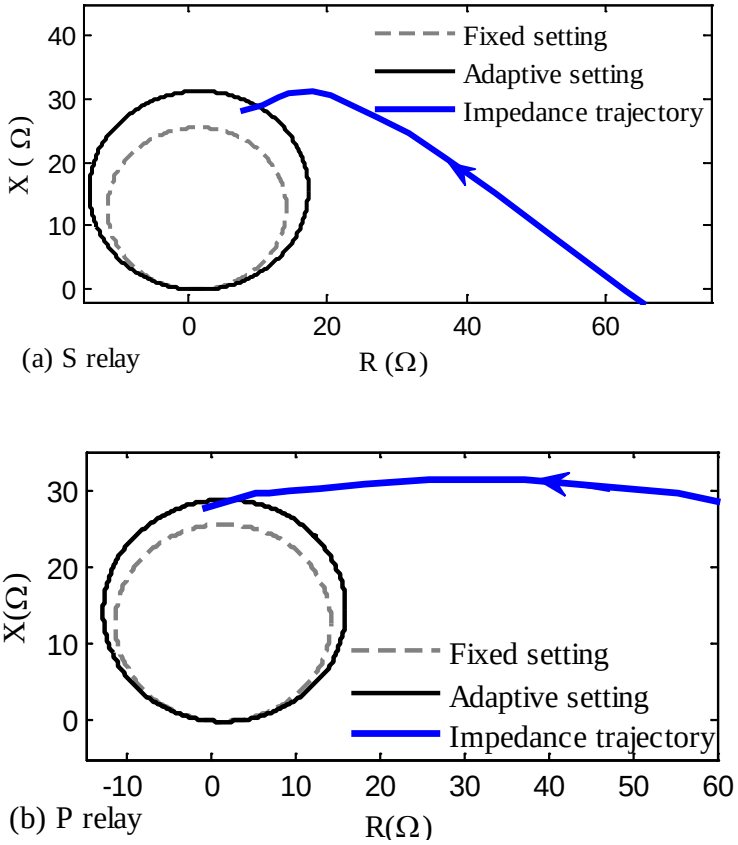

Fig. 3. 6 S and P relays zone 1 adaptive setting for DUTT scheme.

3.6.2 Test for variation in source impedances

The source impedance varies with network topology and generation. The infeed from T-point varies with the variation in source impedance. This in turn affects the overlapping of the zone 1 element of the DUTT scheme. For this case, a prefault system condition of h_1=1.01, δ_1=10˚, h_2=1.06 and δ_2=-20˚ is considered to check the overlapping. Source impedances are changed at fixed voltage magnitude and angle. At S-bus it is decreased by 4 times and at R, P buses decreased 2 times of the corresponding source impedance given in Appendix B.

Synchronized data obtained at three buses are applied to estimate the voltage ratio and phase angle difference. Using this information the overlappings are estimated. Estimated K_S =-84.0 and K_P = -34.9 (refer Table 3.2) with negative values signify the requirement of adaptive setting. Modified S and P relay settings are increased by (3.20) and (3.27) respectively. The adaptive settings obtained by the proposed method for S and P relays are shown in Fig. 3.7 (a) and (b) respectively. The negative $C_S$and $C_P$in Table 3.2, implies the adaptive setting dose not overreach for TP and TS sections for S and P relays respectively. Therefore, adaptive setting of R relay is not required for the situation. Accuracy of adaptive setting is checked by creating a three phase fault at 85% of RP line from R-bus (outside the set boundary of R relay zone 1 characteristic). This fault should be detected by the S and P relays for appropriate operation by the DUTT scheme. Due to the variation in the source impedance at P-bus the fault impedance remains outside the fixed setting as noticed from figures. However, the adaptive setting for the case provides correct solution as evident from the figure.

Table 3.2
Synchronized data and different indices (h_1=1.01, δ_1=-10˚, h_2=1.06 andδ_2=-20˚)

Bus	Voltage (kV)	Line Current (kA)	System condition				Indices			
			h_1	h_2	δ_1(˚)	δ_2(˚)	K_S	K_P	C_S	C_P
S	227.9 ∠-1.7°	1.5 ∠17°	1.01	1.06	-9.03	-19.3	-84	-34.9	-1.65	-2.7
P	243 ∠22°	2.21 ∠-0.07°								
R	229.1 ∠-10°	0.69 ∠-13°								

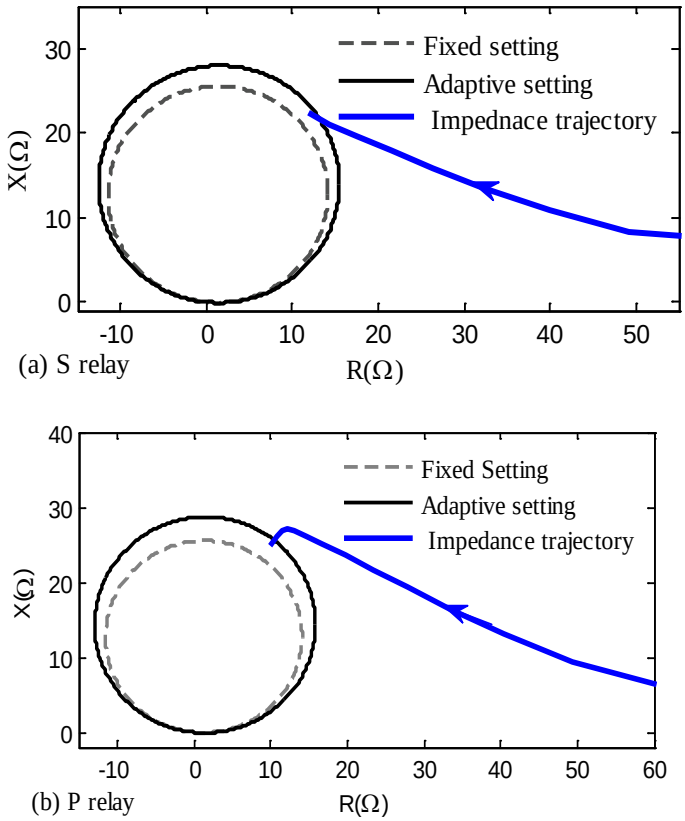

Fig. 3.7. S and P relays zone 1 adaptive setting for source impedance variation.

3.6.3 Simultaneous Adaptive Settings of all three relays

In some cases, where S and P relays settings are increased to maintain the overlapping with R relay, the changed setting may overreach for TP and TS sections. In order to avoid overreach problem, it is required to adapt the relay characteristic at all three buses (also R relay). An example is demonstrated with h_1=1.01, δ_1=-5˚, h_2= 0.96 and δ_2= -10˚ as prefault condition. Synchronized data obtained are used to estimate the voltage ratio, phase angle difference and percentage of overlapping. Estimated K_S= -151.3 and K_P = -2.53 (refer Table 3.3) implies no overlapping available. Next the relay setting of P and S relays are adapted which providesC_S=1.85. This refers that increased S relay setting may over reach TP section. For this case, S and R relays adaptive settings are carried out by (3.25) and (3.33). Adaptive setting for P relay is obtained by increasing ΔZ_P as in (3.27). The fixed and adaptive settings for S, P and R relays are plotted in Fig. 3.8 (a),(b) and (c) respectively.

The accuracy of proposed method is checked by creating a three phase fault at 85% of distance from R bus. During this fault the impedance trajectory is plotted in Fig . 3.8. Impedance trajectory travels from prefault situation to fault point and it is observed form the figure the trajectory finally settles outside the fixed characteristic but inside the adaptive setting. As it is outside the fixed setting the relay will not detect this fault. But the adaptive setting will give a correct decision. This confirms that the adaptive setting is accurate even when all three side relay setting are updated simultaneously

Table 3.3
Synchronized data and different indices (h_1=1.01, δ_1=-5˚, h_2=0.96 and δ_2=-10˚)

Bus	Voltage (kV)	Line Current (kA)	System condition				Indices			
			h_1	h_2	δ_1 (˚)	δ_2 (˚)	K_S	K_P	C_S	C_P
S	242.26 ∠-1.5°	0.98 ∠-2.8°	1.01	0.96	-5.03	-10.3	-151.3	-2.53	1.85	-4.5
P	230.28 ∠-.11°	1.03 ∠-163°								
R	246.46 ∠-4.9°	0.122 ∠106.7°								

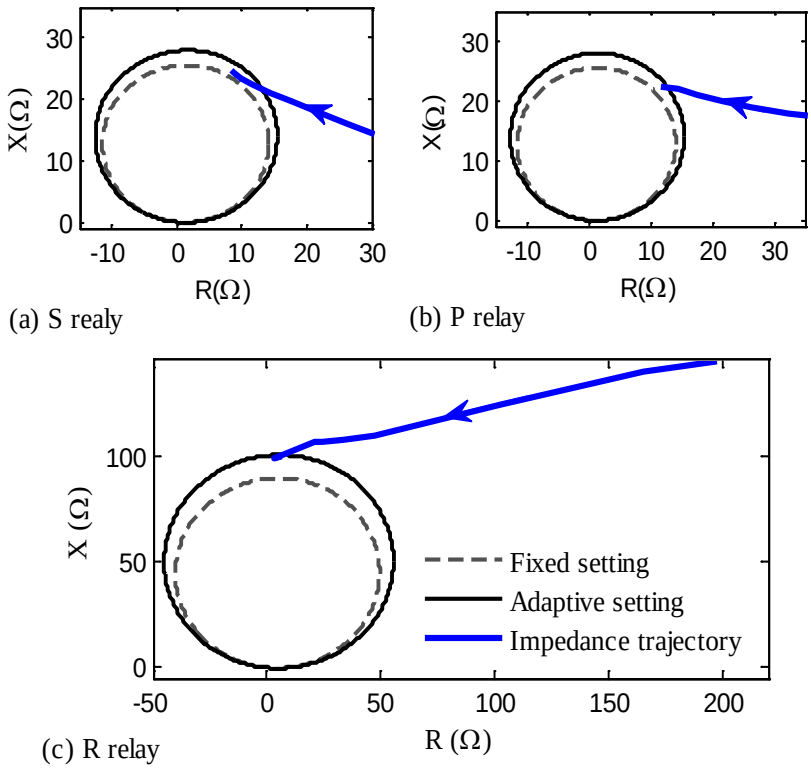

Fig. 3.8. S, R and P relays zone 1 adaptive setting for DUTT scheme.

3.6.4 Test for Unsymmetrical Fault (line-to-ground fault)

All the above cases are tested for symmetrical faults. To check the effect of ground involvement on adaptive setting, a line-to-ground fault with small fault resistance (1 ohm) is simulated at 85% distance of RP from R- bus with same operating condition as in case I. The fault impedance is plotted in the Fig. 3.8, with fixed and adaptive S relay setting obtained in case-I. It is observed from Fig. 3.9 that fault impedance trajectories for line-to-ground type fault settle outside the fixed setting but inside the adaptive setting. This confirms that the adaptive setting is also proper for other types of fault.

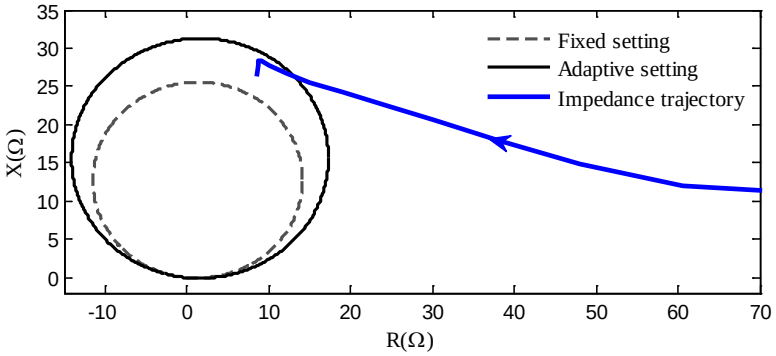

Fig. 3.9. S relay zone 1 adaptive setting for DUTT scheme.

3.6.5 Sensitivity Analysis

The accuracy of the proposed scheme to maintain the overlapping at any operating condition is tested for variation in h and δ with constant source impedance and variation of source impedance with constant h and δ. Table 3.4 provides the accuracy of proposed method for h and δ variation where the source impedances are maintained as in Appendix B.K_S and K_P for adaptive setting during operating condition are calculated with the addition of Z_{err} in (3.15). With conventional setting values of K_S and K_P are negative and when settings are changed adaptively K_S and K_P becomes positive which signifies the overlappings are maintained. Similarly with same h and δ as in case I, source impedances are varied at S and P buses and result is provided in Table 3.5. With adaptive setting, positive values of K_S and K_P are obtained which ensures proper DUTT operation. The calculated fault current used in adaptive setting incurs little error while computing h and δ from WAMs data and therefore 100% overlapping is not obtained.

Table 3.4
Adaptive setting with h and δ variation

Cases	System condition				Power flow(MW) In Sections		Conventional Setting		Adaptive Setting	
	h_1	h_2	δ_1 (°)	δ_2 (°)	TS	TP	K_S	K_P	K_S	K_P
2	1.05	1.05	-15	-15	185	217	-40	-84	97.1	98.2
4	1.01	1.06	-20	-22	134	425	-55	-56	98.5	99.4
5	1.02	1.04	-15	-25	-89	325	-75	-47	97.5	98.9

Table 3.5
Adaptive setting with source impedance variation

Cases	Source Impedance		Conventional setting		Adaptive Setting	
	Times of Z_{1SS}	Times of Z_{1SP}	K_S	K_P	K_S	K_P
1	2	0.5	-25	-107	98.8	97.8
2	3	0.33	-35	-78.2	98.1	98.7
3	4	0.25	-60	-57.7	98.4	98.7

The effect of variation of line length on proposed method is observed by varying the lengths of TP and TS section at the same system condition and length for TR section as in Case I. The first row in Table. 3.6 provide the line lengths as in Case I. Table 3.6 shows overlapping changes with increase in line length for the same condition. Percentage of overlapping is maintained with variations in section lengths by the proposed method. The boundary conditions are studied for provided in Table 3.7 in terms of distance d pu. This is valid for power flow in any directions.

Table 3.6
Effect of line length variation

Case	Length of section (km)		Conventional Setting		Adaptive Setting	
	TS	TP	K_S	K_P	K_S	K_P
1	70	50	-67.2	-54.7	98.8	98.4
2	75	50	-56.46	-19.5	98.8	97.8
3	85	50	-184.6	-10.4	98.1	98.7
4	70	55	-5.6	-28.2	98.4	98.7
5	70	60	-3.4	-24.5	97.5	98.9

Table 3.7
Variation of overlapping with line length

Case	Line Length of Sections (km)			Overlapping
	TP	TS	TR	
1	d	d	4d	large
2	d	d	7d	zero
3	d	0.25d	4d	zero

3.7 Comparative Assessment

While protecting three terminal line DUTT scheme has advantages over differential, POTT and DCB schemes. The comparisons are enumerated below.

3.7.1 Comparison with Current Differential Scheme

Differential relaying using synchronized data has limitations during CT saturation. Differential scheme applied to protect the three terminal line is tested for CT saturation simulating a three phase fault beyond bus R in Fig. 3.1 (outside the three terminal line). CT burden of 30 Ω is selected. The charging current compensation is considered in the differential setting [37]-[38]. The differential relay characteristic plotted in Fig. 3.10 (a) shows, the scheme maloperation due to CT saturation during external fault. For the same case the apparent impedance as seen by R relay is plotted in Fig. 3.10 (b), settles outside the zone 1 characteristic. This signifies DUTT scheme is able to distinguish the fault correctly.

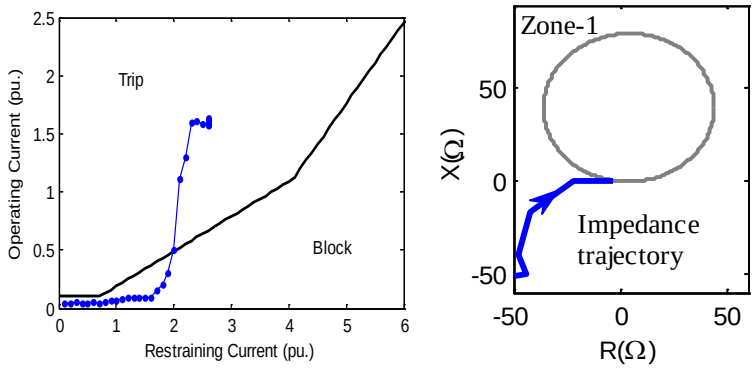

(a) Current differential characteristic (b) R relay for DUTT

Fig. 3.10. Response of differential and DUTT schemes for CT saturation during three phase external fault.

3.7.2 Comparison with POTT and DCB schemes

In an interconnected network R and P buses in Fig. 3.1 may be connected through another path. In this case for fault near bus R on line between T to R current direction may be reversed at P bus. *A* three phase fault is created at 0.1 pu distance from R bus. Corresponding apparent impedance at P bus is plotted in Fig. 3.11 (a) where zone 2 characteristic for POTT scheme is also shown.

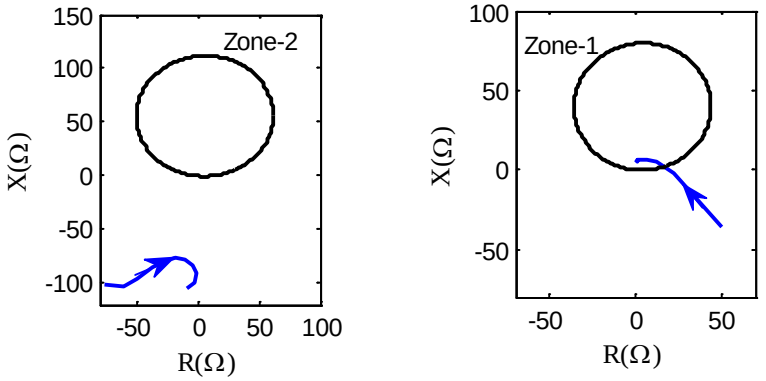

(a) P relay for POTT (b) R relay for DUTT

Fig. 3.11. Apparent impedance at P and R relays during three phase internal fault.

It is observed that the trajectory is well outside the characteristic. As the POTT scheme rely on information from other end, this will cause maloperation of this scheme. On the other hand R bus zone 1 element detect fault and send trip signal to other ends and DUTT scheme will operate correctly for this condition as evident from the Fig. 3.10 (b). The two demonstrations above clearly depict that DUTT is a superior method than differential, POTT and DCB. Next limitation of DUTT will be studied followed by the proposed scheme for 3-terminal line protection

3.8 Conclusions

Conventional DUTT scheme has limited performance in protecting unsymmetrical three terminal line and at certain infeed current fault in a portion of a line remains undetected. An adaptive DUTT scheme for three-terminal line protection is proposed considering infeed current at different operating conditions. Prefault synchronized data at the three terminals are applied to estimate the overlappings between the zone 1 elements. When

these overlappings vanish, the settings are adapted in accordance with infeed condition to ensure reliable operation of the DUTT scheme. In case the adaptive setting has violated the reach of the relay, the adaptive settings are modified, where all three side relay characteristic are modified. The scheme is tested for different operating conditions and different types of faults. Comparison with the conventional DUTT, POTT and differential scheme shows the proposed method has better performance. Test results show its high accuracy.

Synchronized Data Based Adaptive Backup Protection for Series Compensated Line

Apparent impedance seen by the relay is modulated when metal oxide varistor protected series capacitor, is present in a fault loop. At times series compensation may be bypassed due to maintenance purpose or by overvoltage protecting devices. The information on the level of compensation is required for proper protection decision by distance relay if the series capacitor is placed away from the relay. Synchronized data obtained at both ends are applied to calculate the compensation level which is used to adapt the relay setting for backup protection of adjacent line. The mutual coupling in the compensation portion is also considered in the apparent impedance computation. The status of capacitor during fault (bypassed or not) is obtained through impedance calculation during fault and the relay setting is adapted accordingly. Using data simulated through EMTDC/PSCAD for a series compensated line the technique is tested and found to be accurate.

4.1 Introduction

Recent regulatory development, increased electricity demand and restrictions on building new transmission, has an important role in inclusion of series capacitor in long transmission lines. However, series capacitor and MOV protecting it impose challenges to line protection because of subsynchronous resonance, voltage-current inversions, non-linear operation of MOV etc. [24]. Voltage inversion causes maloperation of communication assisted and directional comparison protection schemes [61]. Similarly,

Differential relays performance is compromised for current inversion [59] and CT saturation cases. Failure of these unit protection schemes needs a backup protection and distance relay provides it for long lines.

Distance relay protecting series compensated line suffers from overreaching problem and may trip for a fault beyond zone 1 of the succeeding line. Co-ordination of distance relays can only be achieved when zone 2 settings of the series compensated lines are reduced in accordance with the compensation level [71]. Series capacitors have overvoltage protecting devices like MOV and spark gap, which protects the capacitor during fault. When capacitors are bypassed by its overvoltage protecting devices MOV, spark gap and also for maintenance purpose, the line is treated as uncompensated. During MOV operationthe apparent impedance is also modulated [61]. At these conditions backup protection seeks accurate compensation level present in the line and impedance offered by MOV to improve the relay performance.

In numerical relaying, it is possible to adapt the trip characteristic in accordance with system condition [14]-[15]. In this chapter, an adaptive backup protection of subsequent section of a series compensated line with capacitor placed away from the relay bus is proposed. With the fault current through the capacitor exceeding its protective level, the MOV operates. In the apparent impedance computation for the adaptive setting, the coupling among the sequence networks [62] for the MOV-capacitor combination is taken into account. For adaptive distance relay setting, information on compensation level and operating condition are obtained from prefault synchronized data collected from both the ends. The capacitor and MOV combination may be bypassed at times by the air-gap arrangement when the fault persists for elongated period. The MOV operation is adjudged by the fault current through the capacitor and during the MOV operation the impedance offered by the capacitor and MOV combination is computed using the fault current. For such a situation, synchronized data are used to estimate the status of the capacitor during fault and the relay setting for zone 2/zone 3 is adapted accordingly. Proposed technique is tested for a 400-kV series compensated transmission system. The results from the simulation in EMTDC/PSCAD show high accuracy.

4.2 Apparent Impedance Calculation for Series Compensated Line

Series compensation may be available at the middle, at one or both ends of a line. A two source system is considered for apparent impedance calculation as shown in Fig. 4.1. The series compensation available at middle of line section MN is considered first. Zone 2 of the distance relay located at bus M and in the similar way zone 3 can be studied. The relation for prefault voltages of both sides can be written as,

$$\frac{\bar{\mathrm{E}}_{\mathrm{P}}}{\bar{\mathrm{E}}_{\mathrm{N}}} = he^{-\mathrm{j}\delta} \tag{4.1}$$

where*h* is the voltage magnitude ratio and δ is the phase angle difference between $\bar{\mathrm{E}}_{\mathrm{M}}$ and $\bar{\mathrm{E}}_{\mathrm{P}}$. While deriving the characteristics for zone 2 protection for the system the line segment between the relay and capacitor will have similar characteristics to a normal line. For capacitor portion, two issues arise during faults (i) without and (ii) with the operation of MOV. The subsequent portion of the line beyond the capacitor and 50% of the adjacent line section for zone 2 will have impedances similar to a normal line. For zone 2 protection the seen impedance for the relay at M is obtained by analyzing faults at different points on line MN and 50% of the adjacent line section NP.

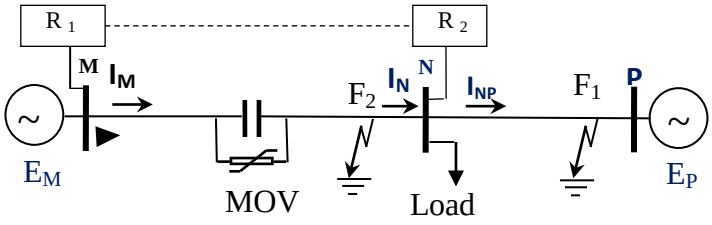

Fig. 4.1. PMUs at the two buses in the series compensation

For the system in Fig. 4.1, consider ag-type fault at a distance ‘d’ pu away from the capacitor. The sequence diagram for the case is shown in Fig. 4.2. The prefault currents through impedances$\mathrm{Z_{SM1}}$,$\mathrm{Z_{LM1}}$, $\mathrm{X_C}$, $\mathrm{Z_{LF1}}$and $\mathrm{Z_{LP1}}$ are $\bar{I}_{\mathrm{SM}}$,$\bar{I}_{\mathrm{LM}}$,$\bar{I}_{\mathrm{Lc}}$, $\bar{I}_{\mathrm{LN}}$and $\bar{I}_{\mathrm{LP}}$ respectively. Using the information on system condition calculated by (4.38), (4.39),(4.1)and compensation level (-j$\mathrm{X_C}$) by (4.37), current $\bar{I}_{\mathrm{LM}}$ is calculated using ABCD parameters approach as,

$$\bar{I}_{SM}=\bar{E}_{M}\left[\frac{D}{B}-\frac{he^{-j\delta}}{B}\right] \tag{4.2}$$

where prefault ABCD parameters are mentioned in (4.3).

$$\begin{bmatrix}A & B\\ C & D\end{bmatrix}=\begin{bmatrix}1 & Z_{SM1}\\ 0 & 1\end{bmatrix}\begin{bmatrix}1 & 0\\ Y_{cM1} & 1\end{bmatrix}\begin{bmatrix}1 & Z_{LM1}\\ 0 & 1\end{bmatrix}\begin{bmatrix}1 & 0\\ Y_{cM1} & 1\end{bmatrix}\begin{bmatrix}1 & -jX_{C}\\ 0 & 1\end{bmatrix}\begin{bmatrix}1 & 0\\ Y_{cN1} & 1\end{bmatrix}\begin{bmatrix}1 & Z_{LN1}\\ 0 & 1\end{bmatrix}$$
$$\begin{bmatrix}1 & 0\\ Y_{cN1} & 1\end{bmatrix}\begin{bmatrix}1 & L\\ 0 & 1\end{bmatrix}\begin{bmatrix}1 & 0\\ Y_{cP1} & 1\end{bmatrix}\begin{bmatrix}1 & Z_{LP1}\\ 0 & 1\end{bmatrix}\begin{bmatrix}1 & 0\\ Y_{cP1} & 1\end{bmatrix}\begin{bmatrix}1 & Z_{SP1}\\ 0 & 1\end{bmatrix} \tag{4.3}$$

Once$\bar{I}_{SM}$ is calculated, $\bar{I}_{LM}$,$\bar{I}_{Lc}$, $\bar{I}_{LN}$ and $\bar{I}_{LP}$ are obtained using network parameters. Considering positive sequence parameters, the prefault voltage at the fault point F is obtained as,

$$\bar{V}_{aF}=\bar{E}_{M}-\bar{I}_{SM}Z_{SM1}-\bar{I}_{LM}Z_{LM1}-\bar{I}_{Lc}(-jX_{c})-\bar{I}_{LS}Z_{LF1} \tag{4.4}$$

For ag-type fault, fault current is calculated by

$$\bar{I}_{F1}=\bar{I}_{F0}=\bar{I}_{F2}=\frac{\bar{V}_{aF}}{Z_{SUM}+3R_{F}} \tag{4.5}$$

where $Z_{SUM}=2\left(\frac{Z_{M1}Z_{P1}}{Z_{M1}+Z_{P1}}\right)+\left(\frac{Z_{M0}Z_{P0}}{Z_{M0}+Z_{P0}}\right)$

Z_{M1} , Z_{P1}andZ_{M0}, $Z_{P0}$are equivalent positive and zero sequence impedances from F to M and F to P side source respectively.

The sequence currents from O to F will be,

$$\bar{I}_{OF1}=\bar{I}_{OF2}=W_{1}\bar{I}_{F1}\ ,I_{OF0}=W_{0}\bar{I}_{F0} \tag{4.6}$$

The distribution factors in (4.6) are defined as:

$$W_{1}=\frac{Z_{P1}}{Z_{M1}+Z_{P1}}\quad,\qquad W_{0}=\frac{Z_{P0}}{Z_{P0}+Z_{M0}}$$

The sequence currents through Z_{LF1}, $Z_{LF2}$and Z_{LF0}will be,

$$\bar{I}_{LF1}=-C_{11}\bar{V}_{1F}+D_{11}\bar{I}_{OF1}\ , \tag{4.7}$$

$$\bar{I}_{LF2}=-C_{12}\bar{V}_{2F}+D_{12}\bar{I}_{OF2}\ , \tag{4.8}$$

$$\bar{I}_{LF0}=-C_{10}\bar{V}_{0F}+D_{10}\bar{I}_{OF0} \tag{4.9}$$

where $\bar{V}_{1F}$, $\bar{V}_{2F}$ and $\bar{V}_{0F}$ are sequence voltages at the fault point. Corresponding ABCD parameters can be expressed as:

$$\begin{bmatrix} A_{11} & B_{11} \\ C_{11} & D_{11} \end{bmatrix} = \begin{bmatrix} 1 & 0 \\ Y_{cF1} & 1 \end{bmatrix} \begin{bmatrix} 1 & Z_{LF1} \\ 0 & 1 \end{bmatrix} \tag{4.10}$$

Similarly C_{12}, D_{12}, C_{10} and D_{10} can be obtained from the negative and zero sequence networks. The sequence currents through capacitor using ABCD parameter approach are given by,

$$\bar{I}_{c1} = -C_{21}\bar{V}_{1F} + D_{21}\bar{I}_{OF1} \tag{4.11}$$

$$\bar{I}_{c2} = -C_{22}\bar{V}_{2F} + D_{22}\bar{I}_{OF2} \tag{4.12}$$

$$\bar{I}_{c0} = -C_{20}\bar{V}_{0F} + D_{20}\bar{I}_{OF0} \tag{4.13}$$

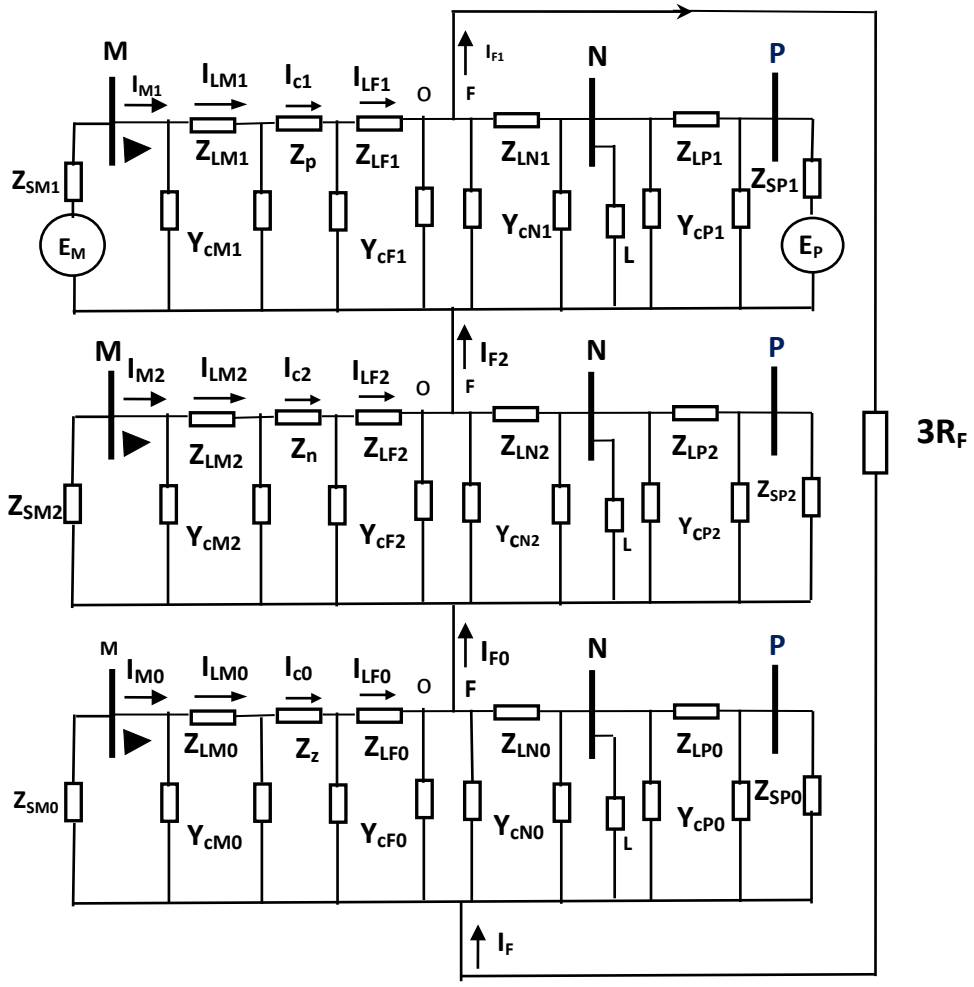

Fig. 4. 2. Sequence diagram for ag -type fault after the series capacitor

whereC_{21} andD_{21}can be expressed as,

$$\begin{bmatrix} A_{21} & B_{21} \\ C_{21} & D_{21} \end{bmatrix} = \begin{bmatrix} 1 & 0 \\ Y_{cF1} & 1 \end{bmatrix} \begin{bmatrix} 1 & Z_{LF1} \\ 0 & 1 \end{bmatrix} \begin{bmatrix} 1 & 0 \\ Y_{cF1} & 1 \end{bmatrix} \tag{4.14}$$

Similarly from negative and zero sequence networks C_{22} ,D_{22},$C_{20}$and D_{20} can be obtained. The capacitor current will be,

$$\bar{I}_{c} = \bar{I}_{Lc} + \bar{I}_{c1} + \bar{I}_{c0} + \bar{I}_{c2} \tag{4.15}$$

$\bar{I}_{Lc}$ is the prefault current through the capacitor. If the ratio of fault current through capacitor and protective level current $I_{pu} = \frac{|\bar{I}_{c}|}{I_{pr}}$, is more than the set value 0.98 the equivalent impedance of the MOV protected series capacitor is given by [65],

$$Z_{eq} = R_{eq} - jX_{eq} \tag{4.16}$$

where

$$R_{eq} = X_{C}\,(0.0745 + 0.49e^{-0.243I_{pu}} - 35.0e^{-5.0I_{pu}} - 0.6e^{-1.4I_{pu}}) \tag{4.17}$$

$$X_{eq} = X_{C}(0.1010 - 0.005749I_{pu} + 2.088e^{-0.8566I_{pu}}) \tag{4.18}$$

The impedance matrix due to the MOV in the three phases is represented as:

$$Z_{eqabc} = \begin{bmatrix} Z_{eqa} & 0 & 0 \\ 0 & Z_{eqb} & 0 \\ 0 & 0 & Z_{eqc} \end{bmatrix} \tag{4.19}$$

Due to the unsymmetrical nature of the impedance in three phases couplings between the sequence networks are present. The symmetrical transformation of the equivalent impedance becomes [132],

$$Z_{eq\_012} = \frac{1}{3}\begin{bmatrix} Z_{h} & Z_{m1} & Z_{m2} \\ Z_{m2} & Z_{h} & Z_{m1} \\ Z_{m1} & Z_{m2} & Z_{h} \end{bmatrix} \tag{4.20}$$

where $Z_{h} = \frac{1}{3}(Z_{eqa} + Z_{eqb} + Z_{eqc})$, $Z_{m1} = \frac{1}{3}(Z_{eqa} + \alpha Z_{eqb} + \alpha^{2} Z_{eqc})$,

$Z_{m2} = \frac{1}{3}(Z_{eqa} + \alpha^{2} Z_{eqb} + \alpha Z_{eqc})$ and $\alpha = e^{-j(2\pi/3)}$

The sequence impedances considering the coupling between the series compensation portion are obtained as $Z_{\mathrm{p}}, Z_{\mathrm{n}}$ and Z_z [130]. Where subscript p, n and z refer to positive, negative and zero respectively.

$$Z_{\mathrm{p}}=\left(\mathrm{Z_h}+\frac{\bar{I}_{\mathrm{c2}}}{\bar{I}_{\mathrm{c1}}}\mathrm{Z_{m1}}+\frac{\bar{I}_{\mathrm{c0}}}{\bar{I}_{\mathrm{c1}}}\mathrm{Z_{m2}}\right) \tag{4.21}$$

$$Z_{\mathrm{n}}=\left(\mathrm{Z_h}+\frac{\bar{I}_{\mathrm{c1}}}{\bar{I}_{\mathrm{c2}}}\mathrm{Z_{m2}}+\frac{\bar{I}_{\mathrm{c0}}}{\bar{I}_{\mathrm{c2}}}\mathrm{Z_{m1}}\right) \tag{4.22}$$

$$Z_{\mathrm{z}}=\left(\mathrm{Z_h}+\frac{\bar{I}_{\mathrm{c2}}}{\bar{I}_{\mathrm{c0}}}\mathrm{Z_{m2}}+\frac{\bar{I}_{\mathrm{c1}}}{\bar{I}_{\mathrm{c0}}}\mathrm{Z_{m1}}\right) \tag{4.23}$$

Since the capacitor current and the equivalent impedance offered by MOV protected capacitor are dependent; the current through the capacitor is solved iteratively using the sequence impedances. The change in capacitor current $\Delta I_c^k = I_c^k - I_c^{k-1}$ is checked for the $\mathrm{k^{th}}$ iteration. If ΔI_c^k in two consecutive iteration becomes negligible then the equivalent impedance offered by the combination for sequence networks $Z_{\mathrm{p}}, Z_{\mathrm{n}}$ and Z_{z} are obtained. If I_{pu} is less than the predefined value 0.98 the MOV will not operate and the equivalent impedance offered by the combination will be

$$Z_{\mathrm{p}} = Z_{\mathrm{n}} = Z_z = -jX_C$$

The sequence currents through $\mathrm{Z_{LM1}}, \mathrm{Z_{LM2}}$ *and* $\mathrm{Z_{LM0}}$ can be now calculated as:

$$\bar{I}_{\mathrm{LM1}} = -\,\mathrm{C_{31}}\bar{V}_{\mathrm{1F}} + \mathrm{D_{31}}\,\bar{I}_{\mathrm{OF1}} \tag{4.24}$$

$$\bar{I}_{\mathrm{LM2}} = -\,\mathrm{C_{32}}\bar{V}_{\mathrm{2F}} + \mathrm{D_{32}}\,\bar{I}_{\mathrm{OF2}} \tag{4.25}$$

$$\bar{I}_{\mathrm{LM0}} = -\,\bar{V}_{\mathrm{0F}} + \mathrm{D_{30}}\,\bar{I}_{\mathrm{OF0}} \tag{4.26}$$

where $\mathrm{C_{31}}$ and $\mathrm{D_{31}}$ are provided in (4.27).

$$\begin{bmatrix}\mathrm{A_{31}} & \mathrm{B_{31}}\\ \mathrm{C_{31}} & \mathrm{C_{31}}\end{bmatrix} = \begin{bmatrix}1 & \mathrm{Z_{LM1}}\\ 0 & 1\end{bmatrix}\begin{bmatrix}1 & 0\\ \mathrm{Y_{cM1}} & 1\end{bmatrix}\begin{bmatrix}1 & \mathrm{Z_p}\\ 0 & 1\end{bmatrix}\begin{bmatrix}1 & 0\\ \mathrm{Y_{cF1}} & 1\end{bmatrix}\begin{bmatrix}1 & \mathrm{Z_{LF1}}\\ 0 & 1\end{bmatrix}\begin{bmatrix}1 & 0\\ \mathrm{Y_{cF1}} & 1\end{bmatrix} \tag{4.27}$$

Similarly $\mathrm{C_{32}}$, $\mathrm{D_{32}}$, $\mathrm{C_{30}}$ and $\mathrm{D_{30}}$ are calculated by using negative and zero sequence line parameters respectively. The sequence current through source impedance at bus Min Fig. 4.2 can be calculated as:

$$\bar{I}_{M1} = -\,C_{41}\bar{V}_{1F} + D_{41}\,\bar{I}_{OF1} \tag{4.28}$$

$$\bar{I}_{M2} = -\,C_{42}\bar{V}_{2F} + D_{42}\,\bar{I}_{OF2} \tag{4.29}$$

$$\bar{I}_{M0} = -\,C_{40}\bar{V}_{0F} + D_{40}\,\bar{I}_{OF0} \tag{4.30}$$

where C_{41} and $D_{41}$are obtained from ABCD parameter in (4.31).

$$\begin{bmatrix} A_{41} & B_{41} \\ C_{41} & C_{41} \end{bmatrix} = \begin{bmatrix} 1 & 0 \\ Y_{cM1} & 1 \end{bmatrix}\begin{bmatrix} 1 & Z_{LM1} \\ 0 & 1 \end{bmatrix}\begin{bmatrix} 1 & 0 \\ Y_{cM1} & 1 \end{bmatrix}\begin{bmatrix} 1 & Z_p \\ 0 & 1 \end{bmatrix}\begin{bmatrix} 1 & 0 \\ Y_{cF1} & 1 \end{bmatrix}\begin{bmatrix} 1 & Z_{LF1} \\ 0 & 1 \end{bmatrix}\begin{bmatrix} 1 & 0 \\ Y_{cF1} & 1 \end{bmatrix} \tag{4.31}$$

The current through relay during ag- type fault for A-phase can be obtained as

$$\bar{I}_{aM} = \bar{I}_{SM} + \bar{I}_{M1} + \bar{I}_{M2} + \bar{I}_{M0} \tag{4.32}$$

where$\bar{I}_{SM}$ is the prefault current mentioned in (4.2). The voltage at bus M with MOV operation is obtained as

$$\bar{V}_{aM}=(\bar{I}_{LN}Z_{LF1} + \bar{I}_{Lc}\,(-jX_C)+\bar{I}_{LM}Z_{LM1})+(2\bar{I}_{LF1}\,Z_{LF1}+\bar{I}_{LF0}Z_{LF0} + \bar{I}_{c1}Z_p +\bar{I}_{c2}Z_n+\bar{I}_{c0}Z_z +2\bar{I}_{LM1}\,Z_{LM1}+\bar{I}_{LM0}Z_{LM0} + 3R_F\bar{I}_F) \tag{4.33}$$

The seen impedance for line-to-ground fault can be calculated from relation,

$$Z_{app} = \frac{\bar{V}_{aM}}{\bar{I}_{aM}+K_0\bar{I}_{M0}} \tag{4.34}$$

where K_0 is the zero sequence compensating factor [26], $K_0 = \frac{Z_{0L}-Z_{1L}}{Z_{1L}}$, with $Z_{0L}$and Z_{1L} be the zero and positive sequence impedances of the line respectively. The K_0 value is different for the fault beyond the capacitor and depends on the MOV operation. However in the study we have used fixed value of K_0, for both setting and decision processes which provides correct results and is addressed in [64].

Since shunt currents sequence network are negligible, apparent impedance can be expressed as in (4.34).

$$Z_{app}=\frac{f_1 + 3R_F}{f_2} \tag{4.35}$$

where$f_1 = dZ_{1L}K_D+2B_{41}W_1 + B_{40}W_0 + ((P_2 - P_3Y_{cM1})(-jX_C) + P_2Z_{LM1})K_T$

$$f_2 = P_1 K_T - \ 2C_{41}Z_{M1}W_1 + 2W_1D_{41} + (1 + K_0)(-C_{40}Z_{M0}W_0 + W_0D_{40})$$

$$K_T = \left[\frac{Z_{SUM} + 3R_F}{P_5}\right], \quad P_1 = \left[\frac{D}{B} - \frac{he^{-j\delta}}{B}\right],$$

$$P_2 = P_1 - [1 - P_1Z_{SM1}]Y_{cM1}, \quad P_3 = P_1 - P_1Z_{SM1} - P_2Z_{LM1},$$

$$P_4 = P_1 - P_1Z_{SM1} - P_2Z_{LM1} - P_2 - P_3Y_{cM1}, K_D = P_2 - P_3Y_{cM1} - P_4Y_{cM1},$$

$$P_5 = 1 - P_1Z_{SM1} - P_2Z_{LM1} - (P_2 - P_3Y_{cM1}) - jX_C - (P_2 - P_3Y_{cM1} - P_4Y_{cM1})dZ_{1L}$$

4.3 Problems with Distance Relay in the presence of Series Compensation

Distance relay face overreach problem for a fault beyond the series compensation. To demonstrate this, trip characteristic is obtained for variation in distance of fault from relay location and up to 50% of the next line and fault resistance from 0 to 200 Ω. The line is 60% compensated at the middle. The quadrilateral trip boundary plotted in Fig. 4.3is shown for two different series compensation levels either with full operation of (60%) or capacitor is bypassed (no compensation). It is to be noted that boundaries for the compensated line for fault distance variation 'd' at fixed R_f (0 or 200 Ω), has an excursion due to the presence of series compensation.

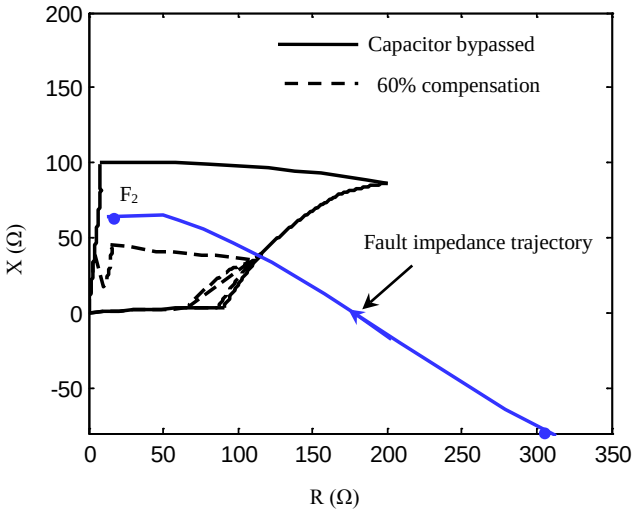

Fig. 4.3. Comparison of zone 2 trip boundaries with 60 % compensation at middle and capacitor bypassed.

Consider an example of a line-to-ground fault at F_2 in the system of Fig. 4.1 when capacitor is bypassed. The fault impedance trajectory is shown in Fig. 4.3. It is evident from the figure that fault trajectory finally settles inside the boundary which is set considering capacitor is bypassed. Thus zone 2/zone 3 setting should be adapted in accordance with status of the capacitor. This is accomplished by using synchronized data obtained from both end relays with GPS facility.

4.4 Proposed Adaptive Backup Scheme

A 400 kV, 50 Hz series compensated power system as shown in Fig. 4.1 is considered. For this case measurement units (distance relays with GPS facility) are considered to be available at the two buses M and N. The buses are connected with a communication system which may be available for any other purpose in the system. Adaptive zone 2 and zone 3 setting of relay at bus M in the system is to be accomplished using power system condition and the level of series compensation. The positive sequence phasor data at a rate of 50 frames per second from the ends are processed at the relay end to obtain the compensation level. The impedance between two buses M and N can be calculated as in [115]:

$$Z_{1\mathrm{MN}}=\frac{(\bar{V}_{\mathrm{M}})^2-(\bar{V}_{\mathrm{N}})^2}{\bar{V}_N\,\bar{I}_{\mathrm{M}}\;+\;\bar{V}_{\mathrm{M}}\bar{I}_{\mathrm{N}}} \tag{4.36}$$

where$\bar{V}_{\mathrm{M}},\bar{I}_{\mathrm{M}}$and $\bar{V}_{\mathrm{N}},\bar{I}_{\mathrm{N}}$ are positive sequence phasors at bus M and N for MN section respectively. The series compensation X_C present in the line is obtained from the imaginary parts of the calculated impedance between bus M and N ($Z_{1\mathrm{MN}}$) and positive sequence impedance of the line ($Z_{1\mathrm{L}}$).

$$\mathrm{X_C}=\mathrm{Im}(Z_{1\mathrm{L}})\;-\;\mathrm{Im}(Z_{1\mathrm{MN}}) \tag{4.37}$$

Using bus N synchronized data, source $\bar{E}_{\mathrm{P}}$ can be written as:

$$\bar{E}_{\mathrm{P}}=\mathrm{A_P}\bar{V}_{\mathrm{N}}-\mathrm{B_P}\bar{I}_{\mathrm{NP}} \tag{4.38}$$

whereA_P and $B_P$are the ABCD parameters for the section between bus N and Pbus source. Similarly $\bar{E}_{\mathrm{M}}$is obtained from the measurements at bus M.

$$\bar{E}_{\mathrm{M}}=\bar{V}_{\mathrm{M}}-\mathrm{Z_{SM1}}\,\bar{I}_{\mathrm{M}} \tag{4.39}$$

whereZ_{SM1} is the source impedance at bus M.

Once compensation level is known using (4.37), zone 2/zone3 setting are obtained at bus M. Zone 2, being the primary protection for the line beyond zone 1, cannot detect faults with a reduced reach when compensation is bypassed. Similarly zone-3 which provides backup for the next line will also face problem. Such problems will be severe when circuit breaker fails in the next line and fault is not detected by backup relay for capacitor bypassed condition. As the delay in data transfer is less than the time setting of zone-2 and zone-3, this method is feasible for zone-2 and zone-3.

The conduction of MOV is adjudged from the capacitor current level and corresponding equivalent impedance of the combination is computed from the relations (4.17)-(4.18). The equivalent impedance offered by MOV and capacitor combination is calculated by iterative way which converges in maximum seven iterations and the extra computation time is not an issue for setting zone 2/zone 3. On the other hand for a MOV-capacitor combination bypassed condition, mutual coupling is not present and the adaptive setting is obtained accordingly.

The series compensation present in the line is computed and the system operating condition is calculated by using the voltage and current phasors obtained from the both end busses. The flow diagram of the proposed algorithm for setting the relay characteristic is shown in Fig. 4.4. The steps of this algorithm are as follows:

Step 1 : Synchronized data from both ends of the line are collected.

Step 2 : h and δ of the equivalent source are computed (4.1), (4.38) and (4.39).

Step 3 : Compensation level is computed in next step and the trip boundary considering MOV operation is generated using (4.35).

Step 4 : During fault compensation level is checked and the characteristic is adapted for compensation bypassed condition.

The MOV operation is adjudged by the fault current through the capacitor. There are two different ways to implement the proposed scheme. One approach, being a protection decision, adaptive distance relay should take the synchronized data as input and the setting calculation are done in the relay. Otherwise, the system condition and level of

compensation can be calculated outside the relay and the setting can be computed which should be transferred to the distance relay for proper decision. The proposed scheme requires a dedicated communication channel. If the data from other ends of the line is not available the proposed scheme will revert back to the conventional scheme.

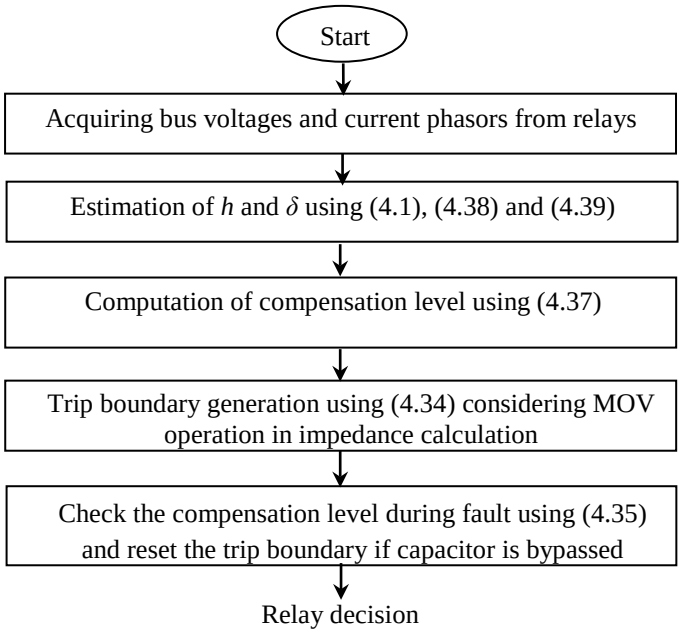

Fig. 4.4. Flow diagram for the proposed adaptive technique.

4.5 Results

The method proposed for adaptive setting of zone 2 is tested with a 3 bus system having series capacitor at (i) middle of line RS as in Fig. 4.1 (ii) at the end of the line. The compensation level is calculated by synchronized voltage and current from both ends of line and the adaptive trip characteristic is obtained by using (4.34). One-cycle discrete Fourier transform is used to compute the phasors from sampled data. At first the influence of MOV operation in the trip boundary is studied. Numerous situations including operation of MOV and series compensation at two different locations are considered for adaptive setting during line-to-ground fault. Besides adaptive setting using prefault data, results are also provided for zone 3 setting during fault by estimating capacitor status. In all cases the source bus P in Fig. 4.1 is considered to be the reference and at 400 kV with phase angle of 0°.

4.5.1. Significance of MOV Operation in the Trip Boundary and Corresponding Modeling

MOV operation depends on fault current. To observe the effects of MOV operation on seen impedance, line-to-ground fault beyond the capacitor is simulated on system of Fig. 4. 1 by varying the fault distance d from the capacitor with negligible fault resistance. Second and third columns of Table 4.1 provide actual impedance with and without MOV operation. It is observed that MOV operation modulates seen impedance significantly and therefore, to calculate trip boundary setting, operation of MOV should be taken into account. In the proposed method MOV modeling is considered in the adaptive setting calculation for the relay.

Table 4.1
Comparison of Calculated Impedance with and Without MOV Operation

Fault distance (d) in p.u.	Actual		Calculated	
	Apparent impedance(Ω) without MOV operation	Apparent impedance(Ω) with MOV operation	Apparent impedance(Ω) without MOV operation	Proposed apparent impedance(Ω) with MOV operation
0.6	5.39+j13.17	11+j26	5.3+j13.07	9.9+j28.89
0.7	6.19+j18.11	10.6+j33.3	6.13+j18.01	11.03+j35.15
0.8	6.89+j22.58	10.9+j37.4	6.79+j22.51	11.52 +j40.93
0.9	7.56+j27.53	12.78+j42.66	7.52+j27.51	11.98 +j44.81
1	8.23+j33.05	14.02+j51.01	8.21+j33.01	13.1 +j53.77
1.1	8.76+j37.83	14.73+j59.57	8.71+j37.79	13.83+ j62.14

Table 4.1 provides a comparative assessment of the proposed method to calculate the apparent impedance during MOV operation. The fourth and fifth columns are for the corresponding values calculated using the boundary settings with and without MOV consideration. It is clearly understood from the results that proposed method has high accuracy advantage over the earlier method. In the next section trip boundary setting is accomplished by the proposed method for different operating conditions.

4.5.2. Inaccuracies in MOV Modeling

MOV modeling considered in the relay setting may be inaccurate as the characteristic may be changing with time. To observe the inaccuracies in MOV modeling the characteristic of the MOV are varied considering a 5% change in its different parameters. The variation in calculated and actual apparent impedances is observed for a line-to-

ground fault at 0.9 pu. fault distance from relay. From the Table 4.2, it is observed that the percentage variations in reactance and resistance with the modified parameters are not significant. Thus variation MOV parameters will not create any problem to the proposed method.

Table 4.2
Variation in Resistance and Reactance Due to Inaccuracies in MOV Modeling

% variation in parameter	Actual R (Ω)	Calculated R (Ω)	% change	Actual X (Ω)	Calculated X (Ω)	% change
2	12.79	12.65	-1.09	42.66	44.7	2.4
-2		12.25	-4.22		43.4	1.7
5		13.01	1.72		44.95	5.5
-5		12.05	-5.7		41.21	-3.4

4.5.3. Boundary Setting for Line-to-ground Fault with 60 % Compensation at the Middle

The technique is evaluated with a prefault system condition of h =1 and δ= 10˚ and the trip boundary is generated for line- to-ground fault. The prefault synchronized data are applied to calculate the compensation level and to estimate the system condition. It is found that at this situation the compensation has Z_C= -j47.86 Ω (Table. 4.3), which confirms the presence of full compensation (60%). Using this information in (4.34) the trip boundary is generated and plotted in Fig. 4.5 (calculated curve). The accuracy of such generated boundary is checked with trip boundary obtained through time-domain simulation using EMTDC/PSCAD for line-to-ground faults with fault resistance varying from 0 Ω to 200 Ω at different locations on the line. For each case, sampled voltage and current data obtained from the simulation, are used to calculate the relay apparent impedance and plotted in Fig. 4.5 (actual curve). From the plot, it is observed that the actual curve closely matches with the boundary generated using (4.34). It confirms that the trip characteristic is accurate for zone 2 setting at this operating condition.

Table. 4.3
Synchronized data with 60 % Compensation at middle with $h = 1$, $\delta = 10^{\circ}$

Relay	Bus Voltage (kV)	Line Current (kA)		Calculated		
				$Z_C(\Omega)$	h	$\delta(^{\circ})$
Bus-M	229.06- j32.37	I_R	0.711+ j0.125	-j47.86	1.0	9.83
Bus-N	223.95-j54.63	I_S	0.67- j0.078			
		I_{ST}	0.458- j0.026			

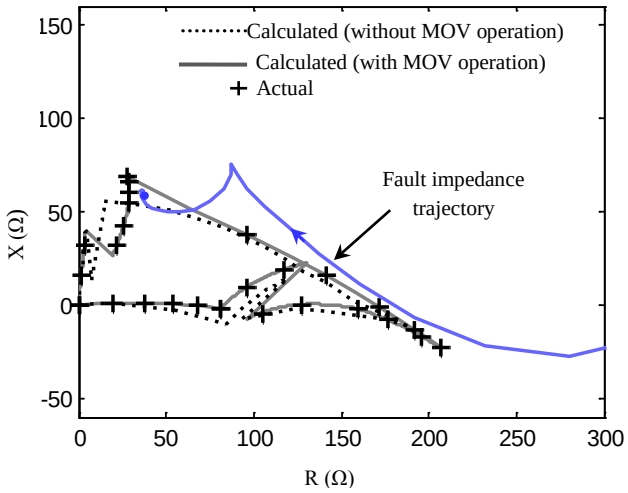

Fig. 4.5 Trip boundary with 60% compensation at middle with $h = 1$, $\delta=10^{0}$.

To see the advantage of the MOV modeling in boundary setting, a line-to-ground fault at 0.9 pu. distance from the M bus in line MN is created and the fault impedance trajectory is plotted in Fig. 4.5 which settles inside proposed boundary. This indicates trip boundary setting is beneficial for proper protection decision.

4.5.4. Trip Boundary with Series Compensation Bypassed at the Middle for a Different System Condition

Sometimes the capacitor may be bypassed due to the unbalance in capacitor banks or for maintenance purpose. When the capacitor bank protective devices operate, it cannot be reinserted to the system immediately. In each case it will lead to an uncompensated line condition. A different example is simulated without series compensation in the line of the system in Fig. 4.1.

Synchronized phasor data collected from the two ends are provided in Table. 4.4. The calculated compensation level Z_C=-j0.61Ω (a low value) shows that the capacitor is bypassed. Using this information the trip boundary is generated by (4.34) and plotted in Fig. 4.6. The generated boundary is compared with the seen impedance obtained from the simulation using EMTDC/PSCAD for line-to-ground faults at different locations varying the fault resistance 0-200 Ω. The results also show the strength of the method in providing trip boundary correctly.

Table . 4.4
Synchronized data for Capacitor Bypassed with h = 0.99, δ = -5˚

Relay	Bus Voltage (kV)	Line Current (kA)		Calculated		
				Z_C(Ω)	h	δ(˚)
Bus-M	210.11-j 90.9	I_M	0.045+j 0.179	-j0.61	0.987	-5.06
Bus-N	217.60-j84.68	I_N	-0.126+j 0.011			
		I_{NP}	-0.332+j0.068			

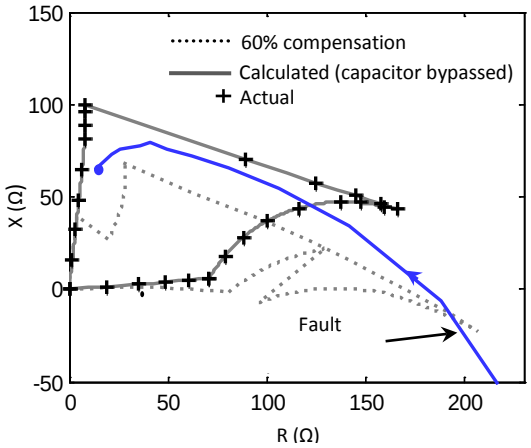

Fig. 4.6. Trip boundary with capacitor bypassed at middle with h = 0.99, δ = -5^0.

To see the advantage of the method a line-to-ground fault at 0.9 pu. from M bus in line MN is simulated. The fault impedance trajectory is shown in Fig. 4.6. The fault impedance trajectory remains outside the set boundary before the fault and inside the adaptive boundary, this clearly shows that by adapting the trip boundary setting the decision can be correct.

4.5.5. Boundary Setting for line-to-ground fault with Compensation bypassed during fault.

During a fault, the capacitor and MOV combination may be bypassed at times by the air-gap arrangement when the fault persists for elongated period. The setting for zone-2 needs to be changed during this condition. Synchrophasor data from both the ends of transmission line are used to obtain the capacitor status correctly and setting can be changed accordingly. To verify this, a system is simulated with the combination bypassed during line-to ground fault. Synchronized phasor data collected from the two ends are provided in Table. 4.5. The estimated compensation level Z_c=-j0.98Ω shows that the capacitor is bypassed with the trip boundary generated by using (4.35) and plotted in Fig. 4.7. The generated boundary compared with the seen impedance obtained from the simulation for line-to-ground faults at different locations varying the fault resistance varying 0-200 Ω. The figure shows the accuracy of the proposed method.

Table. 4.5
Synchronized data for Capacitor Bypassed with h = 1, δ = 10˚

Relay	Bus Voltage (kV)	Line Current (kA)		Calculated $Z_C(\Omega)$
Bus-M	227.94- j32.88	I_M	0.387+ j0.36	-j0.98
Bus-N	188.53-j58.19	I_N	0.341- j0.54	

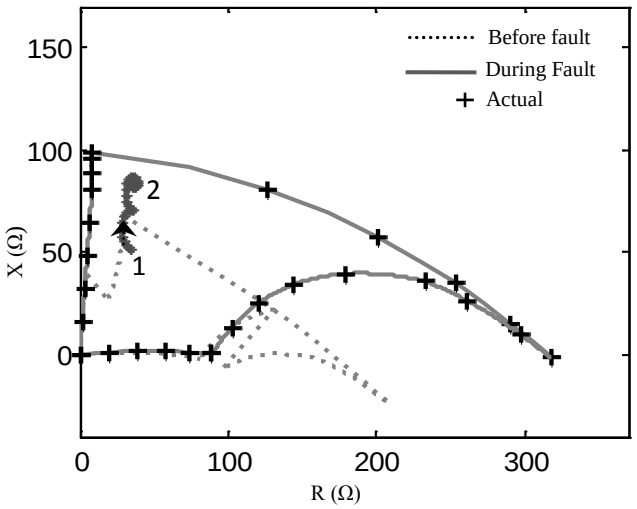

Fig. 4.7. Trip boundary with 60% series compensationbypassed during fault.

A line-to-ground fault with 5Ω fault resistance at d=1.05 is simulated at the same system condition and seen impedance of the relay for this case is plotted on the Fig. 4.7.The inner curve corresponds to the characteristic 60% compensated situation. The initial fault position point-1 is in the plot and then the seen impedance moves to point 2 finally. Thus the setting for zone 2 during different condition of system including series compensation -MOV combination as shown in the figure is justified.

4.5.6. Zone 3 Boundary Setting for line-to-ground fault with series compensation at the end of the line.

The capacitor in a system may be present at the end of section MN as shown in Fig. 4.8. Zone 3 at M bus should be set considering the compensation level for accurate decision. For fault closer to the capacitor, the combination may be bypassed for which zone 3 setting is to be modified. The method is evaluated for 60% compensation at the end of the line.

Before fault, the zone 3 of M bus relay is set considering compensation level in the section MN. The prefault synchronized data are applied to compute the compensation level present in the line. Table 4.6 provides the prefault data for the system before the fault from which compensation level and system condition is obtained. Using (4.37) level of compensation estimated is found to be Z_C=-j 46.17. The zone 3 trip boundary is generated for line-to-ground type fault and plotted in Fig. 4.9(calculated). For this case also apparent impedance boundary (actual) is obtained using PSCAD simulated data and it is found that the two characteristic match closely. Similarly the synchronized data can be applied for adaptive setting during fault.

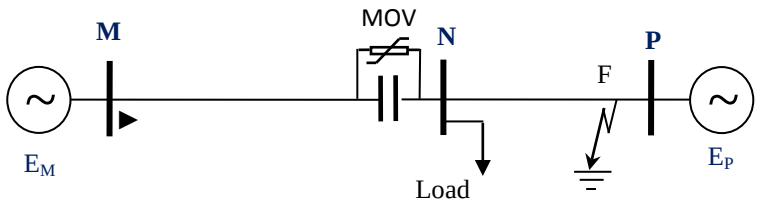

Fig. 4.8. Equivalent two-source system with series compensation at the end.

Table . 4.6
Synchronized data for Capacitor at end of line with h = 0.95, $\delta = 20^{\circ}$

Relay	Bus Voltage (kV)	Line Current (kA)		Calculated		
				Z_C (Ω)	h	$\delta(^{\circ})$
Bus M	219.74+ j5.12	I_M	1.25+ j0.087	-j46.17	0.949	20.0
Bus N	226.22-j37.37	I_N	1.21+ j0.008			
		I_{NP}	1.005+ j0.123			

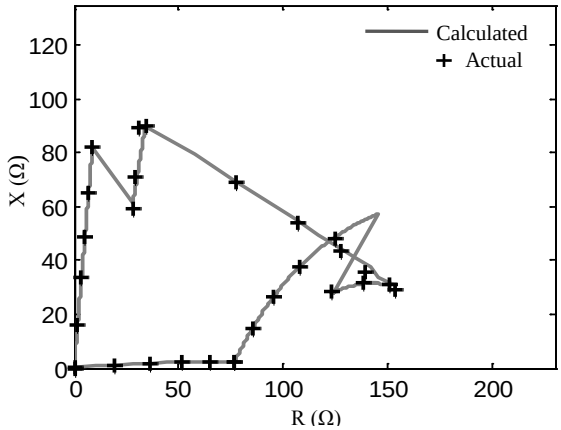

Fig. 4.9. Trip boundary with 60% series compensation at the end.

4.5.7. Zone 3 Boundary Setting for Line-to-ground Fault with Series Compensation Bypassed During Fault at the End of the Line.

The method is evaluated for 60% compensation bypassed during fault at the end of the line. Before fault, the zone 3 of M bus relay is set considering compensation level in the section MN.In the next case, a line-to-ground fault close to bus Nis simulated with a fault resistance of 10 Ω for a system condition of h=0.95 and δ= 20˚. In the initial period of the fault the capacitor was in the circuit and bypassed by the air-gap arrangement after 3 cycles of fault inception. Compensation level available in the line MN is monitored continuously and obtained from positive sequence synchronized data. For this case it is, Z_C=-j0.97 Ω (refer Table. 4.7) and trip boundary generated using this is plotted in Fig. 4.10.

To see the need of adaptive setting, the apparent impedance seen by the relay bus M during this period iscomputed and plotted in Fig. 4.10. It is observed that fault

impedance trajectory reaches to point 1 when series compensation was present in the line and then settles at point 2 following bypassed condition when series compensation is bypassed after 3 cycles(refer marked points in the figure). Out of the relay characteristic plotted, the inside one is for 60% compensation level as set before the fault. The outer relay characteristic corresponding to zero series compensation in the line. It is observed that final fault impedance point at 2 in the trajectory is outside the prefault set characteristic (with 60% compensation) but inside the adaptive setting which is obtained by the scheme. This ensures the advantage of adaptive setting in relay decision.This method can prevent overreaching of the relay and improve the dependability of the system.

Table. 4.7.
Synchronized data series capacitor bypassed at end with $h = 0.95$, $\delta = 20^{\circ}$

Relay	Positive sequence Voltage (kV)	Positive sequence Current (kA)		Calculated Z_C (Ω)
Bus M	214.35+ j7.14	I_M	0.342- j2.43	-j0.97
Bus N	12.03+j0.72	I_N	-0.344- j2.54	

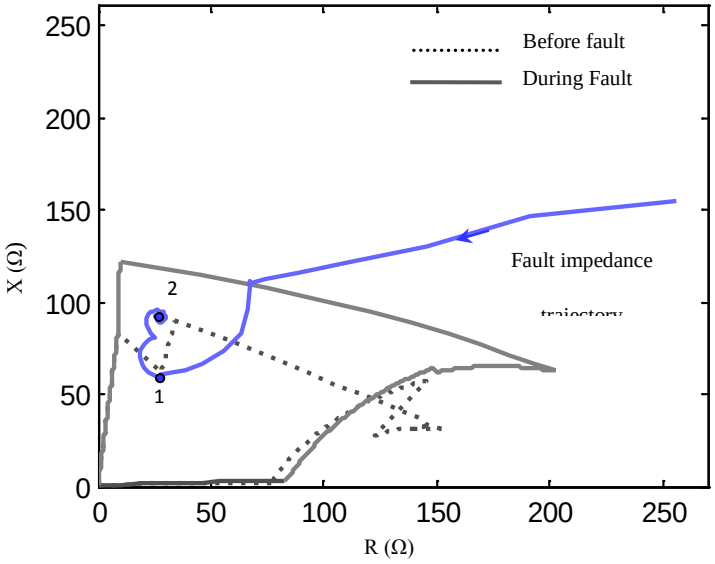

Fig. 4. 10. Trip boundary with compensation bypassed during fault at the end with h = 0.95, $\delta = 20^{0}$.

4.5.8. *Adaptive zone-2 setting for 60% series compensated line in modified 9-bus system.*

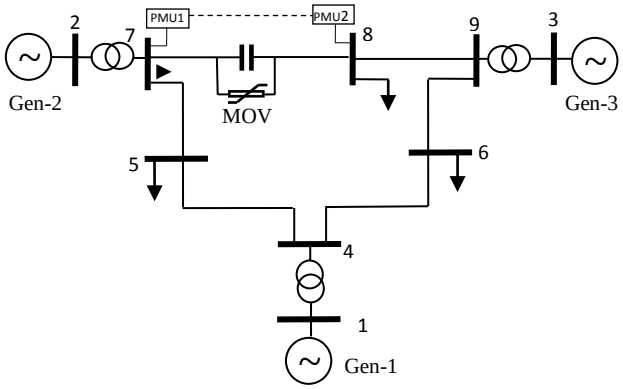

Fig. 4. 11. PMUs with the modified WSCC 9-bus system

Proposed adaptive setting for series compensated network is tested for the modified WSCC 9-bus system as shown in Fig. 11. In the system, line segment between bus-7 and 8 possesses 60% series compensation at the middle. Distance relay at bus-7 is to be adapted in accordance with system condition. The system is first converted to equivalent two port network [130] by using network information. The two equivalent voltage sources are converted to current sources and using delta-star transformation the two port equivalent can be reduced to simple two source equivalent network as in Fig. 4.1.The equivalent source impedances at bus 7 and 9 found to be 1.01+j1.991 Ω and 1.02+j1.981 Ω respectively. The synchronized measurements obtained from both ends of the line connecting between busses are applied to compute the compensation level and the equivalent source voltage.

Estimated compensation level is found to be X_C=-j48.2 Ω (refer Table 4.8). This reveals the presence of full compensation. Using this information and estimated voltage magnitude ratio h , phase angle difference δ from two source equivalent network trip boundary for line-to-ground fault is generated (estimated) and plotted in Fig. 4.12. The characteristic is verified with the apparent impedance for ag-type fault simulated though the EMTDC/PSCAD. The result shows the accuracy of the proposed approach for relay setting.

TABLE 4.8
Synchronized data for 60% Compensation in 9-Bus System

PMU	Bus Voltage (kV)	Line Current (kA)		Z_{1RS} (Ω)	Estimated		
					X_C (Ω)	*h*	$\delta(^\circ)$
1	232.57-j40.78	I_R	0.528+ j0.101	4.43j30.75	-j48.2	1.02	9.88
2	230.16-j56.41	I_S	0.481-j0.110				
		I_{ST}	0.265-j0.057				

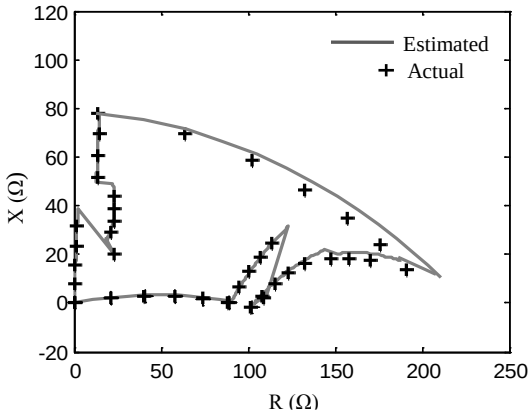

Fig. 12. Trip boundary with 60% compensation at middle of bus 7- 8 modified 9-bus system

4.6 Conclusion

Distance relays protecting series compensated line has limited performance if fault loop includes the series capacitor. However series capacitor may be bypassed due to maintenance purpose or by its protective devices during fault. Distance requires the information on compensation present in the line for accurate operation. In this work Synchronized data at both ends of the line are applied for adaptive zone 2/ zone 3 setting for a series compensated line. Such an adaptive setting is obtained considering MOV operation for apparent impedance derivation using prefault data. The status of capacitor bypassed or not by the air-gap arrangement is confirmed using fault data and the settings are adapted according to the presence of compensation level. The proposed method is evaluated for 400 kV two source equivalent systems for series compensation at various locations of the line and found to be accurate. As evident from the results for numerous cases, the method provides accurate zone 2/zone 3 trip boundary setting for any position of series compensation, level of compensation and operation of MOV protecting the series capacitor.

Secured Zone 3 Protection during Load Encroachment

Three phase fault and load encroachment are balanced phenomena.A load encroachment function is incorporated in distance relay to improve security of protection scheme, confuses with three phase fault during high reactive loading condition.Zone 3 malfunction during such situation often causes cascade line tripping leading to wide area disturbance. In this chapter, voltage phasors of selected buses from a wide area measurement system (WAMs) are used to prevent zone 3 maloperationof a distance relaying scheme during load encroachment. The change in magnitude and phase of bus voltages are used to discriminate three phase fault from load encroachment. Performance of proposed method is tested with New England 39 busand IEEE 118 bus system simulated in EMTDC/PSCAD.

5.1 Introduction

Zone 3 of a stepped distance relay provides remote backup protection for adjacent lines. Due its large reach risk of maloperation increases during heavy system loading condition. At times, load impedance enters into zone 3 and the relay confuses with three phase fault as both are balanced phenomenon and causes undesirable tripping. Investigations on several large area disturbances reveals such maloperation is one of the major cause of cascade tripping in power system [1]-[3].

Zone 3 maloperations can be prevented with certain modifations in the zone 3 characteristic. Modified characteristic like offset mho and lenticular are applied which reduces the dependality of the relay. Load encroachment functions are applied to distance

relay and are set with fixed power factor angle[25] and has limited performance during severe reactive loading condition when the power factor angle varies more than the preset value [86]. As the rate of change of impedance is different for three phase fault and load enchrchment, blinders utilizes this criteria to discriminate heavy loading condition from fault [84]. In literure several methods are proposed to support the zone 3 decision which uses local volatge and current data to derive additional features during disturbance [86]-[88].

Available methods using local information have limited capability in discriminating load to three phase fault. Synchronized phasors, obtained from phasor measurement units (PMUs) placed at specific locations provides wide area visibility. This information can be applied to prevent zone 3 maloperation [101]-[105]. Numerous methods using wide area measurement data are available in the literature to support the zone 3 decisions [106]-[113]. In [112], sequences components at both ends of the line are applied for series compensated to prevent the zone3 maloperation. However, it requiresdata from all the busses of the system.

In this work, to assist zone 3 operation during load encroachment wide area measurement based voltage data areused. During a disturbance, the ratio of change in voltage magnitude and phase angle of selected buses iscomputed to discriminate load encroachment from 3-phase fault thus supplementing zone 3 protection. New England 39 bus and IEEE 118 bus system are used to test the algorithm and results show high accuracy.

5.2 ImpedanceTrajectory during Load Encroachment

The impedance seen by distance relay during a balanced condition can be expressed as,

$$Z_{\text{app}} = \frac{|\bar{V}|^2(\text{P} + j\text{Q})}{\text{P}^2 + \text{Q}^2} \tag{5.1}$$

Where $\bar{V}$ the bus voltage and P, Q are active and reactive powerflowing in the line respectively. From the above relation it is noticed that the apparent impedance decreases with increase in P or Q or both. During this, the apparent impedance locus may enter into zone 3 area and cause maloperation.To prevent this, load encroachment function,

incorporated in distance relay algorithmis based on power factor angleat maximum loading of the line. NERC guidelines define extreme loading conditions as 150% of the emergency current rating of the line with 85% of voltage and a load power factor angle of 30˚ [25]. However under stressed system condition and with high reactive loading, the power factor angle may go beyond 30˚ [82] and the apparent impedance may enter zone 3 outside the set load encroachment area. During this period load encroachment function will fail to prevent zone 3 maloperation [98]-[99].

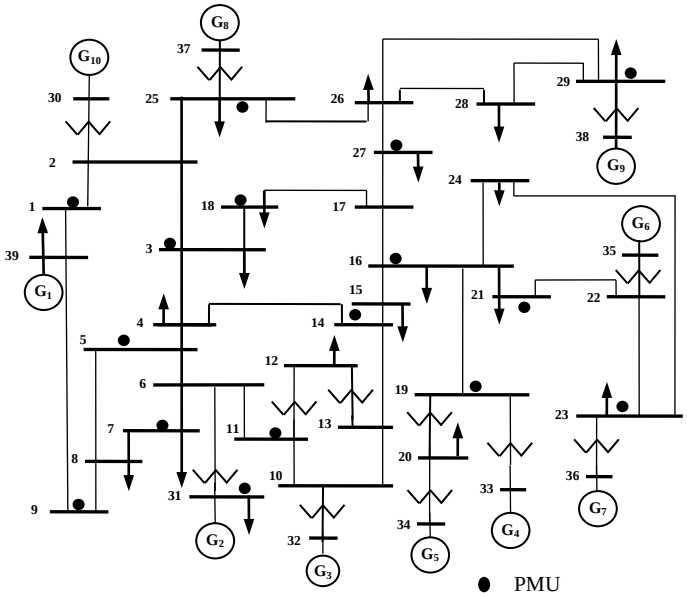

Fig. 5.1. New England 39 bus System.

To demonstrate such a case in New England 39 bus 50 Hz system shown in Fig. 5.1, the relay at bus 29 is selected to observe the effect of increased reactive loading. It is tested for two load encroachment cases (i) normal and (ii) increased reactive loading conditions where the voltage at buses falls to 0.85 pu. The first case, outage of line connecting buses 29 and 28 due to an internal fault, results in the increased loading of line connecting buses 29 and 26. During this period the impedance trajectory seen by the relay at bus 29 for line connecting buses 29 and 26 is shown in curve-1 of Fig. 5.2. This trajectory enters into the set zone 3 characteristic and also falls in load encroachment area. With increased reactive loading at buses 28, 27 and 26 initially and for the same line outage condition, the apparent impedance trajectory at bus 29 enters zone 3 but outside the load encroachment area as observed from curve-2 in Fig. 5.2. Thus during severe

reactive loading condition the conventional load encroachment function applied to supplementing zone 3 will be unable to prevent zone 3 maloperation. In this work, synchronized voltage data obtained from PMUs are used to solve such an issue.

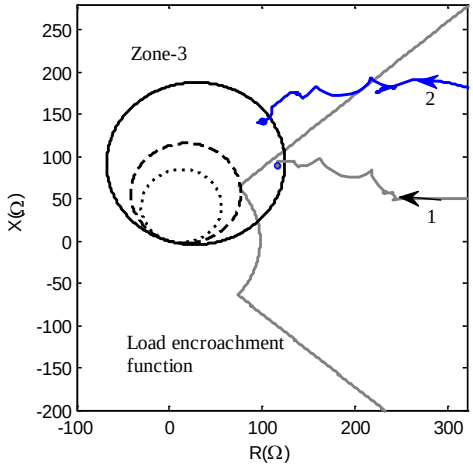

Fig. 5.2. Impedance trajectory at bus-29 for different loading conditions.

5.3 Proposed Sueprvised Scheme

The variation of voltage phasor at different buses of 39 bus New England system is observed for load encroachment and three phase fault for different relays. From this it is observed that voltage magnitude and phase angle variations are different for the two situations. Proposed method utilizes variation of voltages at different buses available from a wide area measurement systemto distinguish heavy loading from three phase fault.

5.3.1 Variation in Voltage Magnitude and Phase Angle during Disturbances

In an interconnected network for a three phase fault, voltage drops at differentbuses become significant whereasfor load increment the drop is within a limit. On the other hand, to meet the power demand, voltage angle change is relatively high. To adjudge this situation an equivalent source and load is considered with a line connecting them as shown in Fig. 5.3.

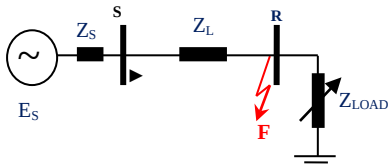

Fig. 5.3. Single line diagram of two bus system.

The voltage at relay bus S during normal loading condition can be expressed as,

$$\bar{V}_{Spre} = \bar{E}_S\left(1 - \frac{Z_S}{Z_S + Z_{LOAD} + Z_L}\right) \tag{5.2}$$

where Z_S = source impedance, Z_L= impedance of the line, Z_{LOAD} = load impedance and $\bar{E}_S$= internal voltage of source. The phasor diagram for such a loading condition is provided in Fig. 5.4(a).

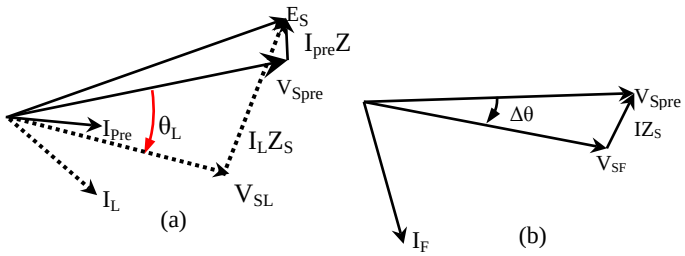

Fig. 5. 4 (a). Phasor diagram for change in voltage at bus S during load increment at bus R.(b) Phasor diagram during three phase fault when voltage equal to 0.85 pu.

With increase in load, current increases from $\bar{I}_{pre}$ to $\bar{I}_L$ and S-bus voltage drops to$\bar{V}_{SL}$ as shown in Fig. 5.4(a). For such a situation with decreased Z_{LOAD}, from (5.2) $\bar{V}_{Spre}$ will have an angle deviation from S- bus voltage $\bar{V}_{SL}$ and is denoted as θ_L. It is noticed that change in voltage magnitude is small as compared to phase change. On the other hand for a three phase fault at the end of the line, voltage at bus S becomes

$$\bar{V}_{SF} = \bar{E}_S\left(1 - \frac{Z_S}{Z_S + Z_L}\right) \tag{5.3}$$

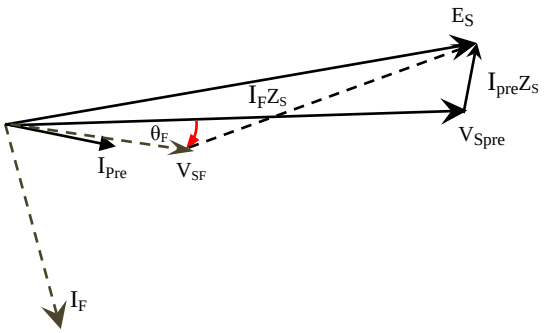

Fig. 5.5. Phasor diagram for change in voltage at bus S for three phase fault.

As phase angles of Z_S and Z_L are of similar order,from (5.3) it can be noticed that during three phase fault the angle of $\bar{V}_{SF}$ is nearly equal to that of E_S. Further the second term in

right hand side of (5.3) is much smaller and angle of $\overline{V}_{Spre}$ is also close to that of $\overline{E}_S$. This implies angle of both $\overline{V}_{Spre}$and $\overline{V}_{SF}$ will be close to $\overline{E}_S$ as observed from the Fig. 5.5. However during fault the current lags nearly 90° and to satisfy the phasor relation in (5.3) the change in voltage magnitude is significant from prefault voltage $\overline{V}_{Spre}$. From both the cases it is observed that phase change of voltage for three phase fault is less compared to load change and change in voltage magnitude during three phase fault is significant.

These two features change in magnitude of voltage and phase angle together can be applied to discriminate three phase fault from load encroachment. A ratio, change in magnitude to change in phase angle of voltage $\frac{\Delta V}{\Delta \theta}$ is selected for this purpose. As discussed, three phase fault results in a sudden change in voltage magnitude compared to phase change, whereas it is being gradual for load change, the ratio will be high for three phase fault and low for load change. To apply such a feature for this purpose, whenever the apparent impedance enters into zone 3, the changes are computed with respect to corresponding values 10 cycles earlier. Such a window length is considered for the discrimination aszone 3 waits 50 cycles to take the decision.

During three phase fault at end of a line which is within the zone 3 reach of a relay, the voltage magnitude deviate significantly at the adjacent buses than the zone 3 relay bus. In some cases, $\frac{\Delta V}{\Delta \theta}$ computed using relay bus voltage will not be enough to confirm athree phase fault. As zone 3 has highest reach, it covers all the lines connected to adjacent bus. Therefore data from nearby buses would fetch more information. With the introduction of wide area measurement system, synchronized data are available from different buses of a power system and are being be utilized for the purpose.

5.3.2 Selection of PMU buses

Synchronized measurements from all buses of a system and associatedcommunication system to collect data are not a cost effective proposition. To address this, PMUs are placed strategically for the application. 39 bus New England system is considered to explain the selection of PMU buses. In literature there are several approaches available to minimize the placement of PMUs for a specific objective [118]-[121]. In order to apply

proposed method PMUs are placed at buses which satisfy following criteria:

1) A PMU must be available to at least one end of a line, remote backup of which needs to be assisted.
2) A non PMU bus must be connected by line to at least one PMU bus.

PMUs in a system are selected using following steps:

1) As the starting point, any generator bus can be selected.
2) Considering a zone 3 relay atthe selected bus,all lines within its reach are listed.
3) Remote ends of all the enlisted lines should be selected for PMU buses.
4) Considering zone 3 relays at those selected buses,new PMU buses are selected considering above two steps and this continues until the placement criteria to assist the backup protection for all lines is fulfilled.

The measurement locations for the 39 bus system are (1,3,5,7,9,10,14,16,18,20,22,23,25,27,29,31).

5.3.3 PMU Group Selection for a Relay

For the purpose to assist the zone 3 decision the measurements from all the buses are not required. Only information from nearby substations or from selected measurements is sufficient. A PMU group is formed for a zone 3 relay considering the criterion; all PMUs available within the zone 3 reach of relay including local PMU (if any) constitute the required group for the relay.The number of PMUs in a group may vary and it depends on the number of lines connected to that bus. PMU groups for 39 bus New England system is provided in Table 5.1.

Table 5.1
PMU groups for 39 bus system

Group No.	Relays at buses to be assisted	PMUs in the group	Group No.	Relays at buses to be assisted	PMUs in the group
1	1, 2,39	25,3,9,1	6	16,17,18	18,27,14,21,19, 3,16
2	3,4	25,18,14,5,3	7	18,17	3,18,27,16,5
3	5, 6,11,10	7,5,11,3,9,14	8	19,21,22,23	23,19,14,21,16
4	7,8,9	5,9,10,7,1,3,14	9	25,26,27	3,1,27,29
5	14,15	16,21,19,18,5,1 4	10	28,29	25,27,29,18

5.3.4 The Discrimination Function

During a disturbance to discriminate three phase fault and load encroachment an indexD derived from a set of PMU data,

$$\mathrm{D} = \max\left(\frac{\Delta V_{1\mathrm{t}}}{\Delta\theta_{1\mathrm{t}}}, \frac{\Delta V_{2\mathrm{t}}}{\Delta\theta_{2\mathrm{t}}}, \ldots\ldots \frac{\Delta V_{\mathrm{nt}}}{\Delta\theta_{\mathrm{nt}}}\right) \tag{5.4}$$

where, n= numberof phasor measurement unitsin a group from which measurement is available and $\Delta\theta_{\mathrm{nt}} = \theta_{\mathrm{nt}} - \theta_{\mathrm{n(t1-0.2)}}$, $\Delta V_{\mathrm{nt}} = V_{\mathrm{nt}} - V_{\mathrm{n(t1-0.2)}}$. Where t_1 is the time (s) when the apparent impedance enters the zone 3 of arelay. Data 10 cycles before (50 Hz system)are useful incase ofslow load increment and used in the calculation of ΔV and $\Delta\theta$.

5.3.5 Threshold selection

The feature $\frac{\Delta \mathrm{V}}{\Delta\theta}$ is high for three phase fault compared to load change. A threshold is set considering following points. A voltage drop for a three phase fault equivalent to the maximum drop during load increase, let the voltage change at S bus has changed from $\mathrm{V_{Spre}}$ to $\mathrm{V_{SF}}$ as in Fig. 5.4(b). With the angle of $\mathrm{Z_S}$ being 90˚ (for lossless line), $\Delta\theta$ can be written as,

$$\Delta\theta = \tan^{-1}\left(\frac{I\mathrm{Z_S}}{V_{\mathrm{SF}}}\right) \tag{5.5}$$

From the above relation, the lower limit of the feature for three phase fault is obtained. Considering the prefault voltage as 1 pu. and voltage drop 0.15 pu. (maximum for load change) the voltage phase angle is obtained as 0.204 (rad) and corresponding feature value becomes 0.73 (pu./rad).

To study the feature, 39 bus New England system is simulated in EMTDC/PSCAD with different system conditions for three phase fault and load change. The change in voltage magnitude and angle during disturbance are obtained at relay bus (whose zone 3 protection is to be assisted) and buses connected to the adjacent lines. The values of ratio $\frac{\Delta \mathrm{V}}{\Delta\theta}$ for 300 cases each for three phase fault and load encroachment are plotted in Fig. 5.6. While simulation of load encroachment cases maximum loading is considered using NERC guide line [25]. Few cases are generated with high reactive loading condition where the power factor angle is greater than 30˚. From the figure it is

observed that the maximumvalue of the ratio for the load encroachment case is 0.51 pu./rad and for three phase fault the minimum index value is 1.17 pu./rad. This provides a way to discriminate three phase fault from load encroachment and a threshold of ξ=0.7 is selected (refer the approximate value obtained above).

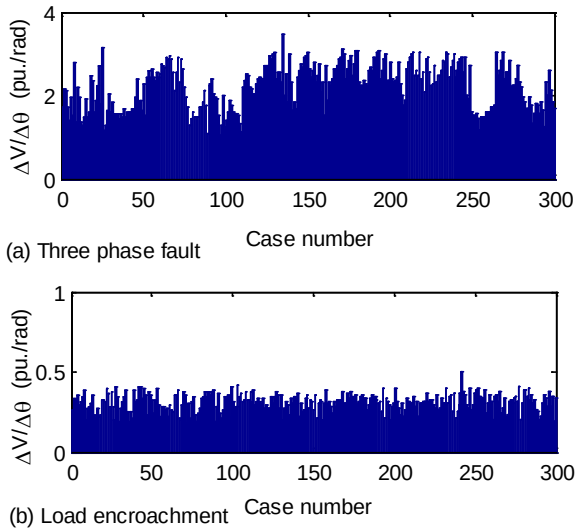

Fig. 5.6. Ratio of change in voltage magnitude and voltage angle for three phase fault and load encroachment.

5.3.6 Steps for Supervised Scheme

The algorithm for the proposed scheme is provided in Fig. 5. 7. The didfferent steps of the algorithm are provided below

Step 1: First, apparent impedance is calculated by using relay voltage and current data.

Step 2:When apparent impedance enters inside the relay zone 3 characteristic, sycnhrophasor volatge data from selected buses are collected and is used to calculate the index D as in (5.4).

Step 3: If D remains greater than the threshold for 0.2 s(10 cycles), a three phase fault is identified. In case of a fault, when local backup fails the supervisory decision is helpful to accelerate the protection decision which can improve the system reliability.

5.3.7 Communication Requirements and Latency Issues

The proposed method takes time in deriving the decision as it uses WAMS data. Delays in availing synchrophasor data are due to phasor computation, communication delay, computation time at PDC and decision transfer delay. The phasor computation delay is around 75 ms [124]. Communication delay depends on the channel available and with fiber optics the latency is 100ms [125]. With high speed processor the computation time is of the order of 1 msec [126]. The derived decision has to be transmitted to a specific relay and is within the range of 3-5 ms [127]. The total time required to derive the decision in within 180 ms which is reasonable to for zone 3 [126].

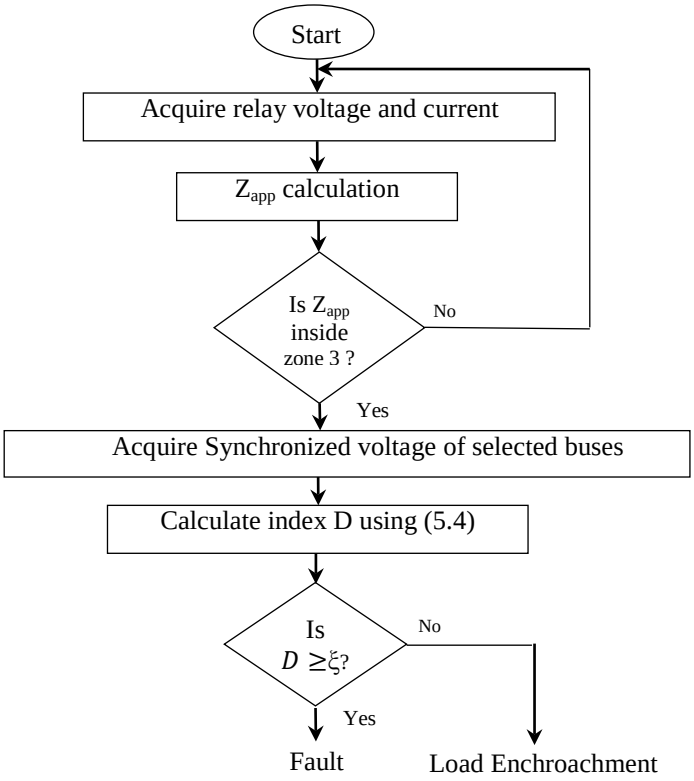

Fig. 5.7. Flow diagram for proposed algorithm.

5.4 Results

To test the proposed method 39 bus New England and IEEE 118 bus systems are simulated in EMTDC/PSCAD. Positive sequence voltage phasors are obtained by using

one cycle DFT. The PMU data are collected at a rate of 50 frames per second for the 50 Hz systems.

5.4.1. Test for Load Encroachment Case with High Reactive Loading

In a system the variation of load is random. For reactive loading two cases arise (i) sudden and (ii) slow increase in reactive loadings. Tests are carried out for the 39 bus system.

5.4.1.1 Sudden reactive load change

The line connecting buses 29 and 26 was heavily loaded. Zone 3 relay at bus 29 is observed for this case. Reactive loading at buses 27, 26 and 28 are increased and the line connecting buses 28 and 29 is tripped simultaneously due to an internal fault. This causes increased loading on the line connecting buses 29 and 26. During this period voltage at selected buses are provided in Fig. 5.8 (a) and (b) .The seen impedance at bus 29 enters into zone 3 at 2.01s but remains outside the applied load encroachment function as observed from Fig. 5.8 (c). The load encroachment function will fail to identify this condition.

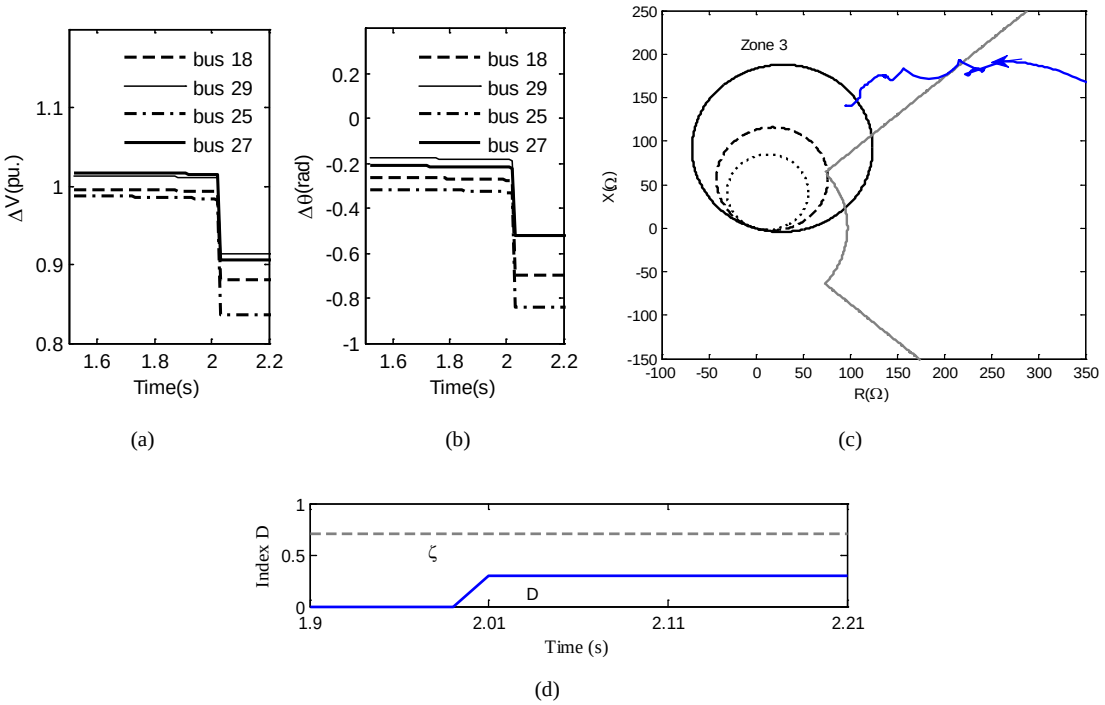

(a) (b) (c)

(d)

Fig. 5.8. (a) Change in voltage magnitude at PMU buses(pu.) (b) Change in Voltage angle (rad) (c) Impedance trajectory for the high reactive loading condition at bus 29. (d) Index D for zone 3 at bus 29 under high reactive loading in 39 bus system.

For these cases measurements from buses 25,27, 29 and 18 are considered to compute the index D as in (5.4). The index is plotted in Fig. 5.8 (d) which remains below the threshold value for 0.2s and confirms a load encroachment. A block signal can be issued to the relay at bus 29. This reveals that the index can prevent zone 3 maloperation even during high reactive loading condition.

5.4.1.2 Slow Reactive Load Change

Sometimes the growth in load is slow. To simulate such a case the line connecting 29 and 28 trips due to a fault and then loads at buses 28, 26 and 27 are increased in 5 steps and simultaneously the generation at bus 25 is decreased. Due to this the line connecting buses 29 and 26 gets overloaded and during this period voltage from buses are provided in Fig. 5.9 (a) and (b). The apparent impedance enters zone 3 relay at bus 29, at 2.02 s as seen from Fig. 5.9 (c) which falls outside the load encroachment function. Thus, conventional load encroachment function is not accurate to distinguish load from fault.

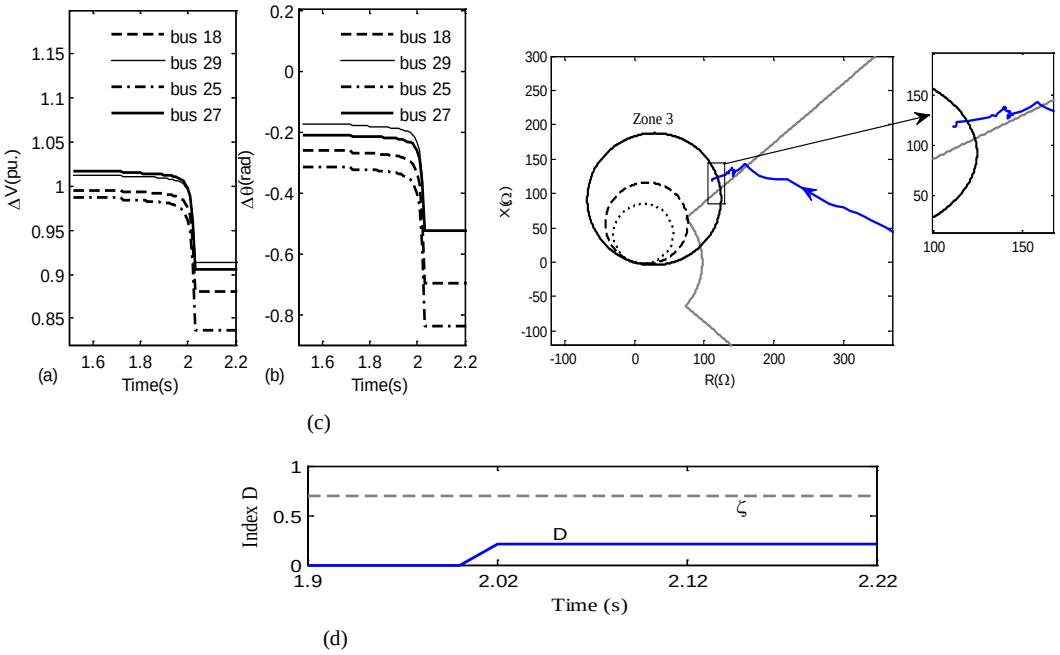

Fig. 5. 9. (a) Change in voltage magnitude at PMU buses (pu.) (b) Change in Voltage angle (rad) (c) Impedance trajectory for the relay at bus 29 during high reactive loading. (d) Index D under slow load increment during high reactive loading in New England 39 bus system.

For the case the changes in voltage magnitude and voltage angle of buses 25,27, 29 and 18 are used to calculate the index D. The index is plotted in Fig. 5.9 (d) and

observed that it is less than the threshold confirming the case as a load encroachment. A signal can be sent to the relay at bus 29 to block the zone 3.

5.4.2 Test for Three Phase Fault during High Reactive Loading Condition

To check the performance of the proposed method for a fault during high reactive loading condition, at buses 27, 26 and 28 reactive loading is increased. Prefault power flow direction remains same as in earlier case. Zone 3 relay at bus 29 is evaluated for a three phase fault in line connecting buses 25 and 26. Change in voltage magnitude and phase angle are plotted in Fig. 5.10 (a) and (b) respectively. Apparent impedance trajectory at bus 29 is plotted in Fig. 5.10 (c) which enters zone 3 characteristic at 2.06s but outside the load encroachment area. Thus available method will be able to correctly identify the fault.

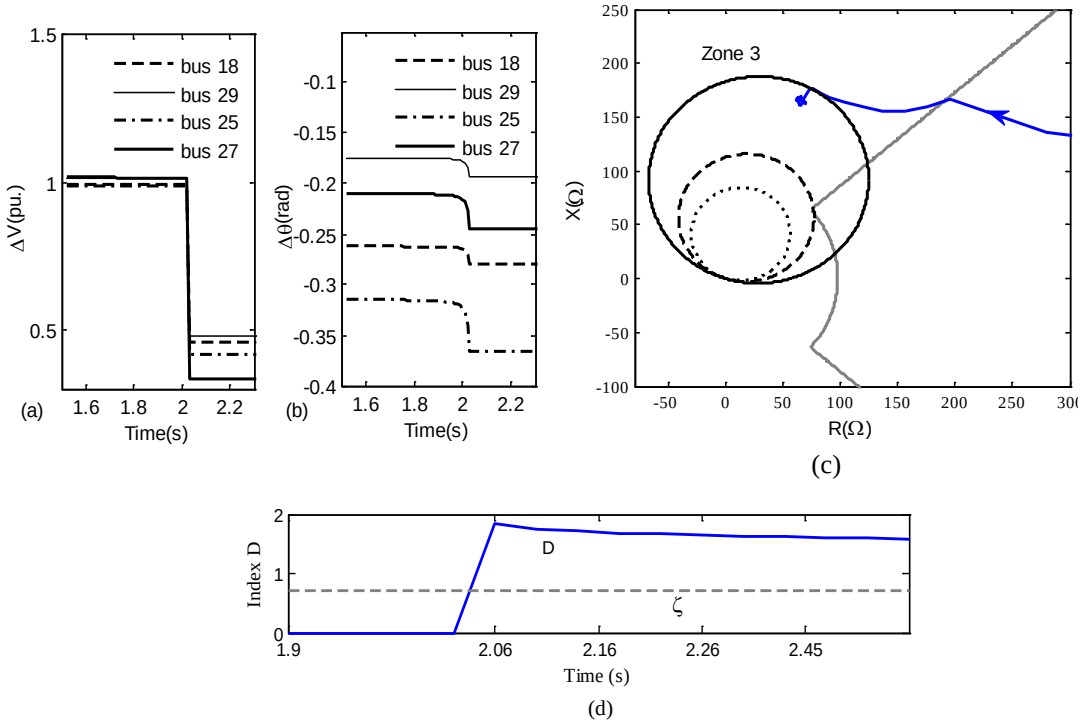

Fig. 5.10. (a) Change in voltage magnitude at PMU busses(pu.) (b) Change in Voltage angle (rad) (c) Impedance trajectory for relay at bus 29. (d) Index D for three phase fault in New England 39 bus system during high reactive condition.

Data from buses 25,27, 29 and 18 are used to calculate the change in voltage magnitude and voltage angle. For index D which is plotted in Fig. 5.10 (d). Trip signal is

sent to the relay at bus 29. From the result it is evident proposed method also identifies three phase fault correctly.

5.4.3 Test with IEEE 118 bus with Series Compensation

IEEE 118 bus system is used to test proposed method. PMUs are placed in the network and enlisted in Appendix E. Zone 3 relay at bus 49 is considered to verify the algorithm during load encroachment and three phase fault. To support the zone 3 relay at bus 49, corresponding group comprises of PMUs at 49, 45, 54, 68, 75, 70 and 77.

Protection of series compensated line is challenging due to the series capacitor and operation of metal oxide varistor and air-gap. The ratings and characteristic of MOV is selected as provided in [117]. The accuracy of the proposed method is also tested for a series compensated line. 60 percentage series compensation is provided in the line connecting buses 69 and 75. The location of capacitor is at bus 69.

5.4.3.1 Load Encroachment Case:

In the presence of series compensation loads are increased at buses 75 and 72. The outage of line connecting buses 49 and 66, when generation is decreased to 100 MW, the voltage is collected from the selected busses and corresponding magnitude and phase angles are plotted in Fig. 5.11 (a) and (b). The apparent impedance enters inside the zone 3 at 3.11 s as shown in the Fig. 5.11 (c). The index D is calculated using the synchronized voltage obtained from busses 49, 45, 54, 68, 75, 70 and 77 and plotted in the Fig. 5.11 (d). From the figure it is observed that the index is below the threshold for 0.2s which ensures a load encroachment case. A blocking signal can be issued to the zone 3 relay at bus 49 preventing relay maloperation.

5.4.3.2 Three phase fault case:

In the presence of series compensation during fault the voltage and current and voltage waveforms are modified. The phasor based techniques will sffer from such modification. Directional relay based scheme will suffer from current inversion cases. In such cases backup protection provided by distance relay is better solution. To see the performance of the proposed method for fault, a three phase fault is simulated in the series compensated line connecting buses 69 and 75 at a distance of 5 km from bus 69. Magnitude of selected

bus voltage and phase angle during this period is given in Fig. 5.12 (a) and (b). The apparent impedance trajectory plotted in the Fig. 5.12 (a) which enters zone 3 at 3.02 s shows that a correct decision will be derived by conventional method. The index D is calculated during the fault and plotted in Fig. 5.12. (d). High values of the index confirms a three phase fault. This implies the proposed has effect of presence of series compensation in the line. However communication based directional comparison based has limited performance during this period.

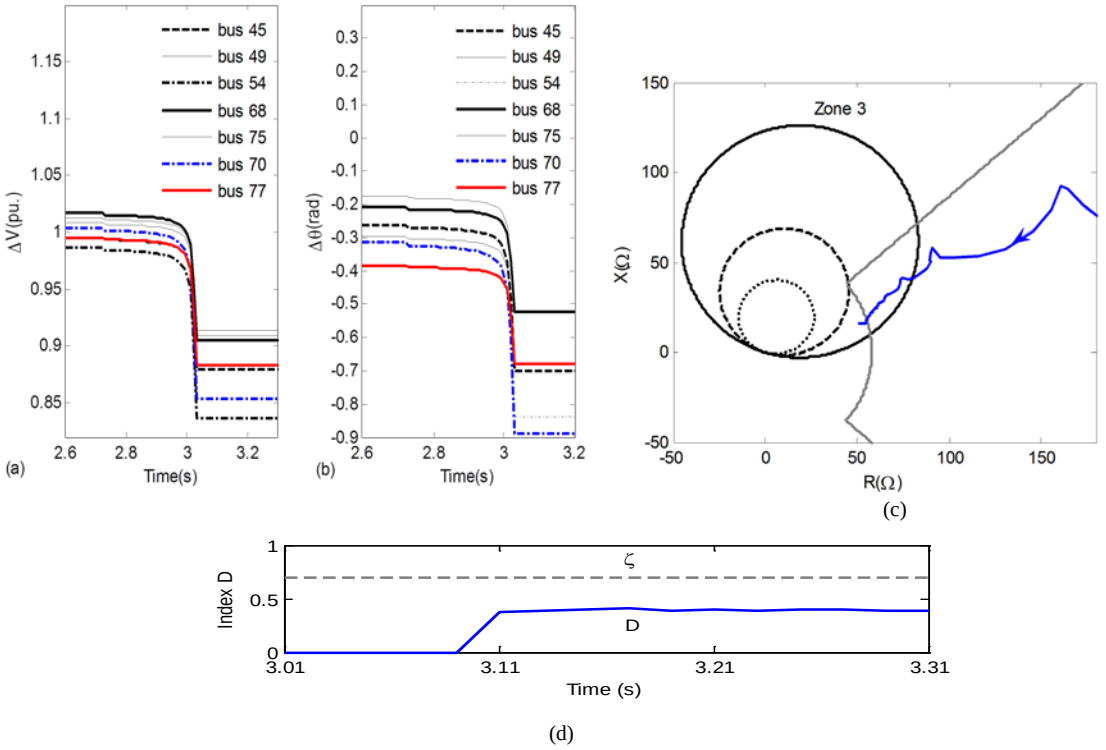

Fig. 5.11. (a) Change in voltage magnitude at PMU buses(pu.) (b) Change in Voltage angle (rad) (c) Impedance trajectory for relay at bus 49 during load increment. (d) Index D during load increment in the presence series compensation in IEEE 118 bus system.

5.4.4 Comparative Assessment

The performance of the proposed method is compeared with other exting method besed on wide area measurement data. Among which two cases are demonstrated below for comparison with the method in [108].

5.4.4.1 Current Inversion case

As proposed method uses magnitude and angle of voltage only, it is not affected by voltage or current inversion in the presence of the series compensation. The voltage at bus 69 and current through line 69-75 of 118 bus system during a three phase fault case in is

provided in Table II. It is observed from the table that the change in current angle is not significant at bus 69. The phase angle change to determine an internal fault must be 3.14 radian. The method in [108], which uses current phase angle of both ends of lines, will maloperate due to current inversion. However the proposed method will operate correctly as it depends only on voltage to derive the decision.

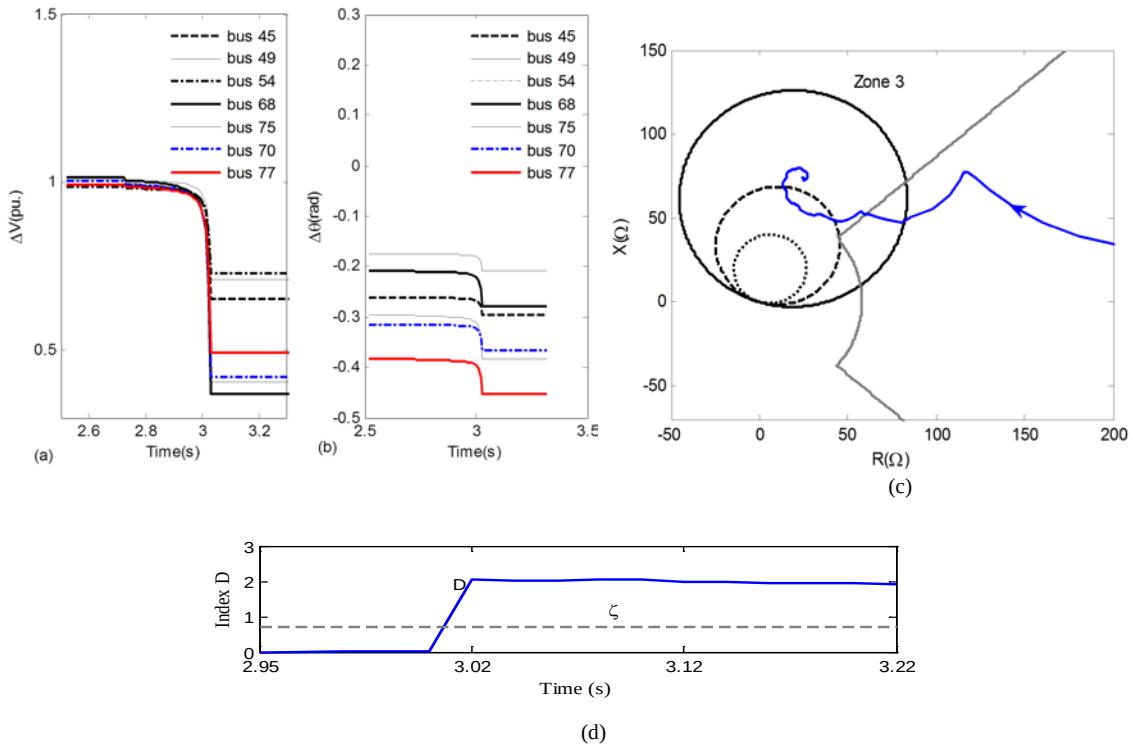

Fig. 5.12. (a) Impedance trajectory for relay at bus 49 during three phase fault. (b) Index D for three phase fault in the presence of series compensated in IEEE 118 bus system.

Table 5.2
Data for three phase fault in the line 69-75

BUS 69	Bus Voltage (pu)	Line Current (pu)	Change in current Angle(rad)
Pre fault	0.9∠0.263	0.4∠0.52	0.07
During fault	0.2∠0.259	2.2∠0.45	

5.4.4.2 Voltage and Line Parameters requirement

The three phase fault discussed in Case C for 118 bus system is considered with outage of the line connecting 69-70. During this period the voltage measurements obtained from

PMU buses reveal a fault situation as voltage deviation at bus 77 is significant. This depicts that proposed method is not affected by changes in system condition. In [108]-[113] data from both ends of the line are required in the decision process. In [114], the method requires line parameters and system data, will face problem due to MOV operation in the series compensated line. Load encroachment problem may not occur in all lines. For lines of importance and where such issue may arise, synchronized voltage of nearby selected buses will supplement protection decision and thus the method does not require data from all busses of the system as in [115]-[118]. Thus realization of the method is feasible.

5.5 Conclusions

Load encroachment during stressed system condition leads to maloperation of zone 3 at times.Whenever zone 3 finds apparent impedance inside its characteristic, the ratios of change in voltage magnitude to change in phase angle of different buses are used to derive an index which can discriminate load encroachment from three phase fault. Proposed method is tested for several system conditions like load increment and three phase fault during high recative loading and low reactive loading. The scheme using WAMS volatge performs correctly for all condition even during high reactive loading condition. The scheme dose require current any branches of the system. Which helps in accurate operation of the scheme even for series compensated line during current inversion. The scheme adavantageous with resect to other schemes as it dosenot depend on information regarding status of the circuit breakers.

Conclusions

6.1 Summary of the Work

Series compensated and multiterminal lines are being increasingly used in power systems in order to meet the power demand and to exploit technical and economic benefits. Available line protection schemes have limited performance for series compensated lines as the compensation level changes with time and the MOV operation modulates the current during the transient process. Infeed in three terminal line varies and imposes problem to distance relay protecting such lines. Alpha plane method using ratio of both end currents is a better scheme than differential relay. Such a scheme has limitation for outfeed condition.

At times, local data based zone 3 relay fails to distinguish fault from load encroachment during heavy loading conditions. This may lead to unwanted line tripping. This thesis investigates on protection schemes for different power networks and proposes adaptive schemes to derive improved performance. This chapter summarizes the salient contributions of the thesis. For extending the work, some feasible future directions are mentioned in subsequent section.

Using both end currents, alpha plane based approach is a powerful technique for line protection. Such relaying principle using phase currents has limitation for high resistance fault. An adaptive alpha plane method is proposed to overcome this. When the ratio of fault currents lies in the conflicting region in the plane, two features; the phase angle between the voltage and current and magnitude of change in current at both ends of the line, are used to confirm an internal fault. The adaptive technique is tested for

numerous situations including fault in series compensated line, high resistance fault, single-pole operation and for communication channel delay. The results show the method work correctly for numerous system conditions. It requires both end voltages data in addition to current. In case the voltage data are not available for any reason at any instant the method uses the conventional alpha plane method.

The performance of DUTT scheme for application to three terminal line depends on the overlapping between the zone 1 elements. For such lines with asymmetrical configuration maintaining overlapping is a challenge. At times a portion of the line remains unprotected when the overlapping vanishes with increase in infeed. An adaptive DUTT scheme is proposed for three-terminal line protection. Prefault synchronized data at the three terminals are applied to estimate the overlappings of the zone 1 elements. When any overlapping vanishes, zone 1 settings are adapted in accordance with the infeed condition to ensure reliable operation of DUTT scheme. To ensure that the adaptive setting does not overreach, all the three relay settings are adapted simultaneously. The schemes requires synchronized voltage and current phasors from all three sides of the system and settings are calculated in each cycle. The source impedance computed using system condition information has adverse effect on the calculated overlapping. In case other end data are not available the scheme will work similar to conventional one.

Series compensation present in the transmission line causes overreaching problem to the distance relay. Nonlinear operation of MOV complicates the problem further. Distance relay requires the information on compensation present in the line at an instant for correct protection decision. Synchronized data are used for adaptive zone 2/ zone 3 setting for a series compensated line. The adaptive setting considers MOV operation by calculating the corresponding current level, using prefault data. To estimate the status of capacitor bypassed or not by the air-gap arrangement at an instant, fault data are used and the relay setting is updated accordingly. As evident from the results for numerous cases, the method provides accurate zone-2/zone-3 trip boundary settings for different levels of compensation or operation of MOV protecting the series capacitor.

To meet the power demand with existing resources system are being operated close to stability limit. At times the apparent impedance enters into the zone 3 characteristic and it is difficult to discriminate it from fault using local data. This causes

maloperation of distance relay and may lead to cascaded tripping. Whenever apparent impedance enters zone 3 in impedance plane the ratios of change in voltage magnitude to change in phase angle from a group of busses are collected through WAMS and are used to derive an index for protection decision. Distance relay algorithm with this index can discriminate load encroachment from three phase fault and thereby improved protection decision can be obtained. The method is tested on 10 machine New England and IEEE 118 bus systems with and without series compensation. The results depict proposed method performs correctly for both slow and sudden changes in loading even under heavy reactive demand condition. The method works accurately for series compensated line even for current inversion and thereby the method is found to be advantageous over existing wide area backup protection schemes.

6.2 Scope of Future Work

The thesis has proposed innovative algorithms to support network protection schemes and to prevent zone 3 maloperation during load encroachment. Performances of remote end data based techniques are studied for several conditions and methods are proposed to improve the protection decision by alpha plane scheme and an adaptive setting for three terminal line is proposed which is immune to stressed power system condition. The performances of proposed algorithms are evaluated for different systems. The findings in the thesis clearly indicate further research direction in the following interesting areas.

Wide area backup protection scheme needs volume of data for processing to derive the decision. Handling lot of information is another area of research. Proposed method can be investigated for data redundancy, noise and other uncertainties. The wide area measurements can also be applied to develop system integrated protection scheme (SIPS) for prevention of blackout or large scale disturbance.

The source impedance used in computation of overlapping in adaptive DUTT scheme for three terminal line is considered as constant. Changes network configuration may cause in change the source impedance. Wide area measurement data which records the online changes can be applied to calculate impedance of equivalent sources.

The proposed adaptive method for series compensated line can also be tested for flexible AC transmission system with devices like thyristor controlled series

compensation (TCSC) and static synchronous compensator (STATCOM). The change in the compensation level paves many challenges to the protection scheme. Reliable relay operation requires accurate value of compensation level present in the line. However system which includes FACTs devices face changes in line parameters and requires computational techniques to estimate the accurate line parameter for correct protection decision.

Power swing is a concern for grid protection. Zone-3 maloperation during power swing is wide discussed problem. Conventional techniques which rely on rate of change of any parameter have limitation in detecting stable and unstable power swing. WAMS data can be applied to develop some technique to identify stable power swing and improved the protection decision. Adaptive out of step protection scheme may be developed using WAMS data which can improve the system stability.

References

[1] IEEE Power System Relay Committee, "Performance of relaying during wide area stressed conditions," 2008. [Online]. Available: www.pes-psrc.org.

[2] D. Novosel, G. Bartok, G. Henneberg, P. Mysore, D. Tziouvaras, and S. Ward, "IEEE PSRC report on performance of relaying during wide area stressed conditions," *IEEE Trans. Power Delivery*, vol. 25, no. 1, pp.3–16, Jan. 2010.

[3] S. P. Wang, A. C. Wen, L. C. Hung, "Efficient splitting for blackout analysis," *IEEE Trans.Power Systems*, vol. 30, no.4, pp. 1775-1783, Jul. 2015..

[4] B. A. Carreras, D.E. Newman, I. Dobson, "North American blackout time series statics and implications for blackout risk," IEEE Trans. Power Systems, In Early Access, 2016.

[5] NERC, August 14, 2003 Blackout: NERC Actions to prevent mitigate the impacts of future cascading blackouts, North American Electric Reliability Council, Princeton, NJ. 10th Feb. 2004.

[6] M.M.Adibi, N. Martins, "Impacts of power system Blackouts," in Proc, Power & energy society Genaral meeting, Denevor, july 26th-30th 2015, pp. 1-15.

[7] D. E. Newman, B. A. Carreras, V. E. Lynch, and I. Dobson, "Exploring complex systems aspects of blackout risk and mitigation," *IEEE Trans. on Reliability*, vol. 60, no. 1, pp. 134–143, 2011.

[8] C. D. Vournas, V. C. Nikolaidis, and A. A. Tassoulis, "Postmortem Analysis and Data Validation in the wake of the 2004 Athens blackout," *IEEE Trans. Power systems*, vol. 21, no. 3, pp. 1331–1339, 2006.

[9] Power grid, "Report of the enquiry committee on grid disturbance in Northern region on 30th July 2012 and in Northern, Eastern and Northern-Eastern Region on 31st July 2012," New Delhi, India, Tech. Rep. 2012.

[10] A. Atputharajah and T. K. Saha, "Power System Blackouts - Literature review," *Fourth International conference on industrial and Automation Systems*, Srilanka, December 2009.

[11] D. Novosel, M. M. Begovic and V. Madani, "Shedding light on blackout," *IEEE Power and Energy Magazine*, vol. 1, no. 2, pp. 32-43, Jan. 2004.

[12] J. S. Thorp, "Protection system in bulk power networks," *PSERC background paper*, 2003.

[13] G. D. Rockefeller, C. L. Wagner, J. R. Linders, K. L. Hicks and D. T. Rizy, "Adaptive Transmission Relaying Concepts for Improved Performance", *IEEE Trans. Power Delivery*, vol. 3, no.4 , pp.1446-1458. Oct. 1988.

[14] M. Adamiak, G. D. Rockefeller, S. H. Horowitz, A. G. Phadke, M. S. Sachdev," Feasibility of control and adaptive protection," *IEEE Trans. Power Delivery* vol. 8, no. 3, pp. 975-983. Jul. 1993.

[15] S. H. Horwitz, A. G. Phadke and J. S. Thorp, "Adaptive Transmission System Relaying", *IEEE Trans. Power Delivery*, vol. 3, no. 4, pp. 1436-1445, Oct. 1988.

[16] A. G. Phadke, "Computer Relaying: Its Impact on Improved Control and Operation of Power Systems", *IEEE Computer Applications in Power*, pp. 5-10, 1988.

[17] A. K. Jampala, S. S. Venkata and M. J. Damborg, "Adaptive Transmission Protection: Concepts and Computational issues", *IEEE Trans. on Power Deliery*, vol. 4, no.1, pp. 177-185, 1989.

[18] Z. Zhizha and C. Deshu, "An adaptive approach in Digital Distance protection", *IEEE Trans. Power Deliv*ery, vol. 6, no. 1, pp.135-142, 1991.

[19] M. J. Damborg, M. Kim, J. Huang, S. S. Venkata, and A. G. Phadke, "Adaptive protection as preventive and emergency control", Proceedings of the IEEE PES Summer Meeting, Seattle, WA, Vol. 2, pp. 1208-1212, Jul. 2000.

[20] D. Tholomier, D. Paraiso and A. Apostolov, "Adaptive protection of transmission lines," *in proc, power system conference PSC'09* Clemson, 2009. pp. 1–14.

[21] S. C. Sun and R. E. Ray, "A current differential relay systems using fiber optics communications," *IEEE Transactions on Power Apparatus and Systems*, vol. PAS-102, no. 2, pp. 410–419, Feb. 1983.

[22] IEEE Power System Relaying Committee, "Protection aspects of multi terminal lines" IEEE Publication No. 79 TH0056-2-PWR 1979.

[23] NERC, A technical document prepared by the systems protection and control task force of the NERC planning committee- "*The complexity of protecting three terminal transmission line*," 2006. [online]. Available: http//www.nerc.com

[24] H. J. Altuve, J. B. Mooney and G. E. Alexander, "Advances in series-compensated line protection," *in 62nd Annu. Conf. at Protective Relay Engineers*, 2009.

[25] NERC, Relay Loadability Exceptions, Determination and application of planning relaying loadability ratings, North American Electric Reliability Council, Princeton, NJ, Sep. 2004.

[26] A. G. Phadke and J. S. Thorp, *Synchronized Phasor Measurements and Their Applications*, New York: Springer, 2008.

[27] V. Terzija, G. Valverde, D. Cai, P. Regulski, V. Madani, J. Fitch, S. Skok, M. M. Begovic, and A. G. Phadke, "Wide-area monitoring, protection, and control of future electric power networks," *IEEE Proceedings*, vol. 99, no. 1, pp. 80-93, Jan. 2011.

[28] "A Survey of Optical Channels for Protective Relaying: Practices and Experience", IEEE Power System Relaying Committee Report, *IEEE Transactions on Power Delivery*, vol. 10, no. 2, pp. 647–658, Apr. 1995.

[29] G. Benmouyal, and J. Mahseredjian, "A combined directional and faulted phase selector element based on incremental quantities," *IEEE Transactions on Power Delivery*, vol. 16, no. 4, 2001.

[30] K. S. Prakash, O. P. Malik, and G. S. Hope, "Amplitude comparator based algorithm for directional comparison protection of transmission lines," *IEEE Trans. Power Delivery*, vol. 4, no. 4. pp. 2032-2041, 1989.

[31] "Line Protection Design Trends in the USA and Canada", IEEE Power System Relaying Committee Report, *IEEE Trans. Power Delivery*, vol. 3, no. 4, pp. 1530-1535, Oct. 1988.

[32] D. A. Tziouvaras, J. Roberts, G. Benmouyal and D. Hou, "The effect of conventional instrument transformer transient on numerical relay elements," *28th Annual Western Protective relay conference*, Spokane, Washington, USA, October 2001.

[33] L. J. Ernst, W. L Hinman, D. H. Quam and J. S. Thorp, "Charge comparison protection of transmission line- relaying concepts," *IEEE Trans. Power Delivery*, vol. 7, no. 4, pp.1834-1852, Oct. 1992.

[34] M. G. Adarmiak, W. Premerlani and G. E. Alexander, "A new approach to current differential protection for transmission Lines," Available online: store.gedigitalenergy.com/faq/documents/l90/ger-3981.pdf

[35] H. Y. Li, E. P. Southern, P. A. Crossley, S. Potts, S. D. A Pickering, B. R. J. Caunce and G. C. Weller, " A new type of differential feeder protection relay using global positioning system for data synchronization," IEEE Trans. Power Delivery., vol. 12, no. 3, pp. 1090-1099, Jul. 1997.

[36] I. Hall, P. G. Beaumont, G. P. Baber, and I. Shuto, " A new line current differential relay using GPS synchronization, " presented at *IEEE Bologna Power Tech Conf.*, Bologna, Italy, Jun. 2003.

[37] G. Houlei, J. Shifang, and H. Jiali, "Development of GPS synchronized digital current differential protection," in *Proc. Int. Conf. Power System Technology*, Apr. 1998, pp. 1177–1182.

[38] Z. Y. Xu, Z. Q. Du, L. Ran, Y. K. Wu, Q. X. Yang, and J. L. He, "A current differential relay for a 1000-kV UHV transmission line," *IEEE Trans. Power Delivery*., vol. 22, no. 3, pp. 1177-1182. Jul. 2007.

[39] A. R. V. C. Warrington, Protective Relays: Their theory and Practice, vol. 1, London, Chapman and Hall, 1962.

[40] A. R. V. C. Warrington, Protective Relays: Their theory and Practice, vol. 1, London, Chapman and Hall, 1969.

[41] B. Kasztenny, D. Taylor and Y. Xia, "Line differential protection under unusual system conditions," Available online: https://www.selinc.com/WorkArea/Download

[42] G. Benmouyal, "The trajectories of line current differential faults in the α-plane," 32nd Annual Wester Protective relay conference, Spokane, WA, October 25-27, 2005.

[43] D. A. Tziouvaras, H. Alturve, G. Benmouyal and J. Roberts, "Line differential protection with an enhanced characteristic ," *Eighth IEE International Conference on* Developments in power system protection, vol.2, no.1, pp. 414-419. April 2004.

[44] G. Benmouyal, J. B. Mooney, "Advanced sequence elements for line current differential protection," Available online: https://www.selinc.com/WorkArea/Download.

[45] L. Bin, L. Chao, H. Jiali, B. Zhiqian and T. Yip, "Novel principle and adaptive scheme of phase correlation line current differential protection," *International Transactions on Electrical Energy Systems*, vol. 23, no.5, pp. 733-750, May. 2013.

[46] *IEEE guide for protective relay applications to transmission lines*, IEEE Std C37-113, 1999.

[47] Network Protection and Automation Guide, 1st ed., Areva T&D, Paris, France.

[48] R. K. Agarwal and A. T. Johns, "The development of a new high speed 3-terminal line protection scheme," *IEEE Trans. Power Delivery*, vol. 1, no. 1, pp. 125- 134, Jan. 1986.

[49] R. K. Aggarwal, A. H. Husseini, and M. A. Redfern, "Design and testing of a new microprocessor based current differential relay for EHV teed feeders," *IEEE Trans. Power Delivery*, vol. 6, no. 3, pp. 991-999, Jul. 1991.

[50] Z. Gajic, I. Brncic, T. Einarsson, and B. Ludqvist, "Practical experience from multiterminal line differential protection installations," *Relay Protection and Substation Automation of Modern Power Systems*, Cheboksary, September 9-13, 2007.

[51] D. R. M. Lyonette, Z. Q. Bo, G. Weller and F. R. Jaing, "A new directional comparison technique for the protection of teed transmission circuits," in*: IEEE Power Engineering Society Winter Meeting*, 23–27th Jan., 2000. pp. 23–27,

[52] *IEEE Guide for the Application of Current Transformers Used for Protective Relaying Purposes*, ANSI/IEEE C37.110-1996.

[53] B. Kasztenny, G. Benmouyal, H. J. Altuve, and N. Fischer, "Tutorial on operating characteristics of microprocessor-based multiterminal line current differential relays," 2011. [Online]. Available: www.selinc.com/20110913, TP6511-01.

[54] M. M. Eissa, "A new digital teed circuit protection using directional element ," *IEEE Trans. Power Delivery, vol.* 24, no. 2, pp. 531–541, Apr. 2009.

[55] R. K. Agarwal and A.T. Johns, "Digital differential relaying scheme for teed circuits based on voltage and current signal comparison," *IEE Proceedings C-Generation Transmission and Distribution*, vol. 137, no. 6, pp. 414-423, Nov. 1990.

[56] B. Bhalja and R. P. Maheshwari, "New differential protection scheme for tapped transmission line," *IET Generation Transmission Distribution*, vol. 2, no. 2, pp. 271–279. 2008.

[57] M. M. Eissa**,** "A new digital relaying scheme for EHV three terminal transmission lines," *Elect. Power Syst. Res.*, vol. 73, no. 2, pp.107–112, Feb. 2005.

[58] K. K. Li, L. L. Lai and A. K. David, "Stand alone intelligent digital distance relay," *IEEE Trans. Power Delivery*, vol. 15, no. 1, pp. 137-142, Feb. 2000.

[59] Y. Q. Xia, K. K. Li and A. K. David, "Adaptive relay setting for standalone digital distance protection*", IEEE Trans. Power Delivery*, vol. 9, no.1, pp. 480–491, Jan. 1994.

[60] D. V. Coury, J. S. Thorp, K. M. Hopkinson and K. P. Birman, "Agent technology applied to adaptive relay setting for multi-terminal line," *IEEE Power Engineering Society Summer Meeting*, July 16–20, pp. 1196–1201, 2000.

[61] D. Erwin, M. Anderson, R. Pineda, et al, "PG&E 500 kV Series- compensated transmission line relay replacement: design requirements and RTDS @ testing," in Protective relay engineers, April, 2001, pp. 191-202.

[62] T. S. Roseburg, M. M. Saha, and J. Zakonjsek, "Testing and operational experiences with high speed distance relay in BPA 500 kV series compensated network," *in Proc. 32nd Annu. Western Protective Relay Conf*erence, 2005, pp. 1-10.

[63] D. Novosel, A. G. Phadke, M. M. Saha, and S. Lindahl, "Problems and solutions for microprocessor protection of series compensated lines," in *Proc. Conf. Developments in Power System Protection*, 1997, pp.18–23.

[64] B. Kasztenny, "Distance protection of series compensated lines-problems and solutions," *28th Annual Western Protective Relay Conference, Spokane*, 22nd -25th Oct., 2001.

[65] T. S. Roseburg, and M. M. Saha, "Testing and operational experiences with high speed distance relay in BPA 500 kV series-compensated network," *presented at the 32nd Annual Western Protective Relay Conference*, Spokane, WA, 25-27th Oct. 2005.

[66] R. Grunbaum, G. Stromberg, and K. Vikstrom, "On the impact of series compensation on line protection and TRV," in proc. *Relay Protection and Substation Automation of Modern Power Systems, Cheboksary,* 9 -13th Sept., 2007.

[67] D. L. Goldsworthy, "A linerised model for MOV-protected series capacitors," *IEEE Trans. Power System*, vol. 2, no. 4, pp. 953-957, Nov. 1987.

[68] M. Coursol, et al, "Modeling of MOV protected series capacitors for short-circuit studies,'' *IEEE Trans. Power Deliv*ery, vol. 8, no. 1, pp. 448-453, Jan. 1993.

[69] J. Mahseredjian. et al, "Superposition technique for MOV-protected series capacitors in short circuit calculations," *IEEE Trans. Power Delivery*, vol. 10, no. 3, pp. 1394-1400, Jan. 1995.

[70] F. Ghassemi, J. Goodarzi, and A. T. Johns, "Method for eliminating the effect of MOV operation on digital distance relays when used in series compensated lines," *in Proc. of the Universities Power Engineering Conf.*, Manchester, UK, Sept. 10–12, 1997, pp. 113-116.

[71] R. J. Marttila, "Performance of distance relay mho elements on MOV-protected series-compensated lines," *IEEE Trans. Power Delivery*, vol. 7, no. 3, pp. 1167–1178, Jan. 1992.

[72] A. Newbould, and I. A. Taylor, "Series compensated line protection: System modelling and relay testing," in *Proc. 4th Int. Conf. Developments in Power Protection*, 1989, pp. 182–186.

[73] A. Y. Abdelaziz, A. M. Ibrahim, M. M. Mansour and H. E. Talaat, "Modern approaches for protection of series compensated transmission lines," *Electric Power Syst. Res.*, vol. 75, pp. 85–98, 2005.

[74] A. I. Megahed, A. M. Moussa and A. E. Bayoumy, "Usage of wavelet transform in the protection of series-compensated transmission lines," *IEEE Trans. Power Delivery*, vol. 21, no. 3, pp. 1213-1221, Jul. 2006.

[75] J. A. S. B. Jayasinghe, R. K. Aggarwal, A. T. Johns, and Z. Q. Bo, " A novel nonunit protection for series compensated EHV transmission lines based on fault generated high frequency voltage signals," *IEEE Trans. Power Delivery*, vol. 13, no. 2, pp. 405–413, Apr. 1998.

[76] R. Dutra, L. Fabiano, W. Oliveira, M. M. Saha and S. Lidstorm, "Adaptive distance protection for series-compensated transmission lines," *in proc. Trans. & Distrib. conference and Exposition*, Latin America, 2004.

[77] A. A. Girgis, A. A. Sallim and A. Karim El- Din, "An Adaptive protection scheme for advanced series-compensated (ACS) transmission lines," *IEEE Trans. Power Delivery*, vol. 13, no. 2, pp.414-420, Apr. 1998.

[78] Q. Y. Xuan, Y. H. Song, A. T. Johns, R. Morgan, and D. Williams, "Performance of an adaptive protection scheme for series compensated EHV transmission systems using neural networks," *Electric Power System Research*, vol. 36, no. 1, pp. 57–66, Jan. 1996.

[79] P. K. Dash, A. K. Pradhan, G. Panda, and A. C. Liew, "Adaptive relay setting for flexible ac transmission systems (FACTS)," *IEEE Trans. Power Delivery*, vol. 15, no. 1, pp. 38-43, Jan. 2000.

[80] R. K. Gajbhiye, B. Gopi, S. A. Soman, "Computationally efficient methodology for analysis of faulted power systems with series-compensated transmission line: a phase coordinate approach," *IEEE Trans. Power Delivery*, vol. 23, no. 2, pp. 1394-1400, Jan. 2008.

[81] A. R. Singh, N. R. Patne, and V. S. Kale, "Adaptive distance protection setting in presence of mid-point STATCOM using synchronized measurement," *Int. J. Electric Power Energy System.*, vol. 67, pp. 252–260, 2015.

[82] S. H. Horowitz and A.G. Phadke, "Third zone revisited," *IEEE Trans. Power Delivery*, vol. 21, no. 1, pp.23-29, Jan. 2006.

[83] T. Seegers and E. Krizauskas, "Transmission line protective systems loadability," Power system Relay Committee of Power Engg. Soc., Tech. Rep.,2001

[84] IEEE Power System Relaying committee of the IEEE Power Engg. Soc., Transmission line protective systems loadability, Rep. PSRC WG, March 2001.

[85] M. Jin and T. S. Sidhu, "Adaptive load encroachment prevention scheme for distance protection," *Electric Power Syst. Res.*, vol. 78, no.10, pp.1693-1700, 2008.

[86] H. K. Zadeh and Z. Li, "Adaptive load blinder for distance protection," *Electric Power Syst. Res*., no. 33, pp. 861-867, Apr. 2011.

[87] C. H. Kim, J. Y. Heo and R. K. Aggarwal, "An enhanced Zone 3 algorithm of a distance relay using transient components and state diagram," *IEEE Trans. Power Delivery*, vol. 20, no. 1, pp. 87–96, Jan.2005.

[88] M. Jonsson, and J. E. Daalder, "An adaptive scheme to prevent undesirable distance protection operation during voltage instability," *IEEE Trans. Power Delivery*, vol. 18, no. 4, pp. 1174–1180, Oct. 2003.

[89] P. K. Nayak, A. K. Pradhan and P. Bajpai, "Secured zone 3 protection during stressed condition," *IEEE Trans. Power Delivery*, vol. 30, no. 1, pp. 89-96, Feb. 2015.

[90] S. Lim, C. C. Liu, S. J. Lee, M. S. Choiand S. J. Rim, "Blocking of zone-3 relays to prevent cascaded events," *IEEE Trans. Power Delivery*, vol. 23, no. 2, pp. 747-754, May. 2008.

[91] S. Jamali, F. Namdari, and P. A. Crosslet, "Anatomy of a secured wide area backup protection," in proc. 9th *IET international conference on developments in power system protection*, Glasgow, Mar. 2008. pp. 332–337.

[92] A. G. Phadke and J. S. Thorp, *Computer Relaying for Power Systems*, 2nd ed., John Wiley and Sons, Ltd., Publication, 2009.

[93] J. D. L. Ree, V. Centeno, J. S. Thorp, and A. G. Phadke, "Synchronized phasor measurement applications in power systems," *IEEE Trans. Smart Grid*, vol. 1, no. 1, pp. 20–27, Jun. 2010.

[94] *IEEE Standard for Synchrophasors for Power Systems*, IEEE Standard C37.118-2005 (Revision of IEEE Std 1344-1995).

[95] D. Woodward, "SEL-421 Relay Fast Messages," SEL Application Guide (AG2002-14), 2002. available: http://www.selinc.com/aglist.html.

[96] G. Benmouyal, E. O. Schweitzer and A. Guzan, "*Synchronized phasor measurements in protective relays for protection , control and analysis of power systems*"[online]. Available: http://www.selinc.com/work area/download/assets.

[97] A. Guzman, S. Samineni, and M. Bryson, "*Protective relay synchrophasor measurements during fault conditions*," 2005. [Online]. Available: www.selinc.com/20050920, TP6214-01.

[98] Power System Relaying Committee Report of Working Group C-14 of the System Protection Subcommittee, Use of synchrophasor measurements in protective relaying applications, Draft 6.3, 4.4.2012.

[99] M. G. Adamiak, A. P. Apostolov, M. M. Begovic, C. F. Henville, K. E. Martin, G. L. Michel, A. G. Phadke, and J. S. Thorp, "Wide area protection-technology and infrastructures," *IEEE Trans. Power Delivery*, vol. 21, no. 2, pp. 601–609, Apr. 2006.

[100] X. N. Lin, Z. T. Li, K. C. Wu, and H. L. Weng, "Principles and implementations of hierarchical region defensive systems of power grid," *IEEE Trans. Power Delivery*, vol. 24, no. 1, pp. 30–37, Jan. 2009.

[101] M. K. Neyestanaki and A. M. Ranjbar, "An Adaptive PMU-Based Wide Area Backup Protection Scheme for Power Transmission Lines," *IEEE Trans. Smart Grid*, vol. 6, no. 3, pp. 1550–1559, 2015.

[102] S. Sheng, K. K. Li, W. L. Chan, Z. X. Jun, and D. X. Zhong, "Agent based self-healing protection system," *IEEE Trans. Power Delivery*, vol. 21, no. 2, pp. 610–618, Apr. 2006.

[103] X. Y. Tong, X. R. Wang, and K. M. Hopkinson, "The modeling and verification of peer-to-peer negotiating multi agent colored petri nets for wide-area backup protection," *IEEE Trans. Power Delivery*, vol. 24, no. 1, pp. 61–72, Jan. 2009.

[104] Z. He, Z. Zhang, W. Chen, O. P. Malik, and X. Yin, "Wide-area backup protection algorithm based on fault component voltage distribution," *IEEE Trans. Power Delivery*, vol.26, no. 4, pp. 2752–2760, Oct. 2011.

[105] P. Mohammadi and H. El-kishky, "A robust initialization algorithm for k-Means clustering in power distribution networks with PMU-based adaptive protection System," *in proc. International Power modulator and high voltage conference*, 1-4th Jun. 2014. pp. 252–255.

[106] J. Ma, J. Li, J. S. Thorp, A. G. Phadke et al, "A faulty steady state component-based wide area backup protection algorithm," *IEEE Transaction on Smart Grid*, vol. 2, no. 3, pp. 468-475, Sep. 2011.

[107] A. El-Hadidy and C. Rehtanz, "Blocking of distance relays zone 3 under load encroachment conditions – A new approach using phasor measurements technique,"14th *International Middle East Power Systems Conference (MECON'10),Cairo University, Egypt, 19*-21st Dec. 2010.

[108] M. M. Eissa, M. E. Masoud and M. M. M. Elanwar, "A novel back up wide area protection technique for power transmission grids using phasor measurement unit," *IEEE Trans. Power Delivery*, vol.25 , no. 1, pp. 270-278 , Jan. 2010.

[109] P. V. Navalkar and S. A. Soman, "Secure remote backup protection of transmission lines using synchrophasors," *IEEE Trans. Power Delivery*, vol. 23, no. 1, pp. 87–96, Oct. 2011.

[110] J. C. Tan, P. A. Crossley, D. Kirscen, J. Goody and J. A. Downes, "An expert system for the back-up protection of a transmission network," *IEEE. Trans. Power Delivery*, vol. 15, no. 2, pp. 508-514, Apr. 2000.

[111] P. Kundu and A. K. Pradhan, "Synchrophasor assisted zone-3 operation," *IEEE Trans. Power Del*ivery, vol. 29, no. 2, pp. 660-667, Apr. 2014.

[112] P. K. Nayak, A. K. Pradhan and P. Bajpai, "Wide area measurement based backup protection for power network with series compensation," *IEEE Trans. Power Delivery*, vol. 29, no. 4, pp. 1970-1977, Feb. 2014.

[113] Z. Zare, F. Aminifar, and M. Sanaye-Pasand, "Synchrophasor-based wide-area backup protection scheme with data requirement analysis," *IEEE Trans. Power Delivery*, vol. 30, no. 3, pp. 1410-1419, Jun. 2015.

[114] C. S. Chen, C. W. Liu, and J. A. Jiang, "Three-terminal transmission line protection using synchronized voltage and current phasor measurements," *Transmission and Distribution Conference and Exhibition 2002: Asia Pacific, IEEE PES*, 6-10th Oct. 2002.

[115] H. K. Zadeh and Z. Li, "Phasor measurement unit based transmission line protection scheme design," *Electric Power System Research*, vol. 81, no. 2, pp. 421–429, Feb. 2011.

[116] A. M. I. Taalab, H. A. Darwish, and E. S. Ahmed, "Performance of power differential relay with adaptive setting line protection," *IEEE Trans. Power Delivery*., vol. 22, no. 1, pp. 50-58, Jan. 2007.

[117] S. Dhambhare, S. A. Soman, and M. C. Chandorkar, "Adaptive current differential scheme for transmission line protection," *IEEE Trans. Power Delivery*, vol. 24, no. 4, pp. 1832-1841, Oct. 2009

[118] Q. Li, T. Cui, Y. Weng, R. Negi, F. Franchetti and M. D. Ilic, "An information-theoretic approach to PMU placement in electric power systems," *IEEE. Trans. Smart Grid*, vol. 4, no.1, pp. 446-456, Jul. 2013.

[119] K. P. Lien, C. W. Liu, C. S. Yu and J. A. Jiang, "Transmission network fault location observability with minimal PMU placement," *IEEE. Trans. Power Delivery*, vol. 21, no.3, pp. 1128-1135, Jul. 2006.

[120] B. K. Saharoy, A. K. Sinha and A. K. Pradhan, "An optimal placement technique for power system observability," *Electric Power Syst. Research*, vol. 42, no. 1, pp. 71-77, 2012.

[121] R. Kavasseri and S. K. Srinivasan, "Joint placement of phasor and conventional power flow measurements for fault observability of power systems," *IET Generation, Transmission & Distribution*, vol. 5, no. 10 , pp. 1019-1024, Oct. 2011.

[122] T. Gonen, *Electric Power Transmission System Engineering Analysis and design*, CRC Press, Taylor and Francis Group, 2009.

[123] D. Woodward, "*SEL-421 Relay fault messages*," SEL application (AG2002-14), 2002, http:// www. Selinc.com/aglist.html.

[124] B. Naduvathuparambil, and A. Feliachi, "Communication delays in wide area measurement systems," in Proc. *IEEE 34th Syst. Theory*, pp. 118-122, 2002.

[125] G. Benmouyal, E. O. Schweitzer and A. Guzan, Synchronized phasor measurements in protective relays for protection control and analysis of power systems," http:// www. Selinc.com/workarea/download/assests.

[126] A. G. Phadke, and J. S. Thorp, "Communication needs for wide area measurement applications," Critical Infrastructure (CRIS), 5th International Conference, September 2010.

[127] D. Wang, S. Miao, X. Lin, P. Liu, Y. Wu, and D. Yang, "Design of a novel wide-area backup protection system," *in Proc. of the IEEE 2005 PES Transmission & Distribution Conference & Exhibition*: Asia and Pacific Dalian, China.

[128] P. M. Anderson, *Power System Protection*, (IEEE Press, 1999, Reprint 2012).

[129] S. H. Horowitz and A. G. Phadke, *Power System Relaying*, Wiley, 2008.

[130] A. N. D. Tleis, *Power Systems Modeling and Fault Analysis, Theory and Practice. Elsevier*, 2009

[131] P. Kundur, *Power System Stability and Control*, The EPRI Power System Engineering Series, Tata McGraw-Hill Publ. Comp. Ltd., New Delhi, 1994.

[132] P. W. Sauer and M. A. Pai, *Power System Dynamics and Stability*, Prentice Hall, Upper Saddle River, 1998.

[133] IEEE Power Engineering Society, *Downed Power Lines: Why They Can't Always Be Detected*, New York: IEEE, 1989.

[134] J. Carr, G. L. Hood, "High Impedance Fault Detection on Primary Distribution Systems," CEA Final Report, Project No. 78–75, Nov. 1979.

[135] D. Hou and N. Fischer, "Deterministic High-Impedance Fault Detection and Phase Selection on Ungrounded Distribution Systems," in *2005 32nd Annual Western Protective Relay Conference Proceedings*

Appendix A

System Data for WSCC 3-Machine 9-Bus Power System (Chapter 2)

Generators:

Gen-1: 600MVA, 22 kV, 50 Hz.

Gen-2: 465MVA, 22 kV, 50 Hz.

Gen-3: 310 MVA, 22 kV, 50 Hz.

X_d = 1.81 p.u., $X_d^{'}$ = 0.3 p.u., $X_d^{''}$ = 0.23 p.u., $T_{do}^{'}$ = 8 s, $T_{do}^{''}$ = 0.03 s, X_q = 1.76 p.u., $X_q^{''}$ = 0.25 p.u., $T_{qo}^{''}$ = 0.03 s., R_a = 0.003 p.u., X_p (Potier reactance) = 0.15 p.u.

Transformers:

T1: 600MVA, 22/400 kV, 50 Hz, Δ/Y.

T2: 465MVA, 22/400 kV, 50 Hz, Δ/Y.

T3: 310MVA, 22/400 kV, 50 Hz, Δ/Y.

X = 0.163 p.u., X_{core} = 0.33 p.u., R_{core} = 0.0 p.u., P_{copper} = 0.00177 p.u.

Transmission lines:

Length of line 7-8 = 320 km., line 8-9 = 400 km., line 7-5 = 310 km., line 5-4 = 350 km., line 6-4 = 350 km., line 6-9 = 300 km.

Positive-sequence impedance = 0.03293 + j 0.327 Ω/km.

Zero-sequence impedance = 0.309 + j 1.297 Ω/km.

Positive-sequence capacitive reactance = $280.1X10^3$ Ω.km.

Zero-sequence capacitive reactance = $461.2546X10^3$ Ω.km.

Loads:

Load A = 300 + j 100 MVA, Load B = 200 + j 75 MVA, Load C = 150 + j 75 MVA.

Appendix B

System Data for 400-kV Three Terminal Line

(Chapter 3)

400 kV, 50 Hz system data are provided below.

Source parameters: Z_{1s}=0.55+j 7.98 Ω , Z_{0s}=1.5+j 23.94 Ω

Line parameters:

Line lengths between bus S to T is 70 km, bus P and T is 50 km

R and T is 300 km

Z_{1L}=0.032+j 0.03184Ω/km,

Z_{0L}=0.2586+j 1.174Ω/km

Shunt capacitance:

C_1=0.01163 µF/ km,

C_0=0.0076764 µF/ km

CT ratio=800:5,

PT ratio = 400 kV: 110 V

(1 and 0 refers to positive and zero sequence respectively)

Positive and negative sequence impedances are equal for all cases.

Appendix C

System Data for Series Compensated Line

(Chapter 4)

400 kV, 50 Hz system data are provided below.

Source parameters:

$Z_{SR1} = Z_{ST1}$ =0.06979+j 1.99 Ω

$Z_{SR0} = Z_{ST0}$=0.2093+j 5.99 Ω

Line parameters:

Line length: R-S = 250 km, S-T=100 km,

Z_{1L}=0.032+j 0.3184Ω/km, Z_{0L} =0.2586+j 1.174Ω/km

Shunt capacitance: C_1=0.01163 µF/ km,C_0=0.0076764 µF/ km

Load =50 MW, CT ratio=800:5, PT ratio = 400 kV: 110 V

1 and 0 refers to positive and zero sequence respectively.

Positive and negative sequence impedances are equal.

Appendix D

System Data for Ten Machine 39-bus New England Power System (Chapter 5)

Generator:

Parameters for the two-axis model of the synchronous machines are shown in Table as follows:

Unit No.	H	Ra	x'd	x'q	xd	xq	T'do	T'qo	xl
1	500.0	0	0.006	0.008	0.02	0.019	7.0	0.7	0.003
2	30.3	0	0.0697	0.170	0.295	0.282	6.56	1.5	0.035
3	35.8	0	0.0531	0.0876	0.2495	0.237	5.7	1.5	0.0304
4	28.6	0	0.0436	0.166	0.262	0.258	5.69	1.5	0.0295
5	26.0	0	0.132	0.166	0.67	0.62	5.4	0.44	0.054
6	34.8	0	0.05	0.0814	0.254	0.241	7.3	0.4	0.0224
7	26.4	0	0.049	0.186	0.295	0.292	5.66	1.5	0.0322
8	24.3	0	0.057	0.0911	0.290	0.280	6.7	0.41	0.028
9	34.5	0	0.057	0.0587	0.2106	0.205	4.79	1.96	0.0298
10	42.0	0	0.031	0.008	0.1	0.069	10.2	0.0	0.0125

Generator and load data:

Bus	Type	Voltage [PU]	Load		Generator		
			MW	MVar	MW	MVar	Unit No.
1	PQ	-	0.0	0.0	0.0	0.0	
2	PQ	-	0.0	0.0	0.0	0.0	
3	PQ	-	322.0	2.4	0.0	0.0	
4	PQ	-	500.0	184.0	0.0	0.0	
5	PQ	-	0.0	0.0	0.0	0.0	
6	PQ	-	0.0	0.0	0.0	0.0	
7	PQ	-	233.8	84.0	0.0	0.0	
8	PQ	-	522.0	176.0	0.0	0.0	
9	PQ	-	0.0	0.0	0.0	0.0	
10	PQ	-	0.0	0.0	0.0	0.0	
11	PQ	-	0.0	0.0	0.0	0.0	
12	PQ	-	7.5	88.0	0.0	0.0	
13	PQ	-	0.0	0.0	0.0	0.0	
14	PQ	-	0.0	0.0	0.0	0.0	
15	PQ	-	320.0	153.0	0.0	0.0	
16	PQ	-	329.0	32.3	0.0	0.0	
17	PQ	-	0.0	0.0	0.0	0.0	
18	PQ	-	158.0	30.0	0.0	0.0	
19	PQ	-	0.0	0.0	0.0	0.0	
20	PQ	-	628.0	103.0	0.0	0.0	
21	PQ	-	274.0	115.0	0.0	0.0	
22	PQ	-	0.0	0.0	0.0	0.0	

23	PQ	-	247.5	84.6	0.0	0.0	
24	PQ	-	308.6	-92.0	0.0	0.0	
25	PQ	-	224.0	47.2	0.0	0.0	
26	PQ	-	139.0	17.0	0.0	0.0	
27	PQ	-	281.0	75.5	0.0	0.0	
28	PQ	-	206.0	27.6	0.0	0.0	
29	PQ	-	283.5	26.9	0.0	0.0	
30	PV	1.0475	0.0	0.0	250.0	-	Gen10
31	PV	0.9820	9.2	4.6	-	-	Gen2
32	PV	0.9831	0.0	0.0	650.0	-	Gen3
33	PV	0.9972	0.0	0.0	632.0	-	Gen4
34	PV	1.0123	0.0	0.0	508.0	-	Gen5
35	PV	1.0493	0.0	0.0	650.0	-	Gen6
36	PV	1.0635	0.0	0.0	560.0	-	Gen7
37	PV	1.0278	0.0	0.0	540.0	-	Gen8
38	PV	1.0265	0.0	0.0	830.0	-	Gen9
39	PV	1.0300	1104.0	250.0	1000.0	-	Gen1

Transmission lines and transformer tap:

All values shown are in per unit at 60Hz on a 100MVA base.

Line Data					Transformer Tap	
From Bus	To Bus	R	X	B	Magnitude	Angle
1	2	0.0035	0.0411	0.6987	0.000	0.00
1	39	0.0010	0.0250	0.7500	0.000	0.00
2	3	0.0013	0.0151	0.2572	0.000	0.00
2	25	0.0070	0.0086	0.1460	0.000	0.00
3	4	0.0013	0.0213	0.2214	0.000	0.00
3	18	0.0011	0.0133	0.2138	0.000	0.00
4	5	0.0008	0.0128	0.1342	0.000	0.00
4	14	0.0008	0.0129	0.1382	0.000	0.00
5	6	0.0002	0.0026	0.0434	0.000	0.00
5	8	0.0008	0.0112	0.1476	0.000	0.00

6	7	0.0006	0.0092	0.1130	0.000	0.00
6	11	0.0007	0.0082	0.1389	0.000	0.00
7	8	0.0004	0.0046	0.0780	0.000	0.00
8	9	0.0023	0.0363	0.3804	0.000	0.00
9	39	0.0010	0.0250	1.2000	0.000	0.00
10	11	0.0004	0.0043	0.0729	0.000	0.00
10	13	0.0004	0.0043	0.0729	0.000	0.00
13	14	0.0009	0.0101	0.1723	0.000	0.00
14	15	0.0018	0.0217	0.3660	0.000	0.00
15	16	0.0009	0.0094	0.1710	0.000	0.00
16	17	0.0007	0.0089	0.1342	0.000	0.00
16	19	0.0016	0.0195	0.3040	0.000	0.00
16	21	0.0008	0.0135	0.2548	0.000	0.00
16	24	0.0003	0.0059	0.0680	0.000	0.00
17	18	0.0007	0.0082	0.1319	0.000	0.00
17	27	0.0013	0.0173	0.3216	0.000	0.00
21	22	0.0008	0.0140	0.2565	0.000	0.00
22	23	0.0006	0.0096	0.1846	0.000	0.00
23	24	0.0022	0.0350	0.3610	0.000	0.00
25	26	0.0032	0.0323	0.5130	0.000	0.00
26	27	0.0014	0.0147	0.2396	0.000	0.00
26	28	0.0043	0.0474	0.7802	0.000	0.00
26	29	0.0057	0.0625	1.0290	0.000	0.00
28	29	0.0014	0.0151	0.2490	0.000	0.00
12	11	0.0016	0.0435	0.0000	1.006	0.00
12	13	0.0016	0.0435	0.0000	1.006	0.00
6	31	0.0000	0.0250	0.0000	1.070	0.00
10	32	0.0000	0.0200	0.0000	1.070	0.00
19	33	0.0007	0.0142	0.0000	1.070	0.00
20	34	0.0009	0.0180	0.0000	1.009	0.00
22	35	0.0000	0.0143	0.0000	1.025	0.00
23	36	0.0005	0.0272	0.0000	1.000	0.00
25	37	0.0006	0.0232	0.0000	1.025	0.00
2	30	0.0000	0.0181	0.0000	1.025	0.00
29	38	0.0008	0.0156	0.0000	1.025	0.00
19	20	0.0007	0.0138	0.0000	1.060	0.00

Appendix E

IEEE 118-bus Single Line Diagram

(Chapter 5)

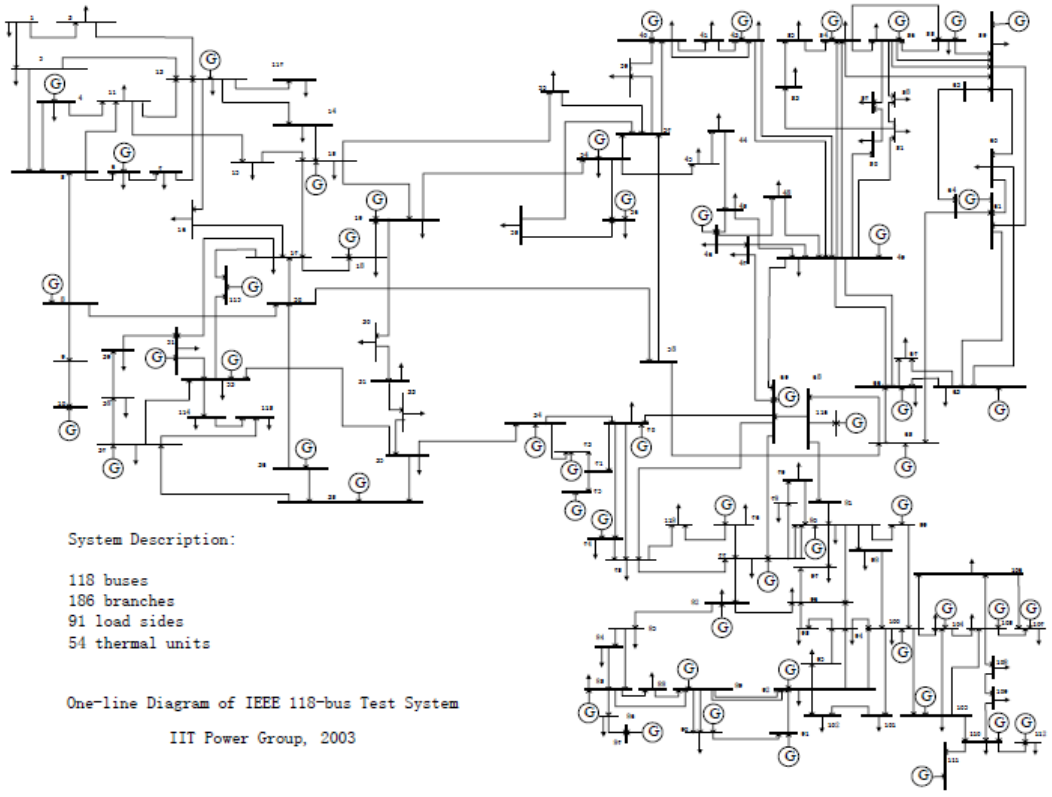

Measurement buses for IEEE 118 bus System

PMUs	1,5,7,9,12,11,15,17,19,21,23,26,27,29,30,32,36,37,41, 43,45,46,49,52,54,55,57,58,59,61,64,65,66,68,70,72,73,75,77 79,80,83,85,87,89,91,92,94,96,100,102,103,105,109,111, 112,114,

Appendix F

IEEE 118-bus Power System Data

(Chapter 5)

Generator and load data:

Unit	Bus No.	Unit Cost Coefficients			Pmax (MW)	Pmin (MW)
		a (MBtu)	b (MBtu/MW)	c (MBtu/MW^2)		
1	4	31.67	26.2438	0.069663	30	5
2	6	31.67	26.2438	0.069663	30	5
3	8	31.67	26.2438	0.069663	30	5
4	10	6.78	12.8875	0.010875	300	150
5	12	6.78	12.8875	0.010875	300	100
6	15	31.67	26.2438	0.069663	30	10
7	18	10.15	17.8200	0.012800	100	25
8	19	31.67	26.2438	0.069663	30	5
9	24	31.67	26.2438	0.069663	30	5
10	25	6.78	12.8875	0.010875	300	100
11	26	32.96	10.7600	0.003000	350	100
12	27	31.67	26.2438	0.069663	30	8
13	31	31.67	26.2438	0.069663	30	8
14	32	10.15	17.8200	0.012800	100	25
15	34	31.67	26.2438	0.069663	30	8
16	36	10.15	17.8200	0.012800	100	25
17	40	31.67	26.2438	0.069663	30	8
18	42	31.67	26.2438	0.069663	30	8
19	46	10.15	17.8200	0.012800	100	25
20	49	28	12.3299	0.002401	250	50
21	54	28	12.3299	0.002401	250	50
22	55	10.15	17.8200	0.012800	100	25
23	56	10.15	17.8200	0.012800	100	25
24	59	39	13.2900	0.004400	200	50
25	61	39	13.2900	0.004400	200	50
26	62	10.15	17.8200	0.012800	100	25
27	65	64.16	8.3391	0.010590	420	100
28	66	64.16	8.3391	0.010590	420	100

29	69	6.78	12.8875	0.010875	300	80
30	70	74.33	15.4708	0.045923	80	30
31	72	31.67	26.2438	0.069663	30	10
32	73	31.67	26.2438	0.069663	30	5
33	74	17.95	37.6968	0.028302	20	5
34	76	10.15	17.8200	0.012800	100	25
35	77	10.15	17.8200	0.012800	100	25
36	80	6.78	12.8875	0.010875	300	150
37	82	10.15	17.8200	0.012800	100	25
38	85	31.67	26.2438	0.069663	30	10
39	87	32.96	10.7600	0.003000	300	100
40	89	6.78	12.8875	0.010875	200	50
41	90	17.95	37.6968	0.028302	20	8
42	91	58.81	22.9423	0.009774	50	20
43	92	6.78	12.8875	0.010875	300	100
44	99	6.78	12.8875	0.010875	300	100
45	100	6.78	12.8875	0.010875	300	100
46	103	17.95	37.6968	0.028302	20	8
47	104	10.15	17.8200	0.012800	100	25
48	105	10.15	17.8200	0.012800	100	25
49	107	17.95	37.6968	0.028302	20	8
50	110	58.81	22.9423	0.009774	50	25
51	111	10.15	17.8200	0.012800	100	25
52	112	10.15	17.8200	0.012800	100	25
53	113	10.15	17.8200	0.012800	100	25
54	116	58.81	22.9423	0.009774	50	25

Transmission lines and transformer tap:

All values shown are in per unit at 60Hz on a 100MVA base

Line No.	From Bus	To Bus	Circuit ID	R (pu)	X (pu)	B (pu)	Flow Limit (MW)
1	1	2	1	0.0303	0.0999	0.0254	175
2	1	3	1	0.0129	0.0424	0.01082	175
3	4	5	1	0.00176	0.00798	0.0021	500
4	3	5	1	0.0241	0.108	0.0284	175
5	5	6	1	0.0119	0.054	0.01426	175
6	6	7	1	0.00459	0.0208	0.0055	175
7	8	9	1	0.00244	0.0305	1.162	500
8	8	5	1	0	0.0267	0	500
9	9	10	1	0.00258	0.0322	1.23	500
10	4	11	1	0.0209	0.0688	0.01748	175
11	5	11	1	0.0203	0.0682	0.01738	175

12	11	12	1	0.00595	0.0196	0.00502	175
13	2	12	1	0.0187	0.0616	0.01572	175
14	3	12	1	0.0484	0.16	0.0406	175
15	7	12	1	0.00862	0.034	0.00874	175
16	11	13	1	0.02225	0.0731	0.01876	175
17	12	14	1	0.0215	0.0707	0.01816	175
18	13	15	1	0.0744	0.2444	0.06268	175
19	14	15	1	0.0595	0.195	0.0502	175
20	12	16	1	0.0212	0.0834	0.0214	175
21	15	17	1	0.0132	0.0437	0.0444	500
22	16	17	1	0.0454	0.1801	0.0466	175
23	17	18	1	0.0123	0.0505	0.01298	175
24	18	19	1	0.01119	0.0493	0.01142	175
25	19	20	1	0.0252	0.117	0.0298	175
26	15	19	1	0.012	0.0394	0.0101	175
27	20	21	1	0.0183	0.0849	0.0216	175
28	21	22	1	0.0209	0.097	0.0246	175
29	22	23	1	0.0342	0.159	0.0404	175
30	23	24	1	0.0135	0.0492	0.0498	175
31	23	25	1	0.0156	0.08	0.0864	500
32	26	25	1	0	0.0382	0	500
33	25	27	1	0.0318	0.163	0.1764	500
34	27	28	1	0.01913	0.0855	0.0216	175
35	28	29	1	0.0237	0.0943	0.0238	175
36	30	17	1	0	0.0388	0	500
37	8	30	1	0.00431	0.0504	0.514	175
38	26	30	1	0.00799	0.086	0.908	500
39	17	31	1	0.0474	0.1563	0.0399	175
40	29	31	1	0.0108	0.0331	0.0083	175
41	23	32	1	0.0317	0.1153	0.1173	140
42	31	32	1	0.0298	0.0985	0.0251	175
43	27	32	1	0.0229	0.0755	0.01926	175
44	15	33	1	0.038	0.1244	0.03194	175
45	19	34	1	0.0752	0.247	0.0632	175
46	35	36	1	0.00224	0.0102	0.00268	175
47	35	37	1	0.011	0.0497	0.01318	175
48	33	37	1	0.0415	0.142	0.0366	175
49	34	36	1	0.00871	0.0268	0.00568	175
50	34	37	1	0.00256	0.0094	0.00984	500
51	38	37	1	0	0.0375	0	500
52	37	39	1	0.0321	0.106	0.027	175
53	37	40	1	0.0593	0.168	0.042	175
54	30	38	1	0.00464	0.054	0.422	175
55	39	40	1	0.0184	0.0605	0.01552	175
56	40	41	1	0.0145	0.0487	0.01222	175

57	40	42	1	0.0555	0.183	0.0466	175
58	41	42	1	0.041	0.135	0.0344	175
59	43	44	1	0.0608	0.2454	0.06068	175
60	34	43	1	0.0413	0.1681	0.04226	175
61	44	45	1	0.0224	0.0901	0.0224	175
62	45	46	1	0.04	0.1356	0.0332	175
63	46	47	1	0.038	0.127	0.0316	175
64	46	48	1	0.0601	0.189	0.0472	175
65	47	49	1	0.0191	0.0625	0.01604	175
66	42	49	1	0.0715	0.323	0.086	175
67	42	49	2	0.0715	0.323	0.086	175
68	45	49	1	0.0684	0.186	0.0444	175
69	48	49	1	0.0179	0.0505	0.01258	175
70	49	50	1	0.0267	0.0752	0.01874	175
71	49	51	1	0.0486	0.137	0.0342	175
72	51	52	1	0.0203	0.0588	0.01396	175
73	52	53	1	0.0405	0.1635	0.04058	175
74	53	54	1	0.0263	0.122	0.031	175
75	49	54	1	0.073	0.289	0.0738	175
76	49	54	2	0.0869	0.291	0.073	175
77	54	55	1	0.0169	0.0707	0.0202	175
78	54	56	1	0.00275	0.00955	0.00732	175
79	55	56	1	0.00488	0.0151	0.00374	175
80	56	57	1	0.0343	0.0966	0.0242	175
81	50	57	1	0.0474	0.134	0.0332	175
82	56	58	1	0.0343	0.0966	0.0242	175
83	51	58	1	0.0255	0.0719	0.01788	175
84	54	59	1	0.0503	0.2293	0.0598	175
85	56	59	1	0.0825	0.251	0.0569	175
86	56	59	2	0.0803	0.239	0.0536	175
87	55	59	1	0.04739	0.2158	0.05646	175
88	59	60	1	0.0317	0.145	0.0376	175
89	59	61	1	0.0328	0.15	0.0388	175
90	60	61	1	0.00264	0.0135	0.01456	500
91	60	62	1	0.0123	0.0561	0.01468	175
92	61	62	1	0.00824	0.0376	0.0098	175
93	63	59	1	0	0.0386	0	500
94	63	64	1	0.00172	0.02	0.216	500
95	64	61	1	0	0.0268	0	500
96	38	65	1	0.00901	0.0986	1.046	500
97	64	65	1	0.00269	0.0302	0.38	500
98	49	66	1	0.018	0.0919	0.0248	500
99	49	66	2	0.018	0.0919	0.0248	500
100	62	66	1	0.0482	0.218	0.0578	175
101	62	67	1	0.0258	0.117	0.031	175

102	65	66	1	0	0.037	0	500
103	66	67	1	0.0224	0.1015	0.02682	175
104	65	68	1	0.00138	0.016	0.638	500
105	47	69	1	0.0844	0.2778	0.07092	175
106	49	69	1	0.0985	0.324	0.0828	175
107	68	69	1	0	0.037	0	500
108	69	70	1	0.03	0.127	0.122	500
109	24	70	1	0.00221	0.4115	0.10198	175
110	70	71	1	0.00882	0.0355	0.00878	175
111	24	72	1	0.0488	0.196	0.0488	175
112	71	72	1	0.0446	0.18	0.04444	175
113	71	73	1	0.00866	0.0454	0.01178	175
114	70	74	1	0.0401	0.1323	0.03368	175
115	70	75	1	0.0428	0.141	0.036	175
116	69	75	1	0.0405	0.122	0.124	500
117	74	75	1	0.0123	0.0406	0.01034	175
118	76	77	1	0.0444	0.148	0.0368	175
119	69	77	1	0.0309	0.101	0.1038	175
120	75	77	1	0.0601	0.1999	0.04978	175
121	77	78	1	0.00376	0.0124	0.01264	175
122	78	79	1	0.00546	0.0244	0.00648	175
123	77	80	1	0.017	0.0485	0.0472	500
124	77	80	2	0.0294	0.105	0.0228	500
125	79	80	1	0.0156	0.0704	0.0187	175
126	68	81	1	0.00175	0.0202	0.808	500
127	81	80	1	0	0.037	0	500
128	77	82	1	0.0298	0.0853	0.08174	200
129	82	83	1	0.0112	0.03665	0.03796	200
130	83	84	1	0.0625	0.132	0.0258	175
131	83	85	1	0.043	0.148	0.0348	175
132	84	85	1	0.0302	0.0641	0.01234	175
133	85	86	1	0.035	0.123	0.0276	500
134	86	87	1	0.02828	0.2074	0.0445	500
135	85	88	1	0.02	0.102	0.0276	175
136	85	89	1	0.0239	0.173	0.047	175
137	88	89	1	0.0139	0.0712	0.01934	500
138	89	90	1	0.0518	0.188	0.0528	500
139	89	90	2	0.0238	0.0997	0.106	500
140	90	91	1	0.0254	0.0836	0.0214	175
141	89	92	1	0.0099	0.0505	0.0548	500
142	89	92	2	0.0393	0.1581	0.0414	500
143	91	92	1	0.0387	0.1272	0.03268	175
144	92	93	1	0.0258	0.0848	0.0218	175
145	92	94	1	0.0481	0.158	0.0406	175
146	93	94	1	0.0223	0.0732	0.01876	175

147	94	95	1	0.0132	0.0434	0.0111	175
148	80	96	1	0.0356	0.182	0.0494	175
149	82	96	1	0.0162	0.053	0.0544	175
150	94	96	1	0.0269	0.0869	0.023	175
151	80	97	1	0.0183	0.0934	0.0254	175
152	80	98	1	0.0238	0.108	0.0286	175
153	80	99	1	0.0454	0.206	0.0546	200
154	92	100	1	0.0648	0.295	0.0472	175
155	94	100	1	0.0178	0.058	0.0604	175
156	95	96	1	0.0171	0.0547	0.01474	175
157	96	97	1	0.0173	0.0885	0.024	175
158	98	100	1	0.0397	0.179	0.0476	175
159	99	100	1	0.018	0.0813	0.0216	175
160	100	101	1	0.0277	0.1262	0.0328	175
161	92	102	1	0.0123	0.0559	0.01464	175
162	101	102	1	0.0246	0.112	0.0294	175
163	100	103	1	0.016	0.0525	0.0536	500
164	100	104	1	0.0451	0.204	0.0541	175
165	103	104	1	0.0466	0.1584	0.0407	175
166	103	105	1	0.0535	0.1625	0.0408	175
167	100	106	1	0.0605	0.229	0.062	175
168	104	105	1	0.00994	0.0378	0.00986	175
169	105	106	1	0.014	0.0547	0.01434	175
170	105	107	1	0.053	0.183	0.0472	175
171	105	108	1	0.0261	0.0703	0.01844	175
172	106	107	1	0.053	0.183	0.0472	175
173	108	109	1	0.0105	0.0288	0.0076	175
174	103	110	1	0.03906	0.1813	0.0461	175
175	109	110	1	0.0278	0.0762	0.0202	175
176	110	111	1	0.022	0.0755	0.02	175
177	110	112	1	0.0247	0.064	0.062	175
178	17	113	1	0.00913	0.0301	0.00768	175
179	32	113	1	0.0615	0.203	0.0518	500
180	32	114	1	0.0135	0.0612	0.01628	175
181	27	115	1	0.0164	0.0741	0.01972	175
182	114	115	1	0.0023	0.0104	0.00276	175
183	68	116	1	0.00034	0.00405	0.164	500
184	12	117	1	0.0329	0.14	0.0358	175
185	75	118	1	0.0145	0.0481	0.01198	175
186	76	118	1	0.0164	0.0544	0.01356	175

Publications from the Thesis

A. Journals published

[1] S. Sarangi and A. K. Pradhan, "Synchronised data-based adaptive backup protection scheme for series compensated line," *IET Gen. Trans. & Distribution.*, vol. 8, no. , pp. 1979–1986, Dec. 2014.

[2] S. Sarangi and A. K. Pradhan, "Adaptive direct underrecahing transfer trip protection scheme for three terminal line," *IEEE Trans. Power Del.*, vol. 30, no. 6, pp. 2383–2391, Dec. 2015.

[3] S. Sarangi and A. K.Pradhan, "An adaptive alpha Plane Line Differential Protection," *IET Generation Transmission & Distribution*, 2017.(Accepted)

B. Book Chapter

[1] P. Kundu, S. Sarangi and A. K. Pradhan, "Wide area measurement based power network protection," *IET Gen. Trans. & Distribution.*, 2016. In Early Access.

C. Conference proceedings

[1] S. Sarangi and A. K. Pradhan, "Adaptive relay setting of series compensated line using phasor measurement unit data," presented in ICEPES-2010, MNIT, Bhopal.

[2] S. Sarangi and A. K. Pradhan, "Apply PMU data for zone-2 setting of series compensated line," presented at the *IEEE International Conference on Energy, Automation and Signal*, S.O.A. University, Bhubaneswar, Odisha, India, Dec., 2011.

[3] S. Sarangi and A. K. Pradhan, "Adaptive POTT scheme for series compensated line using synchrophasors," presented RAMPS-2012,VSSUT, Burla, Dec., 2012.

[4] S. Sarangi and A. K. Pradhan, R. Mohanty, "Preventing zone 3 maloperation during load encroachment," presented RAIEE-2014, VSSUT, BURLA, India, Dec., 2014.

[5] S. Sarangi and A. K. Pradhan, "Enhanced alpha plane line protection," presented in National Power System Conference, IIT Bhubaneswar, Odisha, India, Dec., 2016.

Author's Biography

Saumendra Sarangi was born in Cuttack, Odisha, India, on 25th June, 1980, He received the bachelor degree in Electrical Engineering from Utkal University, Bhubaneswar, India in 2003 and master degree in Power Control and Drives from National Institute of Technology Rourkela, India, and currently pursuing PhD in Power System Protection at Indian Institute Technology, Kharagpur, India. He worked in project titled "Protecting Power system using Wide area measurement" during 2009-2012, sponsored by Department of Science Technology, India. His current research interest is Adaptive Relaying using Synchronized data. He can be contacted at: usomsam@gmail.com. He has 3 years of teaching experience and is currently working as an Assistant Professor at NIT Uttarakhand.